UNIVERSITY OF BIRMINGHAM

Co-channel Interference Reduction in Optical Code Division Multiple Access Systems

By

Mohammad Hossein Zoualfaghari

A Thesis submitted to
The University of Birmingham
for the degree of

DOCTOR OF PHILOSOPHY

SCHOOL OF ELECTRONIC, ELECTRICAL AND COMPUTER ENGINEERING
COLLEGE OF ENGINEERING AND PHYSICAL SCIENCE
April 2015

ABSTRACT

In this thesis few new code sets and a multi-user interference (MUI) cancellation scheme have been proposed for Optical Code Division Multiple Access (OCDMA) systems, which can be employed in the next generation of global communication networks to enhance their existing systems' performance dramatically. The initial evaluation of the proposed code sets shows that their implementation improves the performance, decreases the BER and increases security considerably. Also the proposed MUI cancellation scheme totally removes all the cross-talk and interference between the active users within the network. These novel schemes and codes can be easily implemented in the optical packet switched networks. Optical switching has the ability of bandwidth manipulation at the wavelength level (e.g. with optical circuit/packet/burst switching); the capability to accommodate a wide range of traffic distributions, and also to make dynamic resource reservations possible.

This thesis first gives a brief overview of co-channel interference reduction in OCDMA networks, then proposes two novel code sets, Uniform Cross-Correlation Modified Prime Code (UC-MPC) and Transposed UC-MPC (T-UCMPC), along with their evaluation and analysis in various systems, including IP routing over an OCDMA network. Thereafter, the new MUI cancellation scheme is proposed and then the proposed code sets and the MUI cancellation scheme are implemented and analysed in a laboratory-based experimental test bed. Finally the conclusion of this research is discussed.

ACKNOWLEDGEMENTS

Words cannot describe my feelings and gratitude to my research supervisor Dr Hooshang Ghafouri-Shiraz, for his continuous paternal support, technical advice and sponsorship during the period of my PhD. This was a meandering path up a mountain and without his selfless dedication, I would not have been able to reach the peak. Hereby I send my sincere gratitude to Dr Shiraz for every second of his time and support.

I express my heartfelt gratitude to my beloved wife Yasamin Mehrabadi for her perpetual support and for realising my circumstances. Her true love and patience have always been my hopes and my eternal love and appreciation goes to her as she brings happiness to my life.

I am eternally gratefully to my family for their pure love, faith and support. I proudly dedicate this thesis to the memory of my father Rahmat (1941-2013); his selfless support and dedication is the backbone of my whole life's success. I am sure he is watching me from the heavens and smiles as the seed he had planted flourishes. My mother Flor Famili nourished my soul with her pure maternal love and dedicated her heart to inspire me on the way of my progress. Without her prayers and encouragement I would have got lost in this stormy ocean. My brother Mohammad Reza Zolfaghari was always standing beside me in the front line of the battle with my problems during my PhD programme; not only as a brother, but also as my best friend. My beloved grandmother Robabeh Taheri, taught me how to love and how to live.

In addition, I would like to thank all of the lecturers and staff of the University of Birmingham, as they have constructed the robust foundation of my knowledge.

Finally, I am grateful to my dear friends Dr Abubakar Tariq, Hamid Mahmoudi, Shahrouz Norouzi, Farzad Hayati and all of my other friends and colleagues, for their precious encouragements, supports and selfless friendship.

LIST OF PUBLICATIONS

[1] Zoualfaghari, Mohammad Hossein, and Hooshang Ghafouri-Shiraz. "A Novel Multi User Interference Cancellation Scheme for Synchronous OCDMA Networks." *Journal of Lightwave Technology* 31.11 (2013): 1813-1820.

[2] Zoualfaghari, M. H., and H. Ghafouri-Shiraz. "A Novel Transposed Uniform Cross-Correlation Modified Prime Code for Enhancement of Capacity and Spectral Efficiency of Networks." *Microwave and Optical Technology Letters* 55.12 (2013): 2952-2955.

[3] Zoualfaghari, Mohammad Hossein, and H. Ghafouri-Shiraz. "Enhancement of Network Capacity and Spectral Efficiency Using Transposed Uniform Cross-Correlation Modified Prime Code." *International conference on Electrical and Electronics Engineering (ICEEE)*, 2013, accepted.

[4] Zoualfaghari, M. H., and H. Ghafouri-Shiraz. "Analysis of a novel prime code in IP transmission and routing over FSK-OCDMA in an optical network unit." *Microwave and Optical Technology Letters* 54.12 (2012): 2852-2856.

[5] Zoualfaghari, Mohammad Hossein, and H. Ghafouri-Shiraz. "Uniform cross-Correlation modified prime code for applications in synchronous optical CDMA communication systems." *Lightwave Technology, Journal of* 30.18 (2012): 2955-2963.

LIST OF PATENTS

[1] Zoualfaghari, M.H., "OPTICAL CLOCK DISTRIBUTION FOR OCDMA NETWORKS", European Patent Office (EPO), File No.: EP14192568, 10 November 2014, Patent Pending

[2] Zoualfaghari, M.H., "PRESET TRANSMITTER DELAYS FOR OCDMA SYNCHRONISATION", European Patent Office (EPO), File No.: EP14192570, 10 November 2014, Patent Pending

TABLE OF CONTENT

TABLE OF TABLES

TABLE OF FIGURES

TABLE OF EQUATIONS

LIST OF ABBREVIATIONS

2PC	2^n Prime Code
A-OCDMA	Asynchronous Optical Code Division Multiple Access
AC	Auto-Correlation
APD	Avalanche Photo-Diode
BER	Bit Error Rate
BPSK	Binary Phase Shift Keying
BT	British Telecom
CC	Cross-Correlation
CDMA	Code Division Multiple Access
DAQ	Data Acquisition
DPMPC	Double-Padded Modified Prime Code
EPC	Extended Prime Code
FEC	Forward Error Correction
FPC	Fresh Prime Code
FPMPC	Full-Padded Modified Prime Code
FSK	Frequency Shift Keying
FTTC	Fibre to the Cabinet

FTTH	Fibre to the Home
GF	Galois Field
GPC	Generalised Prime Code
GS	Generalisation Strategy
IB	Injected Bits
IC	Interference Cancellation
IP	Internet Protocol
MAI	Multi Access Interference
MPC	Modified Prime Code
MUI	Multi User Interference
MZI	Mach-Zehnder Interferometer
NPC	Novel Prime Code
NRZ	Non-Return to Zero
OCDMA	Optical Code Division Multiple Access
ONU	Optical Network Unit
OOC	Optical Orthogonal Codes
OOK	On–Off Keying
OPPM	Overlapping Pulse-Position Modulation
OPS	Optical Packet Switch

PC	Prime Code
PD	Photo-Detector
PDF	Probability Density Function
PER	Packet Error Rate
PMPC	Padded Modified Prime Code
PON	Passive Optical Network
PPM	Pulse-Position Modulation
ROM	Read Only Memory
S-OCDMA	Synchronous Optical Code Division Multiple Access
TDMA	Time Division Multiple Access
TMPC	Transposed Modified Prime Code
UCMPC	Uniform Cross-Correlation Modified Prime Code
UHD	Ultra High Definition
UPMPC	Unit-Padded Modified Prime Code
WDMA	Wavelength Division Multiple Access
WLAN	Wireless Local Area Networks
ZPMPC	Zero-Padded Modified Prime Code

Chapter 1

INTRODUCTION

This chapter provides a brief introduction for this research, as well as current challenges and motivations in this research area. Furthermore, in this chapter aims and objectives of this research are illustrated, and the thesis organisation is explained.

1.1 Existing Challenges

To maintain the outstanding performance of the existing communications networks, it is necessary to invest in new network infrastructures, new communication schemes and the enhancement of the current resources. The future of the Internet requires a higher bit-rate and ultra-fast services, such as streaming over the internet protocol (IP) e.g. cloud drives, video-on-demand (VoD) and IPTV. Due to its tremendous resources of bandwidth and extremely low loss, fibre-optics can be the best physical transmission medium for telecommunications and computer networks [1].

In the last decade, the backbone of the UK and global telecommunications has been improved dramatically, according to this demand; however, the access networks could not match up with these changes. While the network operators provide the backbone bandwidth of 10 Gb/s by multiple high-capacity links, still the current super-fast fibre optic access networks can only support up to 152 Mb/s down-streaming for the end users. This technology is trying to bring the fibre as close as possible to the end user, and is divided into two main models (i) Fibre to the Cabinet (FTTC) and (ii) Fibre to the Home (FTTH), which are usually both implemented in the passive optical networks (PON) [2, 3]. Moreover, the current LTE (4G) access network can offer up to 12 Mb/s and 5Mb/s for download and upload, respectively. Therefore the access network is the critical weak point which limits the speed of communication [1, 4].

Accordingly, to get benefit of the backbone's high bandwidth, it is necessary to propose a revolutionary infrastructure, technique or method to mitigate this access network's limitation. Having this concept in mind, that any proposed scheme, system or network

should be able to be adapted for current subscribers, infrastructures and applications; the challenge is to design a new system with the highest compatibility and the lowest cost which can reduce the interferences and increase the performance and efficiency.

1.2 Research Motivations

One of the best solutions to tackle the issues mentioned in the previous section is the use of multiple access techniques, especially in high-speed and bursty traffics. This allows several simultaneous subscribers to share the existing resources (i.e. huge fibre's bandwidth). Multiple access techniques are divided into three main sections: (i) Wavelength Division Multiple Access (WDMA), which shares the frequencies; (ii) Time Division Multiple Access (TDMA), which shares the time slots and (iii) Code Division Multiple Access (CDMA), which shares both time and frequency among the subscribers.

Optical CDMA (OCDM) has potential to enhance the spectral efficiency and security. It is also suitable for asynchronous communications and has been exponentially investigated and implemented in the past few years [5-8], and would be the first candidate for the next generation of PON access networks [2, 9, 10].

On the other hand, beside all the outstanding characteristics of the OCDMA, Multiple Access Interference (MAI), which is introduced from other subscribers, is the OCDMA's weak point. This would decrease the network capacity and increase the BER [11-13]. As a result, realisation and development of a practical OCDMA network is still one of the hottest research areas.

This thesis demonstrates research directed towards the reduction of these interferences in the OCDMA networks, and it is believed that, with the backbone of the performed research in this area and its prospective possibilities for the future global networks, the continuation of this research to implementation level in the industry can bring an excellent, long-term and high quality contribution to the countries' economy and their people's quality of life.

1.3 Aims and Objectives

In this PhD research, the aims are as follows:

1) To propose a new CDMA code set to enhance the bit error rate and the overall system performance.
2) To reconfigure and extend the proposed code set into the new CDMA spreading code families.
3) To implement and examine the proposed new code set into the existing OCDMA systems with various advanced optical modulations.
4) To evaluate the proposed code set in established optical networks and IP transmissions.
5) To design and analyse a multi-user interference cancellation scheme in order to suppress the MUI effect in CDMA networks.
6) To design and examine an end to end network structure, based on the proposed MUI cancellation scheme and OCDMA prime code families.

7) To simulate and model an optical network unit in the laboratory; to obtain a realistic evaluation of the existing spreading codes including the proposed code set, in the presence of the implemented proposed MUI cancellation scheme.

Based on the mentioned aims, the following corresponding objectives are defined:

1) To provide a theoretical approach in the design process of the new spreading code set, in order to formulise and generalise the generation of the code set.
2) To develop new code sets, by modifying the existing code families.
3) To evaluate the new code's performance and behaviour in theory in the OCDMA networks implementing different modulations; to make sure that the Bit Error Rate (BER), security and correlation properties of the new code outperform the other codes.
4) To investigate the implementation of the proposed code in an IP transmission in OCDMA.
5) To design a new multi user cancellation scheme for asynchronous OCDMA transmission, to reduce the BER and improve the system's capacity.
6) To reconfigure existing transceivers and to propose a new architecture which implements the proposed MUI cancellation scheme.
7) To design, implement and examine the proposed code set and MUI cancellation scheme in practice and investigate the practical performance evaluation of the existing prime spreading code sets in a point to point optical network in the laboratory.

1.4 Software Packages used in this Research

In this research, most of the analyses have been performed using the MATLAB® package (code and Simulink) provided by MathWorks. Using this software gives the flexibility to analyse data, develop algorithms, model real structures and generate new applications used in this thesis. MATLAB was chosen because it is very fast in matrix operations and is the best choice for programming, numerical computations and visualisation.

In addition, the proposed architectures and modelled networks in this thesis are implemented in the evaluated version of OptiSystem, a product from the Optiwave package. This software has been used because it gives flexibility to design, evaluate and simulate optical links of modern optical networks in the transmission layer.

It should be mentioned that MATLAB has also been used in connection and implemented within OptiSystem, to add more flexibility to the proposed model and extend its abilities.

1.5 Thesis Structure

Following this chapter, Chapter 2 is dedicated to the literature review and to past studies performed on the Optical Code Division Multiple Access (OCDMA). This includes a brief introduction about OCDMA and its benefits. Moreover, this chapter reports on the previous research on the generations of the 1D orthogonal spreading code sets, including prime codes.

Chapter 3 introduces a new CDMA prime code, named as the Uniform Cross-Correlation Modified Prime Code (UC-MPC), which enhances the network's performance and security. In addition, in this chapter the construction process of this code set is explained in details. This includes the construction of a Novel Prime Code (NPC) and a Modified Novel Prime Code (M-NPC). Moreover, the correlation properties of this novel code set are examined and analysed in this chapter.

The performance analysis of UC-MPC is then analysed theoretically in Chapter 4 . In this chapter, the behaviour of UC-MPC is studied and compared with other prime code families in different schemes. These code sets are analysed in incoherent Pulse Position Modulation (PPM) systems with and without interference cancellation, and Manchester coding.

Chapter 5 is dedicated to the implementation of UC-MPC in the IP transmission and routing over the FSK-OCDMA scheme. This also covers an analytical evaluation of UC-MPC's performance in such a system. The comparison is then performed based on the network capacity, BER, security and the total number of simultaneous active users which can be accommodated in the system.

In Chapter 6 another new spreading prime code, named as the Transposed UCMPC (T-UCMPC) is proposed, which is the transposed version of the UC-MPC code set, introduced previously in Chapter 3 . In this chapter it has been shown that this code set also suppresses the BER and increases the capacity and security of the network, as compared with other prime spreading codes.

After proposing new code sets and evaluating them in different networks with different schemes, a new multi-user interference (MUI) cancellation scheme has been designed and implemented for the OCDMA systems in Chapter 7 . This chapter also contains the design process and implementation of this scheme. Moreover, this chapter shows that some prime code families, including the proposed codes, have been evaluated and compared with each other in this architecture.

Furthermore, an end-to-end network has been modelled in the laboratory to validate the analytical results. Chapter 8 includes this experimental setup. Also the observed performance results of a few prime code sets in a real network have been demonstrated in this chapter.

Finally, the conclusion of this research is explained in Chapter 9 . All the achievements and the outcomes of this research are summarised in this chapter. At the end, this chapter introduces some possible research topics, which are worthwhile to be investigated in the future.

1.6 Summary

This chapter was a quick introduction of this thesis, where the challenges, aims, objectives, software packages used and the thesis architecture have been discussed.

REFERENCES

[1] M. M. Karbassian, "Design and Analysis of Spreading Code and Transceiver architectures for Optical CDMA Networks," Birmingham, PhD Thesis, 2009.

[2] K. Ohara, A. Tagami, H. Tanaka, M. Suzuki, T. Miyaoka, T. Kodate, *et al.*, "Traffic analysis of Ethernet-PON in FTTH trial service," in *Optical Fiber Communication Conference*, p. ThAA2, 2003.

[3] K.-i. Kitayama, X. Wang, and N. Wada, "OCDMA over WDM PON—Solution path to gigabit-symmetric FTTH," *Journal of Lightwave Technology*, vol. 24, p. 1654, 2006.

[4] K. M. Sivalingam and S. Subramaniam, *Emerging optical network technologies: architectures, protocols and performance*: Springer, 2005.

[5] H. M. Shalaby, "Chip-level detection in optical code division multiple access," *Lightwave Technology, Journal of*, vol. 16, pp. 1077-1087, 1998.

[6] M. Azizoglu, J. A. Salehi, and Y. Li, "Optical CDMA via temporal codes," *Communications, IEEE Transactions on*, vol. 40, pp. 1162-1170, 1992.

[7] M. Kavehrad and D. Zaccarin, "Optical code-division-multiplexed systems based on spectral encoding of noncoherent sources," *Lightwave Technology, Journal of*, vol. 13, pp. 534-545, 1995.

[8] T. Ohtsuki, "Performance analysis of direct-detection optical CDMA systems with optical hard-limiter using equal-weight orthogonal signaling," *IEICE transactions on communications*, vol. 82, pp. 512-520, 1999.

[9] G. C. Gupta, M. Kashima, H. Iwamura, H. Tamai, T. Ushikubo, and T. Kamijoh, "A simple one-system solution COF-PON for metro/access networks," *Journal of Lightwave Technology*, vol. 25, pp. 193-200, 2007.

[10] B.-g. Ahn and Y. Park, "A symmetric-structure CDMA-PON system and its implementation," *Photonics Technology Letters, IEEE*, vol. 14, pp. 1381-1383, 2002.

[11] A. B. Cooper, J. B. Khurgin, S. Xu, and J. U. Kang, "High spectral efficiency phase diversity coherent optical CDMA with low MAI," in *Quantum Electronics and Laser Science Conference*, p. JTuA129, 2007.

[12] H. M. H. Shalaby, "Cochannel interference reduction in optical PPM-CDMA systems," *Communications, IEEE Transactions on*, vol. 46, pp. 799-805, 1998.

[13] C.-L. Lin and J. Wu, "Channel interference reduction using random Manchester codes for both synchronous and asynchronous fiber-optic CDMA systems," *Journal of lightwave technology*, vol. 18, p. 26, 2000.

Chapter 2

LITERATURE REVIEW

This chapter is an introduction to and a revision of all components mentioned in this research. Moreover, all the recent research performed in these fields is also covered, from which the nature of this research can be formed.

2.1 Optical Code Division Multiple Access

This research focuses on the Co-Channel Interference Reduction in Optical Code Division Multiple Access (OCDMA). The applications of Code Division Multiple Access (CDMA) techniques in optical networks have been studied intensively since the 1980s [1]. The OCDMA technique offers simultaneous access to the network using the same channel at the same time. This can be achieved by using orthogonal code sets in OCDMA systems. Subscribers' data are encoded with the unique code sequences in the transmitters and are mixed and sent to the destinations. Each receiver has its own unique code sequence and the received data can be separated and retrieved in the receivers [2-4].

Code-Division Multiple-Access (CDMA) technology was developed and deployed with great success in the second and third generation cellular systems and in the Long-Term Evolution (4G LTE) systems, as the major multiple access technology. It has many promising advantages, such as universal frequency reuse, soft hand-off and high spectrum efficiency. In addition, the interference-limited capacity of a CDMA system can effectively support multiplexing among multimedia traffic flows. These advantages make CDMA very promising for use as the air interface in the generic distributed network model. CDMA also is supported by the spread spectrum technology that is used in the current Wireless Local Area Networks (WLAN). The next-generations of networks are expected to have a simple infrastructure with distributed control.

There has been an increasing interest in utilizing code-division multiple-access (CDMA) techniques in fibre-optic local area networks (LAN's) in recent years. This is the result of the wide bandwidth and extra-high signal processing speed, offered by optical

components [5]. As a result, a larger number of simultaneous users can be accommodated with Optical CDMA (OCDMA), rather than radio frequency techniques.

Moreover, in comparison with dynamic allocation of bandwidth in Time Division Multiple Access (TDMA), OCDMA is more immune to the packet collisions and offers a better BER [6]. Also, in a high-traffic communication, OCDMA offers a larger tele-traffic capacity compared with the Wavelength Division Multiple Access (WDMA) [7].

Both synchronous and asynchronous techniques have been studied in the literature. In a synchronous technique, the possible number of subscribers and the number of simultaneous users –that can be accommodated for a given probability of error– are greater than with an asynchronous technique. However, synchronisation subsystems must be used in this technique [8, 9].

2.1.1 Synchronous OCDMA (S-OCDMA)

Synchronous OCDMA (S-OCDMA) systems perform much more efficiently in comparison with Asynchronous OCDMA (A-OCDMA) systems. In S-OCDMA systems, the correlation value of the incoming signal with the code sequence in the corresponding receiver at the output of the correlator is only investigated in the chip intervals. Therefore, the codes used in synchronous systems are defined by three factors: (N, w, R); where 'N' is the number of codes in the code set; 'w' is the code weight and 'R' is the correlation value. It should be mentioned that each code signature in the code set implemented in the synchronous OCDMA can be allocated to a subscriber. On the other hand these systems need a synchronisation unit and have more complexity.

2.1.2 Asynchronous OCDMA (A-OCDMA)

A-OCDMA systems can accommodate fewer subscribers in order to be able to offer acceptable BER and performance. Different code sets have different correlation properties, especially when they are implemented in asynchronous communications. Therefore, the asynchronous correlation properties of code sets in the asynchronous systems should be considered, in order to preserve the orthogonality of the code sequences.

To do so, it is necessary to either decrease the code weight or increase the frame length, to preserve the asynchronous cross-correlation of each of the two signatures at less than two. When the code length increases, both transmission time and system complexity increase consequently. Furthermore, when code weight decreases the signal power and its correlation properties (i.e. difference between auto-correlation and cross-correlation) degrade. However, therefore it is inevitable to discard the asynchronous communications.

2.2 Prime Codes

One approach to reduce the interferences and BER in the synchronous and asynchronous OCDMA systems is to design, propose and implement more efficient code sets in the network.

Over the last four decades, coding and its application to communication systems and networks have been studied in a vast amount of the literature. In the late 1970s, Prime Codes (PC) were first introduced, but due to the rapid development of optical and wireless technologies, serious work on the mathematical and application aspects of prime codes has featured on and off in journals over the last 20 years [1].

Various prime code families and their performance analysis in different OCDMA networks and communication systems have been studied, particularly original prime codes (PC) [1, 9], extended prime codes [1], modified prime codes (MPC) [9, 10], new MPC (nMPC) [9, 11], double-padded MPC (DPMPC) [8, 9], 2^n prime codes [1, 12] and generalized prime codes**.** Furthermore, performance analysis of most of these code families is investigated in On–Off Keying (OOK) and Pulse Position Modulation (PPM).

2.2.1 Prime Code (PC)

A prime code set is constructed based on the finite field arithmetic, also known as Galois Field (GF) [13, 14], and was first introduced in [15]. A finite field consists of p elements for a given prime number p, and is presented by $GF(p)=\{0, 1, 2, ..., p-1\}$. All the operations in this Galois field are performed in 'p' modulo arithmetic.

PC family is constructed over *GF(p)*, when p is a prime number. To do so, $S_i=(s_{i,0}, s_{i,1}, s_{i,2}, \ldots, s_{i,j}, \ldots, s_{i,p-1})$ prime sequence is generated by:

$$s_{i,j}(i,j,p) = i * j \pmod p \tag{2.1}$$

where i, j and $s_{i,j}$ belong to the Galois field of p. The overall code index in the code set, n, in the PC family is same as i.

Furthermore, to generate the binary code sequences $C_n=(c_{n,0}, c_{n,1}, c_{n,2}, \ldots, c_{n,k}, \ldots, c_{n,p^2-1})$ out of these prime sequences, each $c_{n,k}$, also named as a chip [4], is defined as:

$$c_{n,k}(i,j,p,k) = \begin{cases} 1, & k = s_{i,j} + j.p \\ 0, & others \end{cases} \tag{2.2}$$

Table 2.1 demonstrates both the prime sequence and binary code set for PC over $GF(p=5)$. As it can be seen, the number of codes in this code set (i.e. cardinality) and the number of ones in a code signature (code weight) are both $p=5$. Moreover, the code length is $p^2=25$.

The discrete correlation function of two code signatures C_n and C_{n_2} is defined as:

$$R_{C_{n_1}C_{n_2}}(m) = \sum_{k=0}^{L-1} c_{n_1,k}.c_{n_2,k+m} \tag{2.3}$$

where $c_{n,k} \in \{0,1\}$ is a periodic sequence with period L, $|m| \leq L-1$ and $L = p^2$ is the PC code length. All the correlation values calculated at the chip synchronization position (i.e. m=0), are named as in-phased or synchronised correlation (i.e. $R_{C_{n_1}C_{n_2}}(0)$).

Auto-Correlation (AC) and Cross-Correlation (CC) are also defined as:

$$R_{C_{n_1}C_{n_2}}(m) = \begin{cases} \text{Auto} - \text{Correlation}, & n_1 = n_2 \\ \text{Cross} - \text{Correlation}, & n_1 \neq n_2 \end{cases} \quad (2.4)$$

To ease the detection in the receivers, it is essential to implement the codes with higher auto-correlation and less cross-correlation (i.e. higher difference between AC and CC); so the receivers can easily distinguish between the codes. It should be mentioned that to have orthogonal codes, the maximum synchronised cross-correlation of prime codes should not exceed one.

TABLE 2.1
PRIME CODE (PC) OVER GF(P=5)

Index	S					C				
i and n	*j=0*	*j=1*	*j=2*	*j=3*	*j=4*	*j=0*	*j=1*	*j=2*	*j=3*	*j=4*
0	0	0	0	0	0	10000	10000	10000	10000	10000
1	0	1	2	3	4	10000	01000	00100	00010	00001
2	0	2	4	1	3	10000	00100	00001	01000	00010
3	0	3	1	4	2	10000	00010	01000	00001	00100
4	0	4	3	2	1	10000	00001	00010	00100	01000

The synched (i.e. $R_{C_{n_1}C_{n_2}}(0)$) and asynced (i.e. $R_{C_{n_1}C_{n_2}}$) auto and cross correlations of PC are introduced as [1]:

$$R_{C_{n_1}C_{n_2}}(0) = \begin{cases} p, & n_1 = n_2 \\ 1, & n_1 \neq n_2 \end{cases} \tag{2.5}$$

$$R_{C_{n_1}C_{n_2}} = \begin{cases} 0 - p, & n_1 = n_2 \\ 1 - 2, & n_1 \neq n_2 \end{cases} \tag{2.6}$$

2.2.2 Extended Prime Code (EPC)

The maximum cross-correlation value of PC can reach two. To reduce this value to one, a new prime code was introduced, named as the Extended Prime Code (EPC) [16]. Each subsequence of the prime code signatures is then zero-padded with p-1 zeros to achieve the binary code sequence *C* presented in Table 2.2.

TABLE 2.2
EXTENDED PRIME CODE (EPC) OVER GF(P=3)

Index	S			C		
i and n	*j=0*	*j=1*	*j=2*	*j=0*	*j=1*	*j=2*
0	0	0	0	10000	10000	10000
1	0	1	2	10000	01000	00100
2	0	2	1	10000	00100	01000

As it can be seen, like PC, the cardinality and the code weight are both *p=3*, whereas the code length is increased to $(2.p-1) \times p = 2.p^2 - p = 15$. Furthermore, synched and asynced auto and cross correlations of EPC are introduced, as in [1]:

$$R_{C_{n_1}C_{n_2}}(0) = \begin{cases} p, & n_1 = n_2 \\ 1, & n_1 \neq n_2 \end{cases} \quad (2.7)$$

$$R_{C_{n_1}C_{n_2}} = \begin{cases} 0-p, & n_1 = n_2 \\ 0-1, & n_1 \neq n_2 \end{cases} \quad (2.8)$$

2.2.3 Modified Prime Code (MPC)

Later, to increase the cardinality of the prime codes so that they can accommodate more users, the PC code set was modified and a Modified Prime Code (MPC) generated; which is also known as a Synchronised Prime Code. This code set is designed for high bandwidth optical networks implementing a multiple access technique [4, 15, 16].

TABLE 2.3
MODIFIED PRIME CODE (MPC) OVER GF(3)

Index			*S*			*C*		
i	*x*	*n*	*j=0*	*j=1*	*j=2*	*j=0*	*j=1*	*j=2*
0	0	0	0	0	0	100	100	100
	1	1	1	1	1	010	010	010
	2	2	2	2	2	001	001	001
1	0	3	0	1	2	100	010	001
	1	4	1	2	0	010	001	100
	2	5	2	0	1	001	100	010
2	0	6	0	2	1	100	001	010
	1	7	2	1	0	001	010	100
	2	8	1	0	2	010	100	001

To do this, each PC's spreading code is time-shifted for *p* times in each group [15]. Group numbers are shown as *i* in Table 2.3. In addition, *x* is the code index within the group, and *n* is the overall code index in the set.

The cardinality of this code set was increased to p^2, while the code weight and length remain as *p* and p^2, respectively.

Moreover, synched and asynced auto and cross correlations of MPC are as follows:

$$R_{C_{n_1}C_{n_2}}(0) = \begin{cases} p, & n_1 = n_2 \\ 0-1, & n_1 \neq n_2 \end{cases} \tag{2.9}$$

$$R_{C_{n_1}C_{n_2}} = \begin{cases} 0-p, & n_1 = n_2 \\ 0-p, & n_1 \neq n_2 \end{cases} \tag{2.10}$$

2.2.4 2^n Prime Code (2PC)

Correlation properties alone cannot be a good sole measure for the performance analysis of the code set. Another measure is the coding configuration [17]. This means the way encoders and decoders placed in the network affect the whole system in different ways [18]. In 1995, the 2^n Prime Code (2PC) was proposed, which is symmetric as are 2^n codes and meanwhile offers the algebraic properties of prime codes [18, 19].

Table 2.4 contains an example of 2^n prime code set, with 2^n=8 over *GF(11)*. With a slight change in Equation (2.2), the binary sequence of 2PC is defined as follows [1]:

$$C_{n,k} = \begin{cases} 1, & k = s_{i,j} + j.p \ and \ s_{i,j} \neq X \\ 0, & others \end{cases} \tag{2.11}$$

The code length, weight and cardinality in this code set are p^2, 2^n and p^2-2. Moreover, synched and asynced auto and cross correlations of 2PC are as follows:

$$R_{C_{n_1}C_{n_2}}(0) = \begin{cases} 2^n, & n_1 = n_2 \\ 0 - 1, & n_1 \neq n_2 \end{cases} \tag{2.12}$$

$$R_{C_{n_1}C_{n_2}} = \begin{cases} 0 - 2^n, & n_1 = n_2 \\ 0 - 2, & n_1 \neq n_2 \end{cases} \tag{2.13}$$

TABLE 2.4
2^N PRIME CODE (2PC) WITH 2^N=8 OVER GF(P=11) [1]

i or n	S_i										
0	X	X	0	0	0	0	0	0	0	0	X
1	X	X	2	3	4	5	6	7	8	9	X
2	X	X	4	6	8	10	1	3	5	7	X
3	X	X	6	9	1	4	7	10	2	5	X
4											
5	X	X	10	4	9	3	8	2	7	1	X
6	X	X	1	7	2	8	3	9	4	10	X
7											
8	X	X	5	2	10	7	4	1	9	6	X
9	X	X	7	5	3	1	10	8	6	4	X
10	X	X	9	8	7	6	5	4	3	2	X

2.2.5 Generalised Prime Code (GPC)

Prime Code (PC) offers a limited cardinality (i.e. $N=p$) for the code length $L=p^2$. It means that to accommodate a higher number of users (N), PC's code length increases

dramatically (i.e. $L = N^2$). This would require higher bandwidth and increases the complexity of the hardware.

To overcome this problem, Generalised Prime Code (GPC) was proposed (Table 2.5), to improve the code's cardinality without ruining the correlation property [1]. This code set offers cardinality of $N=p^k$, code weight of $w=p$ and length of $L=p^{k+1}$ (i.e. $L = N \times p$).

The synched (i.e. $R_{C_{n_1}C_{n_2}}(0)$) and asynced (i.e. $R_{C_{n_1}C_{n_2}}$) auto and cross correlations of GPC are introduced as [20]:

$$R_{C_{n_1}C_{n_2}}(0) = \begin{cases} p, & n_1 = n_2 \\ 1, & n_1 \neq n_2 \end{cases} \tag{2.14}$$

$$R_{C_{n_1}C_{n_2}} = \begin{cases} 0-p, & n_1 = n_2 \\ 0-2, & n_1 \neq n_2 \end{cases} \tag{2.15}$$

TABLE 2.5
GENERALISED PRIME CODE (GPC) WITH K=2 OVER GF(P=3)

i_1	i_2	n	S_{i_1,i_2}			C		
0	0	0	0	0	0	100000000	100000000	100000000
1	0	1	0	1	2	100000000	010000000	001000000
2	0	2	0	2	1	100000000	001000000	010000000
0	1	3	0	3	6	100000000	000100000	000000100
1	1	4	0	4	8	100000000	000010000	000000001
2	1	5	0	5	7	100000000	000001000	000000010
0	2	6	0	6	3	100000000	000000100	000100000
1	2	7	0	7	5	100000000	000000010	000001000
2	2	8	0	8	4	100000000	000000001	000010000

2.2.6 New MPC (nMPC)

It has been proved than increasing the code weight improves the correlation properties and BER. Also increasing the code length enhances the security of the communication.

In 2005 a new code set was introduced by Liu, F and Ghafouri-Shiraz, H in [21], based on the modified prime code (MPC), and named as the New Modified Prime Code (nMPC). The last subsequence of MPC is trailed at the end of the next code signature within the same group. It should be mentioned that this shift within the group is rotational [9].

It should also be noted that increasing the cross-correlation is the main drawback of this code, which can increase the BER.

Table 2.6 illustrates an example of nMPC code set over *GF(3)*. The inserted sub sequences are bolded in the table. The code weight and the code length are increased to *p+1* and p^2+p, respectively. Moreover the cardinality of this code is p^2. Furthermore, the synched and asynced auto and cross correlations of nMPC are introduced as:

$$R_{C_{n_1}C_{n_2}}(0) = \begin{cases} p+1, & n_1 = n_2 \\ 0-2, & n_1 \neq n_2 \end{cases} \tag{2.16}$$

$$R_{C_{n_1}C_{n_2}} = \begin{cases} 0-(p+1), & n_1 = n_2 \\ 0-(p+1), & n_1 \neq n_2 \end{cases} \tag{2.17}$$

It should be pointed out that increasing the cross-correlation is the main drawback of this code, which can increase the BER.

TABLE 2.6
NEW MODIFIED PRIME CODE (NMPC) OVER GF(P=3)

Index			*S*				*C*			
i	*x*	*n*	*j=0*	*j=1*	*j=2*	***j=3***	*j=0*	*j=1*	*j=2*	***j=3***
0	0	0	0	0	0	**2**	100	100	100	**001**
	1	1	1	1	1	**0**	010	010	010	**100**
	2	2	2	2	2	**1**	001	001	001	**010**
1	0	3	0	1	2	**1**	100	010	001	**010**
	1	4	1	2	0	**2**	010	001	100	**001**
	2	5	2	0	1	**0**	001	100	010	**100**
2	0	6	0	2	1	**2**	100	001	010	**001**
	1	7	2	1	0	**1**	001	010	100	**010**
	2	8	1	0	2	**0**	010	100	001	**100**

2.2.7 Double Padded MPC (DPMPC)

In 2007, Karbassian, M. M. and Ghafouri-Shiraz, H. in [8] expanded the idea used in nMPC and proposed Double Padded MPC (DPMPC). An example of this code set over *GF(p=3)* is illustrated in Table 2.7. DPMPC is constructed in the same way as nMPC; the only difference is an extra subsequence which is the same as the last subsequence of MPC (i.e. *j=3* in Table 2.7), which is inserted before the last subsequence of nMPC (i.e. *j=4* in Table 2.7).

The injected subsequence contains another '1' bit, which increases the code weight. The idea was to increase the code weight to enhance the BER. Also, increasing the code length improves the security.

TABLE 2.7
DOUBLE PADDED MODIFIED PRIME CODE (DPMPC) OVER GF(P=3)

Index			*S*					*C*				
i	*x*	*n*	*j=0*	*j=1*	*j=2*	***j=3***	***j=4***	*j=0*	*j=1*	*j=2*	***j=3***	***j=4***
0	0	0	0	0	0	**0**	**2**	100	100	100	**100**	**001**
	1	1	1	1	1	**1**	**0**	010	010	010	**010**	**100**
	2	2	2	2	2	**2**	**1**	001	001	001	**001**	**010**
1	0	3	0	1	2	**2**	**1**	100	010	001	**001**	**010**
	1	4	1	2	0	**0**	**2**	010	001	100	**100**	**001**
	2	5	2	0	1	**1**	**0**	001	100	010	**010**	**100**
2	0	6	0	2	1	**1**	**2**	100	001	010	**010**	**001**
	1	7	2	1	0	**0**	**1**	001	010	100	**100**	**010**
	2	8	1	0	2	**2**	**0**	010	100	001	**001**	**100**

The code weight and the code length are increased to $p+2$ and p^2+2p, respectively. Furthermore, the cardinality of this code is p^2. The synched and asynced auto and cross correlations of DPMPC are introduced as:

$$R_{C_{n_1}C_{n_2}}(0) = \begin{cases} p+2, & n_1 = n_2 \\ 0-3, & n_1 \neq n_2 \end{cases} \tag{2.18}$$

$$R_{C_{n_1}C_{n_2}} = \begin{cases} 0-(p+2), & n_1 = n_2 \\ 0-(p+2), & n_1 \neq n_2 \end{cases} \tag{2.19}$$

Increasing the cross-correlation and system complexity are two main drawbacks of this code set.

2.2.8 Full Padded Modified Prime Codes (FPMPC)

The full Padded Modified Prime Code (FPMPC) was proposed in 2010, as the ultimate solution for the idea used in the construction of nMPC and DPMPC [22]. It means that '*p*' sub-sequences were appended to the end of MPC, to maximize the code weight with the highest possible number of shifted MPC sub-sequences. The first *p-1* sub-sequences are the shifted version of the last MPC sub-sequences within each group. The last subsequence is the group index (i.e. '*i*') in the code set. Table 2.8 shows an example of FPMPC over *GF(p=3)*.

TABLE 2.8
FULL PADDED MODIFIED PRIME CODE (FPMPC) OVER GF(P=3)

Index			S						C					
i	*x*	*n*	*j=0*	*j=1*	*j=2*	***j=3***	***j=4***	***j=5***	*j=0*	*j=1*	*j=2*	***j=3***	***j=4***	***j=5***
0	0	0	0	0	0	**2**	**0**	**0**	100	100	100	**001**	**010**	**100**
	1	1	1	1	1	**0**	**1**	**0**	010	010	010	**100**	**001**	**100**
	2	2	2	2	2	**1**	**2**	**0**	001	001	001	**010**	**100**	**100**
1	0	3	0	1	2	**1**	**2**	**1**	100	010	001	**010**	**100**	**010**
	1	4	1	2	0	**2**	**0**	**1**	010	001	100	**001**	**010**	**010**
	2	5	2	0	1	**0**	**1**	**1**	001	100	010	**100**	**001**	**010**
2	0	6	0	2	1	**2**	**1**	**2**	100	001	010	**001**	**100**	**001**
	1	7	2	1	0	**1**	**0**	**2**	001	010	100	**010**	**001**	**001**
	2	8	1	0	2	**0**	**2**	**2**	010	100	001	**100**	**010**	**001**

In FPMPC, the code weight is *2p*, the code length is $2p^2$ and its cardinality is p^2. Furthermore, the synched and asynced auto and cross correlations of FPMPC are given as:

$$R_{C_{n_1}C_{n_2}}(0) = \begin{cases} 2p, & n_1 = n_2 \\ 1-2, & n_1 \neq n_2 \end{cases} \quad (2.20)$$

$$R_{C_{n_1}C_{n_2}} = \begin{cases} 0-2p, & n_1 = n_2 \\ 0-(2p-1), & n_1 \neq n_2 \end{cases} \quad (2.21)$$

Again, high code length and cross-correlation are the drawbacks of this code set. On the other hand, the large difference between auto-correlation and cross-correlation values, besides the high code weight, is the benefit of FPMPC.

2.2.9 Transposed Modified Prime Codes (TMPC)

With a novel idea in [22], Transposed Modified Prime Codes (TMPC) were constructed from FPMPC in 2010. This code set is the transposed version of FPMPC's binary code sequences. Table 2.9 shows an example of binary code sequences of TMPC over *GF(p=3)*.

The code weight is p, the code length is p^2 and its cardinality is $2p^2$. Furthermore, the synched and asynced auto and cross correlations of FPMPC are given as:

$$R_{C_{n_1}C_{n_2}}(0) = \begin{cases} p, & n_1 = n_2 \\ 0-2, & n_1 \neq n_2 \end{cases} \quad (2.22)$$

$$R_{C_{n_1}C_{n_2}} = \begin{cases} 0-p, & n_1 = n_2 \\ 0-p, & n_1 \neq n_2 \end{cases} \quad (2.23)$$

The strong point of this code is its cardinality. This code can accommodate $2p^2$ simultaneous users. The drawback is its correlation property. The cross-correlation is increased in comparison with MPC, while the auto-correlation remains unchanged.

TABLE 2.9
TRANSPOSED MODIFIED PRIME CODE (TMPC) OVER GF(P=3)

Index			C		
i	*x*	*n*	*j=0*	*j=1*	*j=2*
0	0	0	100	100	100
	1	1	010	010	001
	2	2	001	001	010
1	0	3	100	001	001
	1	4	010	100	010
	2	5	001	010	100
2	0	6	100	010	010
	1	7	010	001	100
	2	8	001	100	001
3	0	9	010	001	001
	1	10	001	100	010
	2	11	100	010	100
4	0	12	001	100	100
	1	13	100	010	001
	2	14	010	001	010
5	0	15	111	000	000
	1	16	000	111	000
	2	17	000	000	111

2.3 Performance Analysis of Prime Codes

According to the discussion in the previous section, introducing a new code set can potentially enhance the performance of a system. To obtain a realistic figure of any new code set, it is essential to implement and evaluate it in various OCDMA networks in order to assess its performance and assay its characteristics. Moreover the efficiency of this proposed code set should be compared with other existing codes in various systems with different modulations. The prime codes mentioned in Section 2.2 have been implemented and evaluated in different OCDMA systems with various modulations in previous research studies.

The fundamental principles and performance analysis of CDMA techniques in optical fibre networks were discussed by Salehi, J. A. in 1989 in [23] and [24]. Also in 1995 Shalaby, M. H. investigated direct-detection optical synchronous CDMA systems with M-array Pulse Position Modulation (PPM) signalling in [25]. Then in 1997, a new code was proposed and evaluated from the original 2^n modified prime code to increase the number of simultaneous subscribers and decrease the code weight and length, by Zhang, J. et al [12].

Later in 1998, Shalaby proposed a multi-user interference reduction technique for optical code-division multiple-access systems in [5]. In this method data symbols from each user are encoded using a PPM scheme before multiplexing. Two years later, Zhang, J. et al in 2000 investigated the cross-correlation and system performance of modified prime codes for all-optical CDMA applications in [26].

The next relevant research project was interference reduction via a cancellation scheme for synchronous optical CDMA systems, which was discussed in 2001 [27]. Authors, Liu, M. et al, also included thermal noise, Avalanche Photo-Diode (APD) noise and interference in their analysis.

Furthermore, a deep insight into the behaviour of OCDMA systems, based on an incoherent, intensity encoding/decoding technique and using a well-known class of codes, namely Optical Orthogonal Codes (OOC), was presented in [28] by Mashhadi S. and Salehi, J. A. in 2006.

Since 2007, the optics team in the School of Electronic, Electrical and Computer Engineering at the University of Birmingham focused on the prime code families and their performance analysis. In 2007 Lui F., Karbassian M. M. and Ghafouri-Shiraz H. proposed a new family of prime codes, named as NPC; also they evaluated their performance in synchronous optical CDMA networks in [11].

In 2007 Karbassian, M. M. and Ghafouri-Shiraz, H. in [8] proposed a new prime spreading sequence, named DPMPC. This code was applied to both Pulse-Position Modulation (PPM) and Overlapping Pulse-Position Modulation (OPPM) code-division multiple-access networks; and their performances were evaluated and compared with existing prime code families. This code set has also been evaluated in Binary Phase Shift Keying (BPSK) modulation in [29].

Finally in 2010, FPMPC and TMPC were proposed and implemented in an on-off keying (OOK) OCDMA system in [22].

2.4 IP Transmission and Routing

As mentioned previously, many multimedia applications are now implemented on new Internet Protocol (IP) [30]. This demand has especially increased dramatically in the last few years because of the advent of many new technologies and concepts such as 4K resolution Ultra-High Definition (UHD), IPTV, Internet of Things (IoT), Machine to Machine (M2M) and Smart Cities.

All of these technologies require high-speed internet-based networks which rely on optical communications. Moreover all the new protocols, such as Weightless, which is heavily used in M2M, like many other well-developed protocols, are based on IP.

Figure 2.1 Internet of Things (IoT)

As a result, having an exponential growth in demanding wearable and Mobiles as Sensor (MaS) technologies, which implement the mentioned technologies and applications supporting various multimedia, the ongoing research on IP routing over OCDMA networks, as the main backbone of these infrastructures, has heavily increased.

One of the existing challenges is the processing speed of the network layer's components, which operate electrically. This speed cannot match the bandwidth which optical fibre offers. Raddo, T. R et al in 2011 proposed a solution to tackle this issue in a multi-rate and multi-class Optical Packet Switch (OPS) [31].

Optical Code Division Multiple Access (OCDMA) supports asynchronous traffic in the network, and Differentiated Services (DiffServ) and Quality of Service (QoS) in the physical layer. Furthermore, the cardinality of the system (i.e. the maximum number of simultaneous users accommodated in the network) can be easily increased in OCDMA [32, 33]. Therefore, in the past few years much research has focused on and converged towards the OCDMA approach.

In addition, since 2009, Karbassian and Ghafouri-Shiraz have carried out deep research in this area and implemented and evaluated prime code signatures in IP routing in coherent OCDMA networks [33-35].

2.5 Multi User Interference Reduction

By implementing a Passive Optical Network (PON) in an OCDMA network (i.e. OCDMA-PON) it is possible to share the network's infrastructure among multiple simultaneous users, both synchronously and asynchronously. This multiple access causes interferences which reduce the network's capacity significantly [36, 37]. Moreover, because the unipolar code sets are quasi orthogonal, these multi user interferences can deteriorate their performance dramatically [38].

In addition to the new code sets which can enhance the network's performance, one of the most efficient ways to reduce the co-channel interference in the system is to reduce or eliminate the interferences caused by multiple accesses in the network, named as Multi User Interference (MUI) or Multi Access Interference (MAI) (Figure 2.1). This requires modification of the existing networks' infrastructures, or the design and proposeal of a new scheme to do so.

There is ongoing research which is heavily focused on proposing MUI cancellation schemes and units to mitigate this problem in CDMA/OCDMA networks; some of them are in [38-42].

As an example of one of the most recent research projects, in March 2014 Seleem, H. et al in [43] proposed an Interference Cancellation (IC) detector, which is more efficient in comparison with other correlation receivers. In addition it is claimed that this detector is more efficient than linear minimum mean-square error detectors.

Therefore, to enhance the performance of the uplink, it is essential to design a cheap and low-complex MUI canceller, which is able to extract and retrieve the emitted signals - coming from the plurality of transmitters- from the noises and interferences introduced by the network [44].

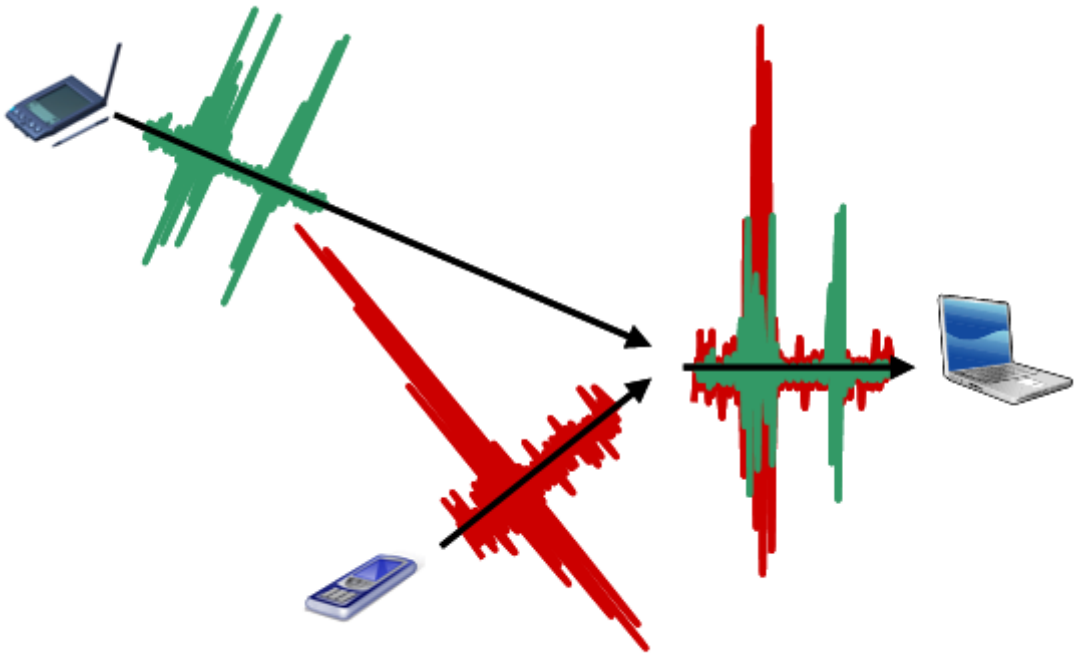

.

Figure 2.2 Multi User Interference (MUI) in CDMA networks

2.6 Experimental setup of an OCDMA Network

In the previous sections of this chapter, various methods of co-channel interference reduction and enhancement of the performance of OCDMA networks were discussed. However, all of these approaches and methods can only truly be validated when implemented and evaluated in simulation, and also in a laboratory-based OCDMA test bed, a test bed which can accommodate multiple simultaneous subscribers and different code signatures, in a node to node OCDMA network.

To utilise these reduction means and methods in the commercial OCDMA systems, the following questions should be answered:

- Does optical code division multiple access offer better performance, compared with other multiple access methods? [45]
- How do the optical orthogonal codes perform in different OCDMA networks?
- How do the multi access interference reduction schemes perform in a real network, and what are their limitations?

Many OCDMA simulations and experimental setups have been implemented and tested previously and also recently; this has been especially to address the mentioned questions and to evaluate the designed optical elements implemented in the physical layer of OCDMA networks. Some of this research includes: investigation of coherent OCDMA's advances [45]; comparison of different code performances in a hybrid 40G OCDMA-PON network [46]; demonstration of 10 G/s transmission over 100km WDM-TDM-

OCDMA-PON [47]; experimental simulation and implementations of coherent OCDMA with heterodyne detection [48] and elastic packet routing in OCDMA [49].

In a close approach to this research, recently in 2013, Idris, S. et al from the University of Strathclyde, proposed an MAI reduction apparatus for OCDMA networks, which included a new incoherent receiver operating at 2.5 Gb/s data rate [50]. This innovation implements a self-synchronisation scheme, using an all-optical clock recovery unit to minimise the unwanted cross-correlations (i.e. MAI). The authors have then developed this receiver and implemented and tested it in a multi-user OCDMA laboratory test bed [49].

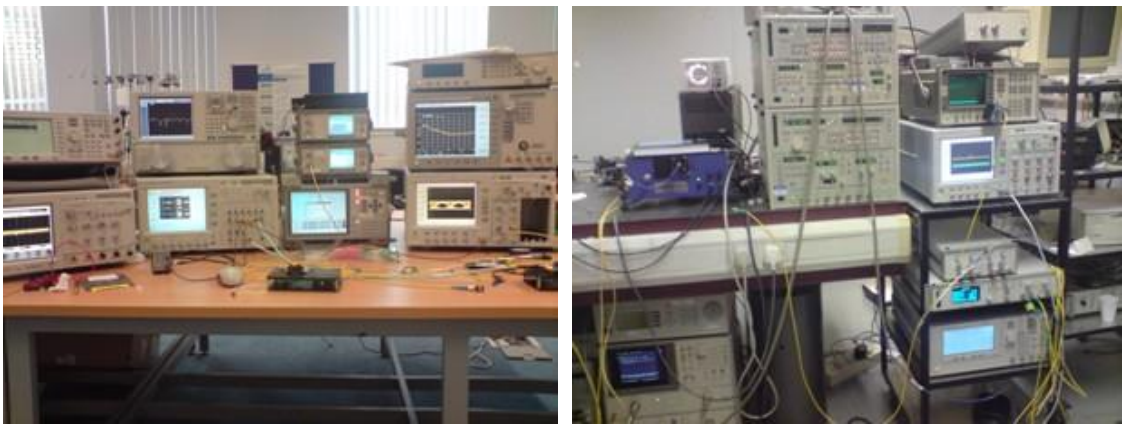

(a) (b)

Figure 2.3 Node to node laboratory based OCDMA test bed
(a) University of Strathclyde, (b) University of Glasgow

2.7 Review of Literature on Co-channel Interference Reduction in OCDMA

An overview of the fundamental OCDMA topics, which were heavily used in this research, was discussed briefly. This included a short review on OCDMA, introducing prime code families and their performance analysis in various OCDMA networks; IP transmission; multi user interference reduction techniques and finally OCDMA experimental test beds.

Although the accelerating trend of interest in OCDMA has resulted in an extensive research history in the past few years, which is noticeably outstanding, there are still many gaps in order to improve the performance of OCDMA systems and mitigate its considerable drawback of multi access interference.

2.7.1 Proposing High Performance Orthogonal Code Sets

Table 2.10 compares all the conventional prime code families together in terms of their characteristics, which are code weight, length, cardinality, and their synchronised and asynchronised correlation properties.

The strong points and drawbacks of each code set have been discussed in previous sections in detail. All of these code sets perform very well, but the common main drawback is the high cross-correlation value. To enhance the performance, mainly the code weight is increased; where extra bits (i.e. sub-sequences) are padded into the existing prime codes. These sub-sequences are the shifted version of existing sub-sequences in the

code signature; and each conventional prime code set has the ultimate possible shifts within the groups. The added sub-sequences are repetitive, duplicated and introduce more collision; subsequently they increase the cross-correlation. Some examples are [8, 21, 22].

In the Chapter 3 it will be shown that the code weight can be increased to generate a new code set, while the correlation properties are also improved. Also in Chapter 6 another new code set is introduced and evaluated, based on the proposed code in Chapter 3 .

TABLE 2.10
PRIME CODE SETS PROPERTIES

Prime Codes	PC	EPC	MPC	2PC	GPC	nMPC	DPMPC	FPMPC	TMPC
Weight	p	p	p	2^n	p	$p+1$	$p+2$	$2p$	p
Length	p^2	$2.p^2 - p$	p^2	p^2	p^{k+1}	$p^2 + p$	$p^2 + 2p$	$2p^2$	p^2
Cardinality	p	p	p^2	p^2-2	p^k	p^2	p^2	p^2	$2p^2$
Synced Auto-Correlation	p	p	p	2^n	p	$p+1$	$p+3$	$2p$	p
Synced Cross-Correlation	1	1	0-1	0-1	1	0-2	0-3	1-2	0-2
Asynced Auto-Correlation	0-p	0-p	0-p	0-2^n	0-p	0-$(p+1)$	0-$(p+2)$	0-$2p$	0-p
Asynced Cross-Correlation	0-2	0-1	0-p	0-2	0-2	0-$(p+1)$	0-$(p+2)$	0-$(2p-1)$	0-p

Therefore the remaining challenge in this area is to produce new and efficient orthogonal code families that can be implemented in the optical communications systems, along with the performance analysis of these codes which has been carried out in Chapter 4 .

2.7.2 Enhancing IP Transmission in OCDMA

As it has been mentioned previously, it is known that there is an exponentially increasing demand for IP-based multimedia and communication services. Also it was discussed that optical CDMA can be a great backbone for IP transmission.

The challenge is to have faster, more secure, and more power-efficient transmission, which can accommodate a greater number of users. A lot of effort has been put into place to investigate the best approaches to tackle this challenge [30, 32-35]. However, even if changing the infrastructure and modifying the physical layer is practical, then this operation is too costly. Therefore, one of the approaches to enhance the performance of IP based networks is to implement a new code set in the system, which enhances the transmission.

In Chapter 5 , the new code set proposed in Chapter 3 is implemented and analysed in an IP based Optical Network Unit (ONU) operating over Frequency Shift Keying (FSK) modulation. The results are promising, and the proposed network delivers an outstanding performance.

2.7.3 Revolutionary MUI Canceller Scheme

As discussed previously, there has been a lot of progress towards the implementation of multi user interference reduction schemes and apparatuses; but there are still a few main weak points in the previously-proposed designs. Their high-complexity is the main disadvantage of these techniques, which will result in costly designs and commercial implementation. Moreover, high speed and powerful computational units are needed to implement these techniques.

Furthermore, in some cases some of these techniques require detailed information about the channel and network. This includes characteristics such as delays, attenuations and phases between each transceiver [51-53]. In addition, it is difficult to obtain this information about the channel, and it requires lots of bandwidth [42].

Some of these proposed MUI cancellation techniques are almost impractical, due to these disadvantages. Also, if it is possible to implement them, they are able to accommodate only a small number of subscribers simultaneously [54, 55].

In Chapter 7 , a new multi user interference canceller scheme is proposed, designed and implemented, which is not only low-complexity, low-cost and channel-independent, but also eliminates the MUI interference totally (i.e. 100%) in a noise-free situation.

2.7.4 Down Streaming the Ongoing Research into the Commercial Implementations

Ideally, the result of each single piece of research is intended to be directly reflected in real-life implementation. As the first step of this procedure, the mediation stage between pure academic research and its commercial implementation is to simulate and test it as a prototype.

Therefore it was essential for this research to design and implement a laboratory-based test bed for an end to end OCDMA network. As mentioned previously, many practical implementations have been performed previously (e.g. [46, 47, 50]). However the capability of each laboratory is firstly limited to its equipment. The point is that this experiment was an essential step for this research in order to evaluate and verify the performance of the proposed code sets and the MUI canceller technique in reality. With limited equipment, the most advanced techniques are designed and implemented in Chapter 8 , which gives the flexibility to test the whole idea of this thesis with all of its components, fully and all together.

REFERENCES

[1] G. C. Yang and W. C. Kwong, *Prime codes with applications to CDMA optical and wireless networks*: Artech House Publishers, 2002.

[2] J. A. Salehi, "Code division multiple-access techniques in optical fiber networks," *Communications, IEEE Transactions on,* vol. 37, pp. 824-833, 1989.

[3] J. A. Salehi and C. A. Brackett, "Code division multiple-access techniques in optical fiber networks. II. Systems performance analysis," *Communications, IEEE Transactions on,* vol. 37, pp. 834-842, 1989.

[4] P. Prucnal, M. Santoro, and F. Ting, "Spread spectrum fiber-optic local area network using optical processing," *Lightwave Technology, Journal of,* vol. 4, pp. 547-554, 1986.

[5] H. M. H. Shalaby, "Cochannel interference reduction in optical PPM-CDMA systems," *Communications, IEEE Transactions on,* vol. 46, pp. 799-805, 1998.

[6] N. G. Tarhuni, T. O. Korhonen, E. Mutafungwa, and M. S. Elmusrati, "Multiclass optical orthogonal codes for multiservice optical CDMA networks," *Lightwave Technology, Journal of,* vol. 24, pp. 694-704, 2006.

[7] S. Goldberg and P. R. Prucnal, "On the Teletraffic Capacity of Optical CDMA," *Communications, IEEE Transactions on,* vol. 55, pp. 1334-1343, 2007.

[8] M. M. Karbassian and H. Ghafouri-Shiraz, "Fresh Prime Codes Evaluation for Synchronous PPM and OPPM Signaling for Optical CDMA Networks," *Lightwave Technology, Journal of,* vol. 25, pp. 1422-1430, 2007.

[9] M. M. Karbassian, "Design and analysis of spreading code and transceiver architectures for optical CDMA networks," University of Birmingham, 2009.

[10] G.-C. Yang and W. C. Kwong, "Performance Analysis of Extended Carrier-Hopping Prime Codes for Optical CDMA," *IEEE Transactions on Communications,* vol. 53, pp. 876-881, May 2005.

[11] F. Lui, M. M. Karbasian, and H. Ghafouri-Shiraz, "Novel Family of Prime Codes for Synchronous Optical CDMA," *Optical and Quantum Electronics,* vol. 39, pp. 79-90, January 2007.

[12] J.-G. Zhang, W. C. Kwong, and A. B. Sharma, "2n Modified Prime Codes for Use in Fiber Optic CDMA Networks," *Electronics Letters,* vol. 33, pp. 1840-1841, October 1997.

[13] R. E. Blahut, *Theory and practice of error control codes*: Addison-Wesley, 1983.

[14] S. Lin and D. J. Costello, "Error Control Coding—Fundamentals and Applications, Vol. 1 of Computer Applications in Electrical Engineering Series," ed: Prentice–Hall, Englewood Cliffs, New Jersey, 1983.

[15] W. C. Kwong, P. A. Perrier, and P. R. Prucnal, "Performance comparison of asynchronous and synchronous code-division multiple-access techniques for

fiber-optic local area networks," *Communications, IEEE Transactions on,* vol. 39, pp. 1625-1634, 1991.

[16] G.-C. Yang and W. C. Kwong, "Performance analysis of optical CDMA with prime codes," *Electronics Letters,* vol. 31, pp. 569-570, 1995.

[17] Z. Jian-Guo, W. C. Kwong, and A. B. Sharma, "2n modified prime codes for use in fibre optic CDMA networks," *Electronics Letters,* vol. 33, pp. 1840-1841, 1997.

[18] W. C. Kwong, G.-C. Yang, and J.-G. Zhang, "2 n prime-sequence codes and coding architecture for optical code-division multiple-access," *Communications, IEEE Transactions on,* vol. 44, pp. 1152-1162, 1996.

[19] W. Kwong and G. Yang, "Construction of 2n prime-sequence codes for optical code division multiple access," *IEE Proceedings-Communications,* vol. 142, pp. 141-150, 1995.

[20] A. Shaar and P. Davies, "Prime sequences: quasi-optimal sequences for OR channel code division multiplexing," *Electronics Letters,* vol. 19, pp. 888-890, 1983.

[21] F. Liu and H. Ghafouri-Shiraz, "Analysis of PPM-CDMA and OPPM-CDMA communication systems with new optical code," in *Asia-Pacific Optical Communications*, pp. 602137-602137-9, 2005.

[22] M. M. Karbassian and F. Kueppers, "Synchronous Optical CDMA Networks Capacity Increase Using Transposed Modified Prime Codes," *Lightwave Technology, Journal of,* vol. 28, pp. 2603-2610, 2010.

[23] J. A. Salehi, "Code Division Multiple Access Techniques in Optical Fiber Networks - Part I : Fundamental Principles," *IEEE Transactions on Communications,* vol. 37, pp. 824-833, August 1989.

[24] J. A. Salehi and C. A. Brackett, "Code Division Multiple Access Techniques in Optical Fiber Networks - Part II : System Performance Analysis," *IEEE Transactions on Communications,* vol. 37, pp. 834-842, August 1989.

[25] H. M. H. Shalaby, "Performance analysis of optical synchronous CDMA communication systems with PPM signaling," *Communications, IEEE Transactions on,* vol. 43, pp. 624-634, 1995.

[26] J.-G. Zhang, A. B. Sharma, and W. C. Kwong, "Letter to the Editor - Cross-correlatin and System Performance of Modified Prime Codes for All-Optical CDMA Applications," *Journal of Optics A: Pure and Applied Optics,* vol. 2, pp. L25-L29, September 2000.

[27] M.-Y. Liu and H.-W. Tsao, "Reduction of Multiple-Access Interference for Optical CDMA Systems," *Microwave and Optical Technology Letters,* vol. 30, pp. 1-3, July 2001.

[28] S. Mashhadi and J. A. Salehi, "Code Division Multiple Access Techniques in Optical Fiber Networks - Part III : Optical and Logic Gate Receiver Structure with Generalized Optical Orthogonal Codes," *IEEE Transactions on Communications*, vol. 54, p. 14571468, August 2006.

[29] M. M. Karbassian, F. Liu, and H. Ghafouri-Shiraz, "Performance Analysis of Novel Prime Code Family in Coherent Optical CDMA Network," in *Communications and Networking in China, 2007. CHINACOM '07. Second International Conference on*, pp. 393-396, 2007.

[30] T. R. Raddo, A. L. Sanches, J. V. dos Reis, and B. H. V. Borges, "Multiservice, multirate IP transmission over OCDMA network," in *Transparent Optical Networks (ICTON), 2013 15th International Conference on*, pp. 1-4, 2013.

[31] T. R. Raddo, A. L. Sanches, J. V. dos Reis, and B. V. Borges, "Performance evaluation of a multirate, multiclass OCDM/WDM optical packet switch," in *Microwave & Optoelectronics Conference (IMOC), 2011 SBMO/IEEE MTT-S International*, pp. 824-828, 2011.

[32] T. R. Raddo, A. L. Sanches, J. V. dos Reis, and B. V. Borges, "A New Approach for Evaluating the BER of a Multirate, Multiclass OFFH-CDMA System," *Communications Letters, IEEE*, vol. 16, pp. 259-261, 2012.

[33] M. M. Karbassian and H. Ghafouri-Shiraz, "IP Routing and Transmission Analysis in Optical CDMA Networks: Coherent Modulation With Incoherent Demodulation," *Lightwave Technology, Journal of*, vol. 27, pp. 3845-3852, 2009.

[34] H. Ghafouri‐Shiraz and M. M. Karbassian, "Optical CDMA Networking," *Optical CDMA Networks: Principles, Analysis and Applications*, pp. 281-346.

[35] M. M. Karbassian and H. Ghafouri-Shiraz, "IP Routing and Traffic Analysis in Coherent Optical CDMA Networks," *Lightwave Technology, Journal of*, vol. 27, pp. 1262-1268, 2009.

[36] E. Wong, "Next-Generation Broadband Access Networks and Technologies," *Lightwave Technology, Journal of*, vol. 30, pp. 597-608, 2012.

[37] S. Yoshima, N. Nakagawa, J. Nakagawa, and K. Kitayama, "10G-TDM-OCDMA-PON systems," in *OptoeElectronics and Communications Conference (OECC), 2010 15th*, pp. 724-725, 2010.

[38] A. O. m'foubat, F. Elbahhar, and C. Tatkeu, "Multiuser interference cancellation in a passive network with PON-OCDMA uncontrolled power," in *Ultra Modern Telecommunications and Control Systems and Workshops (ICUMT), 2011 3rd International Congress on*, pp. 1-5, 2011.

[39] N. Elfade, A. A. Aziz, H. Yousif, M. Musa, A. Aziz, E. Idriss, *et al.*, "Multi-user detection for the OCDMA: Optical Parallel Interference Cancellation with optical limiter," in *Intelligent and Advanced Systems, 2007. ICIAS 2007. International Conference on*, pp. 444-446, 2007.

[40] A. K. Soong and W. A. Krzymien, "CDMA multi-user interference cancellation with reference symbol aided estimation of channel parameters," in

Communications, Computers, and Signal Processing, 1995. Proceedings., IEEE Pacific Rim Conference on, pp. 429-432, 1995.

[41] P. Taeyoon, L. Jaechul, A. Youngshin, L. Seungphil, and C. Jaeho, "Multi-user interference cancellation technique for coded OFDM-CDMA system," in *Global Telecommunications Conference, 2002. GLOBECOM '02. IEEE*, pp. 504-508 vol.1, 2002.

[42] Y. Wen-Bin and K. Sayrafian-Pour, "A Low Complexity Interference Cancellation Technique for Multi-User DS-CDMA Communications," in *Communications (ICC), 2010 IEEE International Conference on*, pp. 1-5, 2010.

[43] H. Seleem, A. Bentrcia, and H. Fathallah, "Penalised and doubly-penalised parallel/successive interference cancellation multi-user detectors for asynchronous upstream optical code division multiple access passive optical network," *Communications, IET*, vol. 8, pp. 626-638, 2014.

[44] A. S. Motahari and M. Nasiri-Kenari, "Multiuser detections for optical CDMA networks based on expectation-maximization algorithm," *Communications, IEEE Transactions on*, vol. 52, pp. 652-660, 2004.

[45] J. P. Heritage and A. M. Weiner, "Advances in Spectral Optical Code-Division Multiple-Access Communications," *Selected Topics in Quantum Electronics, IEEE Journal of,* vol. 13, pp. 1351-1369, 2007.

[46] R. Matsumoto, T. Kodama, S. Shimizu, R. Nomura, K. Omichi, N. Wada, *et al.*, "40G-OCDMA-PON System With an Asymmetric Structure Using a Single Multi-Port and Sampled SSFBG Encoder/Decoders," *Lightwave Technology, Journal of,* vol. 32, pp. 1132-1143, 2014.

[47] Y. Tanaka, T. Kodama, S. Yoshima, N. Kataoka, J. Nakagawa, S. Shimizu, *et al.*, "Ultimate reach 10Gbps dispersion-compensation-free WDM-TDM-OCDMA-PON: Experimental demonstration and theoretical validation," in *Optical Fiber Communication Conference and Exposition (OFC/NFOEC), 2012 and the National Fiber Optic Engineers Conference*, pp. 1-3, 2012.

[48] Y. Yi, K. G. Petrillo, T. Hong-Fu, J. B. Khurgin, A. B. Cooper, and M. Foster, "Simulation and experimental demonstration of coherent OCDMA using spectral line pairing and heterodyne detection," in *Information Sciences and Systems (CISS), 2013 47th Annual Conference on*, pp. 1-6, 2013.

[49] H. Brahmi, G. Giannoulis, M. Menif, V. Katopodis, D. Kalavrouziotis, C. Stamatiadis, *et al.*, "Experimental Demonstration of an Elastic Packet Routing Node Based on OCDMA Label Coding," *Photonics Technology Letters, IEEE,* vol. 24, pp. 721-723, 2012.

[50] S. Idris, T. Osadola, and I. Glesk, "Towards self-clocked gated OCDMA receiver," *Journal of the European Optical Society-Rapid Publications vol 8 13013, 6 pages,* vol. 8, p. 3013, 2013.

[51] R. Fantacci, "Proposal of an interference cancellation receiver with low complexity for DS/CDMA mobile communication systems," *Vehicular Technology, IEEE Transactions on,* vol. 48, pp. 1039-1046, 1999.

[52] P. Patel and J. Holtzman, "Analysis of a simple successive interference cancellation scheme in a DS/CDMA system," *Selected Areas in Communications, IEEE Journal on,* vol. 12, pp. 796-807, 1994.

[53] A. Duel-Hallen, "A family of multiuser decision-feedback detectors for asynchronous code-division multiple-access channels," *Communications, IEEE Transactions on,* vol. 43, pp. 421-434, 1995.

[54] R. Lupas and S. Verdu, "Near-far resistance of multiuser detectors in asynchronous channels," *Communications, IEEE Transactions on,* vol. 38, pp. 496-508, 1990.

[55] R. Lupas and S. Verdu, "Linear multiuser detectors for synchronous code-division multiple-access channels," *Information Theory, IEEE Transactions on,* vol. 35, pp. 123-136, 1989.

Chapter 3

PROPOSING UNIFORM CROSS-CORRELATION MODIFIED PRIME CODE

In this chapter a novel set of formulas are proposed, which are derived to construct an Optical Code Division Multiple Access (OCDMA) prime code, hereby referred to as the "Uniform Cross-Correlation Modified Prime Code (UC-MPC)". Moreover, the correlation properties of this code set are evaluated and compared with other existing prime code sets. The results reveal that UC-MPC has enhanced correlation properties, improves the security and decreases the bit error rate, as compared with the other existing prime code families.

3.1 Introduction

Nowadays, optical networks are improving the quality and speed of multimedia services. One of the factors needed for this improvement is the generation and implementation of optimal code sequences with enhanced features. Although various code sets have been studied in last two decades [1-8], research is still going on to propose more efficient code sets with less co-channel interference reduction.

As the characteristics of a communication network, the security of the system, its efficiency and the maximum number of subscribers which the system can accommodate, should be all investigated. These features are related to the characteristics of the code set implemented in the system, which are the code length, the code weight, the correlation properties of the code set, and its cardinality. These parameters should be considered in the design process of a code set to enhance the performance of the system. Moreover, the performance of an OCDMA system is highly dependent on the receiver topology, the Multiple User Interference (MUI), and the type of modulation used [9].

To enhance the performance of the OCDMA system, it is necessary to reduce the multi-user interference (MUI) effect. To do so, a novel code set, with maximised auto-correlation and minimised cross-correlation, should be developed.

In doing so, a variety of prime code sets have been analysed and evaluated in different OCDMA networks. These include the primary prime code (PC) [1, 8], extended prime code [1, 8], modified prime code (MPC) [1, 8], generalized prime code [8], carrier-hopping [8], multi-carrier prime codes [8],the new MPC (nMPC) [6], padded MPC

(PMPC) [10], 2^n modified prime codes [11] and double-padded MPC (DPMPC) [12]. Moreover, in this research, the performance of these code sets, in different modulations such as Pulse Position Modulation (PPM) and On–Off Keying (OOK), has been analysed in detail. Some of these analysis are included in the next chapters, where few of these codes are compared with each other in various systems.

In this chapter, a new prime code set is introduced which is hereby referred to as the "Uniform Cross-Correlation Modified Prime Code (UC-MPC)". This code set improves the overall performance of the optical communication network. In brief, UC-MPC offers outstanding correlation properties, improves the security of system, decreases the BER and therefore reduces the co-channel interference.

In this chapter the construction process of UC-MPC is discussed in Section 3.2. Sections 3.3 and 3.4 discuss the correlation properties of the novel code set and conclusion, respectively.

3.2 Code Construction

As mentioned in the previous chapter, Modified Prime Code (MPC) [8], which is one of the most famous prime code families, is a shifted version of Prime Code (PC) [8]. In this section initially two novel code sets are proposed, hereby referred to as Novel Prime Code (NPC) and Modified Novel Prime Code (M-NPC). These code sets have the similar properties as those of PC and MPC, respectively. Then the proposed UC-MPC can be constructed by modifying this new code set in the manner that will explain below.

3.2.1 Novel Prime Code (NPC)

Implementing a small change in the PC generation formula, the NPC code set $S_{NPC}(i,j,p)$ can be obtained by [9]:

$$S_{NPC}(i,j,p) = 2^{[i*j \pmod p]} \tag{3.1}$$

where p is a prime number and both i and j are integers belonging to the Galois field $GF(p) = \{0,1,\dots,p-1\}$. Unlike the conventional prime code sequence, to construct the binary code sequence of NPC, $S_{NPC}(i,j,p)$ is directly converted to its associated binary value.

The resulting binary sequence has a length of p^2 and is denoted by $C_{NPC}(i,p)=(c_{i,0}, c_{i,1}, \dots, c_{i,j}, \dots, c_{i,p-1})$, where $c_{i,j}$ is the equivalent binary value of $S_{NPC}(i,j,p)$. Both the number of '1's (code weight) and the cardinality of C_{NPC} are equal to p.

For instance, for $p = 5,\ i = 3\ and\ j = 4$ from (3.1):

$$S_{NPC}(3,4,5) = 2^{[12(mod\ 5)]} = 2^{[2]} = 4$$

$$\text{and hence } c_{3,4} = 00100$$

As a result, the whole binary sequence of $C_{NPC}(3,5) = (c_{3,0}, c_{3,1}, c_{3,2}, c_{3,3}, c_{3,4})$ = (00001 01000 00010 10000 00100). Table 3.1 contains all the possible values of both S_{NPC} and C_{NPC} for $p = 5$.

TABLE 3.1
NEW PRIME CODE (NPC) OVER GF(5) [9]

Index	S_{NPC}					C_{NPC}				
i	j=0	j=1	j=2	j=3	j=4	j=0	j=1	j=2	j=3	j=4
0	1	1	1	1	1	00001	00001	00001	00001	00001
1	1	2	4	8	16	00001	00010	00100	01000	10000
2	1	4	16	2	8	00001	00100	10000	00010	01000
3	1	8	2	16	4	00001	01000	00010	10000	00100
4	1	16	8	4	2	00001	10000	01000	00100	00010

3.2.2 Modified Novel Prime Code (M-NPC)

A modified prime code is generated by shifting the code sequences of the prime code [8]. Applying the same approach to the NPC, the Modified Novel Prime Code (M-NPC) is generated. The proposed formula below converts the NPC sequences to the M-NPC code sequences [9]:

$$S_{M-NPC}(n,j,p) = \left[2^{n\,(mod\ p)}\ .\ S_{NPC}\left(\left\lfloor\frac{n}{p}\right\rfloor, j, p\right)\right]\ \ (mod\ \ [2^p - 1]) \tag{3.2}$$

where *'n'* is the code index ($0 \leq n < p^2$), '*j*' is the sub-sequence index within the code ($0 \leq j < p$), and ⌊ ⌋ is the floor function. The group number is $i=\left\lfloor\frac{n}{p}\right\rfloor$ and the code index within a group $x=n\ (mod\ p)$. The term $2^{n\,(mod\ p)}$ in Equation (3.2) shifts the j^{th} sub-sequence of the i^{th} NPC sequence (i.e. $S_{NPC}(\lfloor n/p \rfloor, j, p)$) by *x*, and the term $(mod\ [2^p - 1])$ enforces the circular shift to generate the M-NPC sub-sequence. Table 3.2 contains all the possible values of both S_{M-NPC} and $C_{M\text{-}NPC}(n,p) = (c_{n,0}, c_{n,1}, \ldots, c_{n,p^2-1})$ of the M-NPC over *GF(p=5)*.

In brief, each bit of a NPC sequence is shifted *p* times to form one group of the M-NPC. To construct Table 3.2, each sequence of Table 3.1 is shifted 5 times as *p=5*. For instance, referring to Table 3.1, $C_{NPC}(0,5) = (00001\ 00001\ 00001\ 00001\ 00001)$. This sequence is the first of the 1st group of the M-NPC (see Table 3.2). Afterwards, by shifting the bits 5 times, 5 new code sequences are generated for the 1st group of the M-NPC. Implementing the same procedure for each of the other NPC sequences given in Table 3.1, p^2=25 M-NPC sequences are obtained (Table 3.2). Similar to the MPC, M-NPC also supports up to p^2 subscribers over *GF(p)*.

TABLE 3.2
MODIFIED NOVEL PRIME CODE (M-NPC) OVER GF(5) [9]

Index			$S_{M\text{-}NPC}$					$C_{M\text{-}NPC}$				
i	x	n	j=0	j=1	j=2	j=3	j=4	j=0	j=1	j=2	j=3	j=4
0	0	0	1	1	1	1	1	00001	00001	00001	00001	00001
	1	1	2	2	2	2	2	00010	00010	00010	00010	00010
	2	2	4	4	4	4	4	00100	00100	00100	00100	00100
	3	3	8	8	8	8	8	01000	01000	01000	01000	01000
	4	4	16	16	16	16	16	10000	10000	10000	10000	10000
1	0	5	1	2	4	8	16	00001	00010	00100	01000	10000
	1	6	2	4	8	16	1	00010	00100	01000	10000	00001
	2	7	4	8	16	1	2	00100	01000	10000	00001	00010
	3	8	8	16	1	2	4	01000	10000	00001	00010	00100
	4	9	16	1	2	4	8	10000	00001	00010	00100	01000
2	0	10	1	4	16	2	8	00001	00100	10000	00010	01000
	1	11	2	8	1	4	16	00010	01000	00001	00100	10000
	2	12	4	16	2	8	1	00100	10000	00010	01000	00001
	3	13	8	1	4	16	2	01000	00001	00100	10000	00010
	4	14	16	2	8	1	4	10000	00010	01000	00001	00100
3	0	15	1	8	2	16	4	00001	01000	00010	10000	00100
	1	16	2	16	4	1	8	00010	10000	00100	00001	01000
	2	17	4	1	8	2	16	00100	00001	01000	00010	10000
	3	18	8	2	16	4	1	01000	00010	10000	00100	00001
	4	19	16	4	1	8	2	10000	00100	00001	01000	00010
4	0	20	1	16	8	4	2	00001	10000	01000	00100	00010
	1	21	2	1	16	8	4	00010	00001	10000	01000	00100
	2	22	4	2	1	16	8	00100	00010	00001	10000	01000
	3	23	8	4	2	1	16	01000	00100	00010	00001	10000
	4	24	16	8	4	2	1	10000	01000	00100	00010	00001

As an example, for a given $p = 5, n = 18\ and\ j = 4$ from (3.2):

$$S_{M-NPC}(18,4,5) = \left[2^{18\ (mod\ 5)}\ .\ S_{NPC}\left(\left\lfloor\frac{18}{5}\right\rfloor, 4,5\right)\right]\ (mod\ [2^5 - 1])$$

$$= [2^3\ .\ S_{NPC}(3,4,5)]\ (mod\ 31)$$

$$= [8 \times 4]\ (mod\ 31) = 1$$

$$\text{Hence } c_{18,4} = 00001$$

The whole binary sequence $C_{M\text{-}NPC}(18,5)$*=(01000 00010 10000 00100 00001).*

3.2.3 Uniform Cross-Correlation Modified Prime Code

By modifying the M-NPC, the proposed UC-MPC is constructed. To do so, the code weight of the M-NPC is increased, while the cross correlation of unity between any two code sequences is maintained in the new code set.

In doing so, *p* bits are injected (which consists of one '1' bit and *p-1* '0' bits) within each M-NPC code sequence. This results in the increment of the code weight from *p* to *p+1*, and the code length from p^2 to $(p^2 + p)$. For instance, for *p=5*, the 1st code sequences of M-NPC (C_{M-NPC}), and the one with injected bits (C_{iM-NPC}), are illustrated below, where the injected bits are highlighted in grey:

$C_{M-NPC}\ (0,5) = 00001$ 00001 00001 00001 00001

$C_{iM-NPC}(0,5) = 00001$ **1** 00001 **0** 00001 **0** 00001 **0** 00001 **0**

In brief, the injected bit "1" is placed after the last bit of the first M-NPC sub-sequence (i.e. 00001 **1**). Likewise, the 2nd, 3rd, 4th and 5th injected bits, which are all zeros, are located after the last bits of the 2nd, 3rd, 4th and 5th M-NPC sub-sequences.

Subsequently, by grouping each 5 bits from the left of $C_{iM-NPC}(0,5)$ sequence, each sub-sequence of the novel UC-MPC can be obtained:

$C_{UC-MPC}(0,5) =$ 00001 **1** 00001 **0** 00001 **0** 00001 **0** 00001 **0**

This regrouping increases the number of sub-sequences from *p=5* to *p+1=6* as shown in Table 3.3:

TABLE 3.3
FIRST CODE SEQUENCE OF UC-MPC OVER GF(5)

i	x	n	*j=0*	*j=1*	*j=2*	*j=3*	*j=4*	*j=5*
0	0	0	00001	**1**0000	1**0**000	01**0**00	001**0**0	0001**0**

The 5th (i.e. *j=4*) UC-MPC sub-sequence "001**0**0" in the Table 3.3 consists of 3 bits (i.e. 001) on the left side of the injected bit, IB (i.e. **0**), which hereby are referred to as the left bits, LB, and one bit on the right side of the injected bit (i.e. 0), which is referred to as the right bit, RB. The right bit belongs to the current M-NPC sub-sequence and the left bits belong to the previous M-NPC sub-sequence. Generally the *p* bits of the j^{th} UC-MPC sub-sequence can be constructed, as indicated in the Table 3.4:

TABLE 3.4
CONSTRUCTION OF J^{TH} UC-MPC SUB-SEQUENCE OVER GF(P) [9]

LB	IB	RB
(j-1) least significant bits of the (j-1)th M-NPC sub-sequence	0 or 1	(p-j) most significant bits of the jth M-NPC sub-sequence

According to these explanations, the UC-MPC code set is formulated as follows [9]:

$$S_{UC-MPC}(n,j,p) = \left[S_{M-NPC}(n,j-1,p) \ (mod\ 2^{j-1})\right].2^{p-j+1} \quad +$$

$$\left\lfloor 1-\left(\frac{j-\left\lfloor\frac{n}{p}\right\rfloor-1}{p}\right)^2\right\rfloor . 2^{p-j} \quad +$$

$$\left\lfloor\frac{S_{M-NPC}(n,j,p)}{2^j}\right\rfloor \tag{3.3}$$

where $0 \le j \le p$, $0 \le n < p^2$ and $S_{M-NPC}(n,j,p)$ is given in (2). Moreover:

$$S_{M-NPC}(n,-1,p) = S_{M-NPC}(n,p,p) \stackrel{\text{def}}{=} 0$$

Table 3.5 shows all possible values of both S_{UC-MPC} and C_{UC-MPC} for $p = 5$. In addition, the following algorithm also explains the construction stages of the UC-MPC:

1. A signature sequence is selected from the M-NPC (e.g. CM-NPC(10,5)= 00001 00100 10000 00010 01000), see Table 3.2.
2. A pair of neighbour sub-sequences (“Parents”) is considered from the above selected signature sequence for breeding the new sub-sequence (e.g. referring to Figure 3.1, Row -1, where $c_{10,2} = 10000$ and $c_{10,3} = 00010$.)
3. A certain number of bits of each selected parent, hereby referred to as a “Chromosome”, is separated from both parent sub-sequences by the first and the third terms of (3.3). In the above example: chromosomes 1 (i.e. LB) and 2 (i.e. RB) are both ”00” (see Figure 3.1, Row-2).

4. Depending on the binary value of the 2nd term in (3.3) a bit 1 or 0 (i.e. IB) is injected between the above mentioned two chromosomes (i.e. "1" in the above example), see Figure 3.1, Row-3.

5. The new generated sub-sequence (e.g. "00100"), hereby referred to as the "Child" sub-sequence, is a part of the construction of the UC-MPC code (see Row-4 in Figure 3.1). This is the 3rd sub-sequence of the 10th UC-MPC sequence ($s_{10,3} = 4$ and $c_{10,3} = 00100$), shown in Table 3.5. The generated child sub-sequence is the *jth* subsequence of the nth UC-MPC sequence. This child sub-sequence, beside 'p' other child sequences, forms the whole UC-MPC sequence.

6. Repeat steps 2 to 5 to construct the remaining sub-sequence pairs of the chosen M-NPC signature sequence. p+1 child sub-sequences are generated for each UC-MPC code sequence.

7. Repeat steps 1 to 6 for p2 times to construct all other UC-MPC code sequences.

TABLE 3.5
UNIFORM CROSS-CORRELATION MODIFIED PRIME CODE (UC-MPC) OVER GF(5) [9]

Index			SUC-MPC						CUC-MPC					
i	x	n	j=0	j=1	j=2	j=3	j=4	j=5	j=0	j=1	j=2	j=3	j=4	j=5
0	0	0	1	16	16	8	4	2	00001	10000	10000	01000	00100	00010
	1	1	2	17	0	16	8	4	00010	10001	00000	10000	01000	00100
	2	2	4	18	1	0	16	8	00100	10010	00001	00000	10000	01000
	3	3	8	20	2	1	0	16	01000	10100	00010	00001	00000	10000
	4	4	16	24	4	2	1	0	10000	11000	00100	00010	00001	00000
1	0	5	1	1	9	1	1	0	00001	00001	01001	00001	00001	00000
	1	6	2	2	10	2	0	2	00010	00010	01010	00010	00000	00010
	2	7	4	4	12	0	4	4	00100	00100	01100	00000	00100	00100
	3	8	8	8	8	8	8	8	01000	01000	01000	01000	01000	01000
	4	9	16	0	24	16	16	16	10000	00000	11000	10000	10000	10000
2	0	10	1	2	4	4	8	16	00001	00010	00100	00100	01000	10000
	1	11	2	4	0	12	17	0	00010	00100	00000	01100	10001	00000
	2	12	4	8	0	21	0	2	00100	01000	00000	10101	00000	00010
	3	13	8	0	17	6	0	4	01000	00000	10001	00110	00000	00100
	4	14	16	1	2	4	4	8	10000	00001	00010	00100	00100	01000
3	0	15	1	4	0	18	2	8	00001	00100	00000	10010	00010	01000
	1	16	2	8	1	0	6	16	00010	01000	00001	00000	00110	10000
	2	17	4	0	18	0	11	0	00100	00000	10010	00000	01011	00000
	3	18	8	1	4	0	18	2	01000	00001	00100	00000	10010	00010
	4	19	16	2	0	9	2	4	10000	00010	00000	01001	00010	00100
4	0	20	1	8	2	0	16	5	00001	01000	00010	00000	10000	00101
	1	21	2	0	20	1	0	9	00010	00000	10100	00001	00000	01001
	2	22	4	1	0	10	0	17	00100	00001	00000	01010	00000	10001
	3	23	8	2	0	16	5	1	01000	00010	00000	10000	00101	00001
	4	24	16	4	1	0	8	3	10000	00100	00001	00000	01000	00011

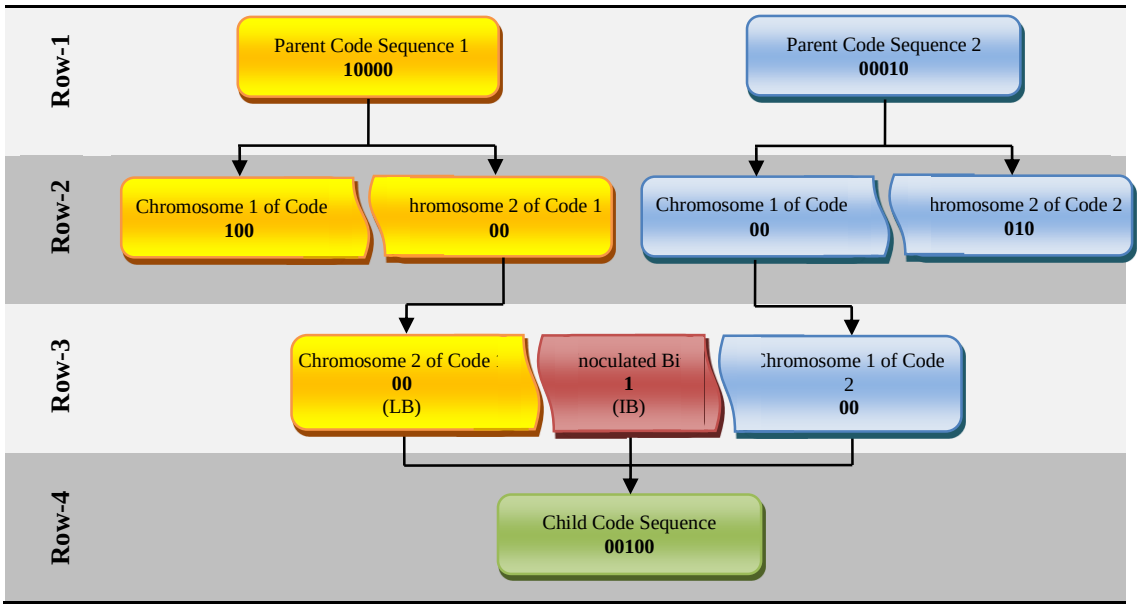

Figure 3.1 UC-MPC Code Sequence Generation Diagram

3.2.4 Examples

The following example is provided to explain the mentioned stages in detail. For instance, for the given *p=5*, *n=13* and *j=2*, from (3.3):

$$S_{UC-MPC}(13,2,5) = [\, S_{M-NPC}(13,1,5) \ (mod\ 2^{2-1})] \ .\ 2^{5-2+1} \ +$$

$$\left\lfloor 1 - \left(\frac{2 - \left\lfloor \frac{13}{5} \right\rfloor - 1}{5} \right)^2 \right\rfloor \ .\ 2^{5-2} \ +$$

$$\left\lfloor \frac{S_{M-NPC}(13,2,5)}{2^2} \right\rfloor$$

$$S_{UC-MPC}(13,2,5) \ = [\, 1 \ (mod\ 2)] \ .\ 2^4 \ + \left\lfloor 1 - \left(\frac{-1}{5} \right)^2 \right\rfloor \ .\ 2^3 + \left\lfloor \frac{4}{4} \right\rfloor$$

$$S_{UC-MPC}(13,2,5) \ = 16 \ + 0 \ + 1 = 17 \text{ and hence } c_{13,2} = 10001$$

The bracket part of the 1st term in (3.3) represents the LB column in Table 3.4. These bits should then be shifted by *p-(j-1)* to the left to form the left part of the new sub-sequence. The shift is performed by the 2^{p-j+1} part of the 1st term in (3.3). As an example, the 1st term in (3.3) for the above mentioned case, where *p=5, n=13* and *j=2,* is obtained as follows:

$$S_{M-NPC}(13,1,5) = 1 = (00001)_2$$

$$[\,S_{M-NPC}(13,1,5)\ \ (mod\ \ 2^{2-1})] = 1 = (0000\mathbf{1})_2$$

$$[\,S_{M-NPC}(13,1,5)\ \ (mod\ \ 2^{2-1})]\ .\ 2^{5-2+1} = 16 = (\mathbf{1}0000)_2$$

In the same way, the third term of (3.3) represents the RB column of Table 3.4. Dividing $S_{M-NPC}(n,j,p)$ by 2^j performs *j*-bits shift to the right and extracts the *p-j* most significant bits of the jth M-NPC sub-sequence. For the above case, there is:

$$S_{M-NPC}(13,2,5) = 4 = (\mathbf{001}00)_2$$

$$\left\lfloor \frac{S_{M-NPC}(13,2,5)}{2^2} \right\rfloor = 1 = (00\mathbf{001})_2$$

For each UC-MPC code, the j^{th} bit of j^{th} sub-sequence ($c_{n,j}$) is the injected bit (IB) which is highlighted in the Table 3.5. Also, for each code in the i^{th} group, the injected '1' bit is located in the *j=i+1* sub-sequence. As an example, for $C_{UC-MPC}(13,5)$*=(01000 00000 10001 00110 00000 00100),* the group number $i = \left\lfloor \frac{13}{5} \right\rfloor = 2$, and the injected '1' bit is the 3rd bit of $c_{13,3} = "00110"$.

The bracket part in the second term of (3.3) generates a single injected bit (0 or 1, see the IB column of Table 3.4) which, as explained earlier, lies between the LB and RB parts to

obtain the UC-MPC sub-sequence. It should be noted that the function of term 2^{p-j} is to shift this IB by $p-j$ to the left, so that it can be fitted between LB and RB. For the above example, the group number is 2, so the 2nd injected bit (i.e. IB for *j=2*) is '0'= $(00000)_2$. Then, after 3 bits (i.e. *p-j*) shift to the left, it becomes $(00000)_2$.

At the end, these three parts (LB, IB and RB) together construct the j^{th} UC-MPC sub-sequence. That is, in this example:

$$
\begin{aligned}
S_{UC-MPC}(13,2,5) &= (\mathbf{1}0000)_2 && (1^{st}\ \text{Term of (3.3)})\\
&+ (0\mathbf{0}000)_2 && (2^{nd}\ \text{Term of (3.3)})\\
&+ (00\mathbf{001})_2 && (3^{rd}\ \text{Term of (3.3)})\\
\hline
S_{UC-MPC}(13,2,5) &= (10001)_2 &&= 17
\end{aligned}
$$

Similarly the remaining *p* UC-MPC sub-sequences can be generated. As has been discussed in the proposed algorithm, the mentioned process can be applied p^2 times, for different values of '*n*', to construct the whole UC-MPC code sequences. The weight, cardinality and length of this new code are $p+1$, p^2 and p^2+p, respectively.

3.3 Analysis of Correlation Properties

The discrete correlation function of two UC-MPC code sequences $C_i(n)$ and $C_j(n)$ is defined as:

$$R_{C_iC_j}(m) = \sum_{n=0}^{L-1} C_i(n).C_j(n+m) \tag{3.4}$$

Where $C_i(n) \in \{0,1\}$ is a periodic sequence with period L, $|m| \leq L-1$, and $L = p^2 + p$ is the UC-MPC code length. Figure 3.2(a) and Figure 3.2(b) illustrate the auto-correlation (AC) and cross-correlation (CC) functions of the UC-MPC, respectively. These figures are generated by using (3.4) for the given p=5 and data stream'11010010'. At each chip synchronization position (T) the value of AC for sequence C_6 is p+1=6 and the value of CC function for code sequences C_3 and C_6 is 1.

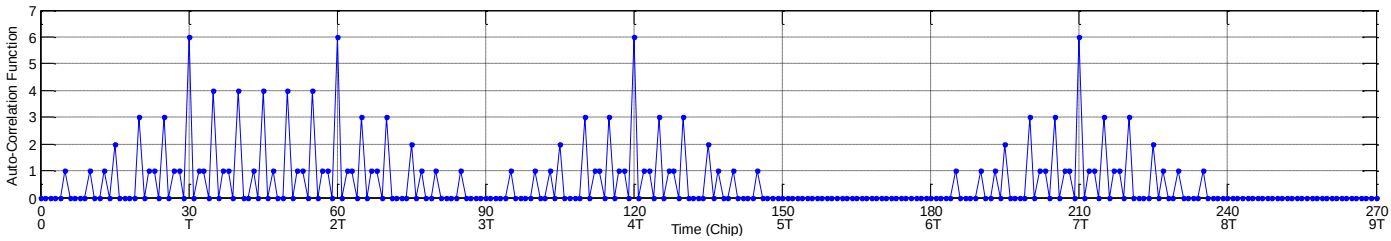

(a) Auto-Correlation function of code sequence C_6 for the data stream '11010010'

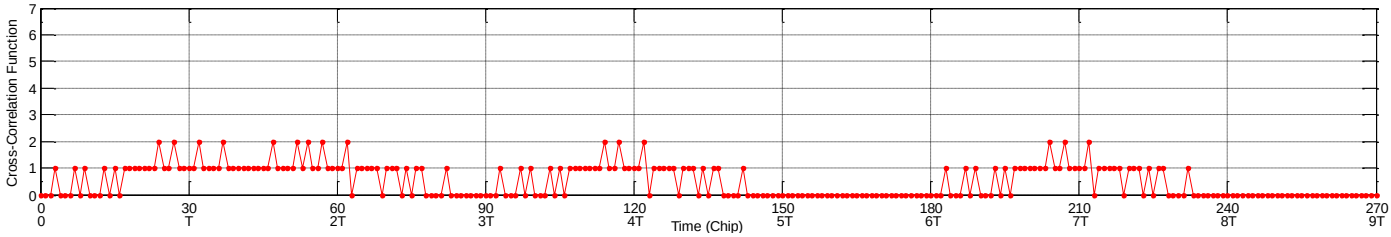

(b) Cross-Correlation function of code sequences C_3 and C_6 for the data stream '11010010'

Figure 3.2 Correlation functions of Uniform Cross-Correlation Modified Prime Code (UC-MPC) over *GF(5)* [9]

It should be noted that the value of AC in the asynchronous communication (i.e. m≠0 in (3.4)) varies from 0 to 6 (see Figure 3.2(a)). Also, in this scenario, the value of CC between C_3 and C_6 varies from 0 to 2 (see Figure 3.2(b)). Generally, when two distinct code sequences are selected within the same group, the CC value can reach as high as *p* (i.e. 5 in this case), and, if the two code sequences are selected from different groups, this value is, at most, four. The minimum and maximum values of correlation functions of all possible combination of any two code sequences in the UC-MPC, for *p=5*, are illustrated in Figure 3.3.

The correlation functions of synchronised PC, MPC, nMPC, DPMPC, and UC-MPC are shown in Figure 3.4(a) to Figure 3.4(e), respectively. All of these figures show the zero-shifted correlation values between each code pair, which are calculated at the chip synchronization position T.

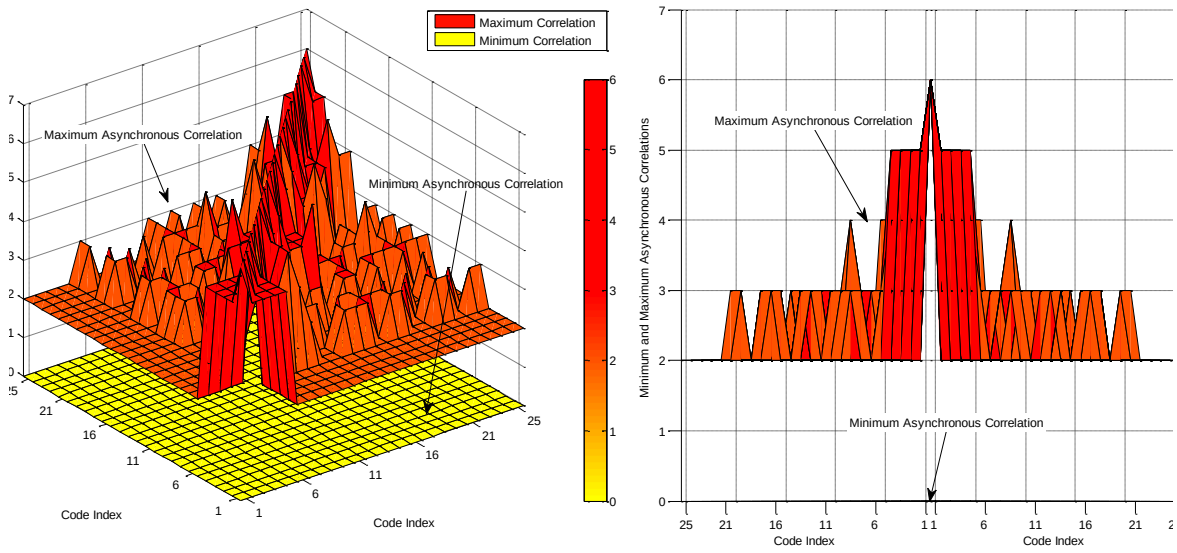

(a) 3D View (b) Front View

Figure 3.3 Minimum and maximum values of correlation function of all possible combination of code sequence pairs in UC-MPC over GF(5) [9]

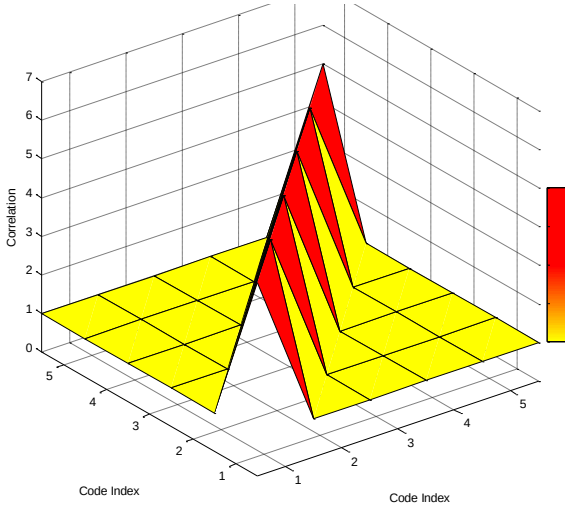

(a) PC (3D View)

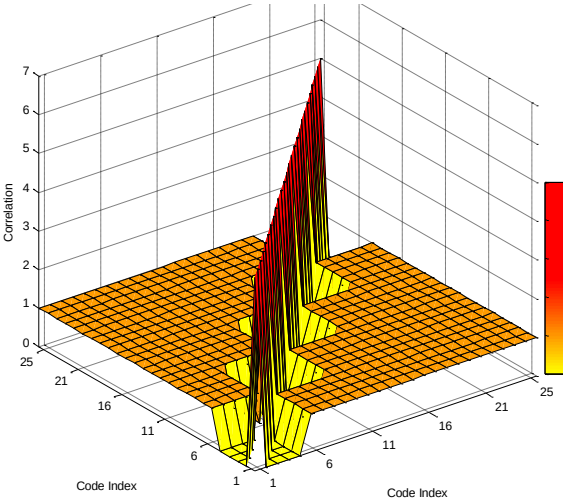

(b) MPC (3D View)

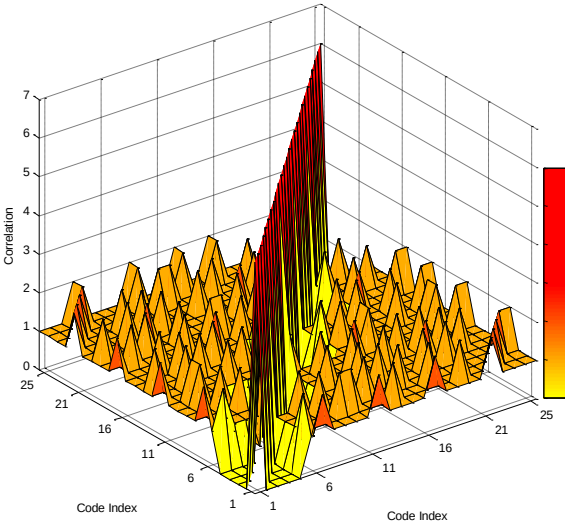

(c) nMPC (3D View)

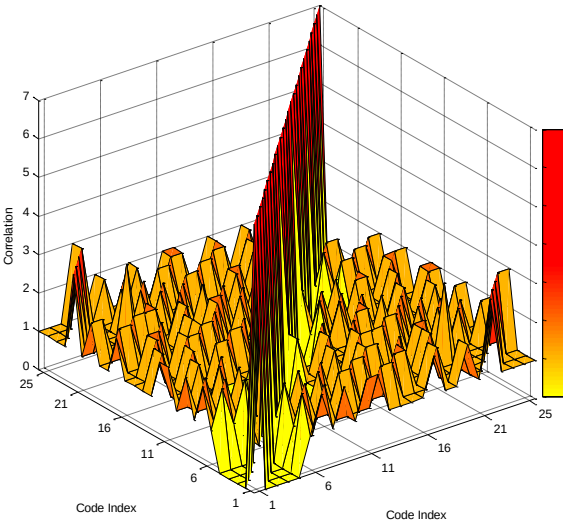

(d) DPMPC (3D View)

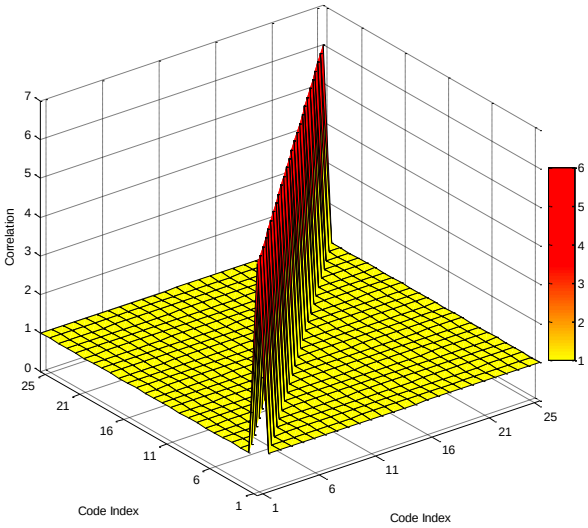

(e) UC-MPC (3D View)

Figure 3.4 Correlation functions of Prime Code families over GF(5) in a synchronised system [9]

The zero-shifted correlation values of all pairs of UC-MPC code sequences are shown in Figure 3.4(e). As can be seen in this figure, for all the combinations the AC (diagonal values) are p+1. Also, the CC between any two code sequences within the code set is always 1, while in case of nMPC (Figure 3.4(c)) and DPMPC (Figure 3.4(d)) the CC values reach 2 and 3, respectively. CC values more than one are considered as high CC values which indicate the higher similarity of code sequences in the code set. This would result in error in the receivers, and therefore deteriorate the performance and increase the BER.

In addition, in this figure, the correlation properties of UC-MPC are compared with the other prime code sets. It can be seen that UC-MPC supports more concurrent users than PC and delivers a higher AC as compared with those of MPC and PC.

Moreover, both Figure 3.4(e) and Table 3.5 illustrate that the UC-MPC code set with uniform and unity CC, offers higher AC and code weight. In the proposed family, the probability of interference between each two code sequences is the same. This is the result of the uniformity of the CC in UC-MPC, while this is not the case in the other prime code sets.

Furthermore, the asynchronous CC functions of UC-MPC, nMPC and DPMPC are compared with each other in Figure 3.5. For the given 1st and 21st UC-MPC signatures over GF(5) from Table 3.5, it can be seen that at the synchronisation time t=T the CC values for UC-MPC, nMPC and DPMPC are 1, 2 and 3, respectively.

As Figure 3.5 shows, the CC value of UC-MPC exceeds one only in two occasions and hence, UC-MPC offers a better asynchronous CC value, as compared with other prime families.

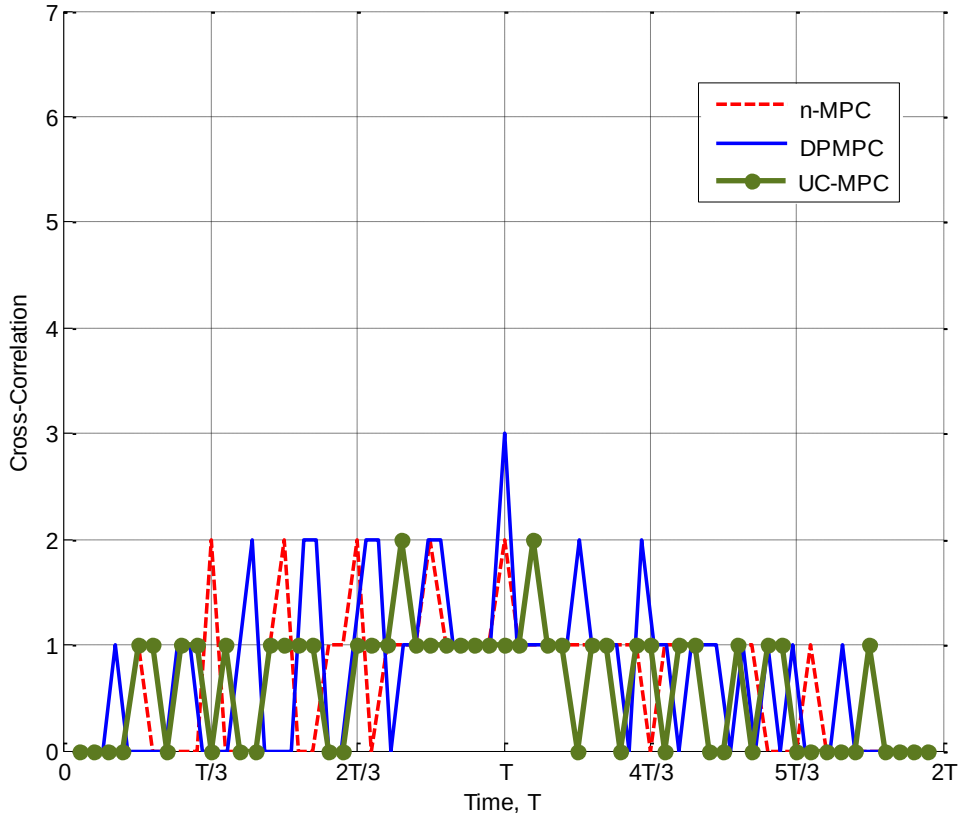

Figure 3.5 Cross-Correlation function of code sequences C_1 and C_{21} for different prime code families over GF(5)

All in all, because of these properties, UC-MPC offers a bigger difference between auto-correlation and cross-correlation values, which eases the decode procedure in the receivers and improves the performance of systems by lowering the BER. This will be discussed in Chapter 4 in detail.

3.4 Summary

In this chapter, a novel set of formulae and a new prime code family with uniform cross-correlation (UC-MPC) are introduced to be implemented in OCDMA systems. Also the correlation properties of the proposed UC-MPC have been analysed and compared the results with other existing prime code sets.

The results reveal that the cross-correlation of UC-MPC is unity and uniform, and this code set delivers much better correlation properties as compared to the other prime code sets. Moreover, an increment of the code length of UC-MPC from p^2 (in NMPC and MPC) to (p^2+p) leads to the increase of chips/symbol, and consequently improves the BER performance and also the security of the system. This will be investigated in Chapter 4 in detail.

Furthermore, the increment of both auto-correlation and weight from p in M-NPC and MPC to $p+1$ in UC-MPC results in lowering the BER of the system, and increases the number of simultaneous active subscribers.

Finally, unlike the other prime code sets, the pattern of the proposed code sequences cannot be predicted easily without the constructor formula. This increases the security of the code dramatically.

REFERENCES

[1] G.-C. Yang and W. C. Kwong, "Performance Analysis of Extended Carrier-Hopping Prime Codes for Optical CDMA," *IEEE Transactions on Communications,* vol. 53, pp. 876-881, May 2005.

[2] H. Hai Jiang, W. Weihua Zhuang, and X. Xuemin Shen, "Distributed Medium Access Control Next-Generation CDMA Wireless Networks," *Wireless Communications, IEEE,* vol. 14, pp. 25-31, 2007.

[3] M. M. Karbassian and H. Ghafouri-Shiraz, "Fresh Prime Codes Evaluation for Synchronous PPM and OPPM Signaling for Optical CDMA Networks," *Lightwave Technology, Journal of,* vol. 25, pp. 1422-1430, 2007.

[4] M. M. Karbassian, F. Liu, and H. Ghafouri-Shiraz, "Performance Analysis of Novel Prime Code Family in Coherent Optical CDMA Network," in *Communications and Networking in China, 2007. CHINACOM '07. Second International Conference on,* pp. 393-396.

[5] W. C. Kwong, P. A. Perrier, and P. R. Prucnal, "Performance comparison of asynchronous and synchronous code-division multiple-access techniques for fiber-optic local area networks," *Communications, IEEE Transactions on,* vol. 39, pp. 1625-1634, 1991.

[6] F. Liu, M. M. Karbassian, and H. Ghafouri-Shiraz, "Novel family of prime codes for synchronous optical CDMA," *Optical and Quantum Electronics,* vol. 39, pp. 79-90, 2007.

[7] H. M. H. Shalaby, "Direct detection optical overlapping PPM-CDMA communication systems with double optical hardlimiters," *Lightwave Technology, Journal of,* vol. 17, pp. 1158-1165, 1999.

[8] G. C. Yang and W. C. Kwong, *Prime codes with applications to CDMA optical and wireless networks*: Artech House Publishers, 2002.

[9] M. H. Zoualfaghari and H. Ghafouri-Shiraz, "Uniform cross-Correlation modified prime code for applications in synchronous optical CDMA communication systems," *Lightwave Technology, Journal of,* vol. 30, pp. 2955-2963, 2012.

[10] M. Y. Liu and H. W. Tsao, "Cochannel interference cancellation via employing a reference correlator for synchronous optical CDMA systems," *Microwave and Optical Technology Letters,* vol. 25, pp. 390-392, 2000.

[11] Z. Jian-Guo, W. C. Kwong, and A. B. Sharma, "2n modified prime codes for use in fibre optic CDMA networks," *Electronics Letters,* vol. 33, pp. 1840-1841, 1997.

[12] M. M. Karbassian and H. Ghafouri-Shiraz, "Performance analysis of heterodyne-detected coherent optical CDMA using a novel prime code family," *Journal of Lightwave Technology,* vol. 25, pp. 3028-3034, 2007.

Chapter 4

CO-CHANNEL INTERFERENCE REDUCTION USING UC-MPC

The Uniform Cross-correlation Modified Prime Code (UCMPC), proposed in the previous chapter, is implemented and evaluated in various OCDMA systems. This chapter presents some of these evaluations, which can be good measures to permit a comparison between this new code and other existing prime codes.

4.1 Introduction

As has been discussed previously in the literature review (Section 2.3), prime codes have been extensively implemented and analysed in OCDMA systems. Pulse Position Modulation (PPM) is one of the well-known modulations, which are heavily used in the OCDMA systems, and implement prime codes. The behaviour of prime codes have been investigated in these systems in [1-5].

Pulse position modulation is an energy-efficient modulation and offers a better average power in comparison with another popular modulation types, i.e. On-Off Keying (OOK). Although the chip time is the weak point of PPM in comparison with OOK, it should be noted that in many communications and devices, the power issues are much more important and critical [4].

In this chapter, performances of the following systems were analysed and compared, based on the new spreading code (i.e. UC-MPC):

1. PPM-OCDMA systems with MAI cancellation, presented in [4]
2. PPM-OCDMA systems with Manchester codes and MAI cancellation, mentioned in [4]
3. PPM-OCDMA systems without any MAI cancellation.

It was found that, in comparison with existing prime code families, the proposed UC-MPC reduces the bit error rate (BER) and increases the network capacity. Furthermore, the implementation and analysis of this code set in the Frequency Shift Keying (FSK) modulation and intensity modulated On-Off Keying (OOK) systems have been demonstrated in Chapter 5 and Chapter 6 , respectively.

4.2 Analysis of UC-MPC in PPM

Easy implementation of the UC-MPC in existing systems employing conventional prime code families can be achieved, with no need to change the hardware. Three mentioned PPM-OCDMA systems in Section 4.1 were analysed, using the proposed signature sequences (UC-MPC), as follow:

4.2.1 PPM-OCDMA Systems without implementing any cancellation scheme

In the previous chapter, for a given prime number (p), p^2 UC-MPC sequences were generated, with length and weight of $L=(p^2+p)$ and $w=(p+1)$, respectively. Accordingly, p groups consisting of p different codes were formed. The correlation function $R_{c_i c_j}$ for any two pairs of UC-MPC code sequences at synchronous time (T) was given as:

$$R_{c_i c_j} = \begin{cases} p+1, & if\ m = n \\ 1, & others \end{cases} \tag{4.1}$$

Below, the UC-MPC is implemented in an M-ary PPM-OCDMA system, which can accommodate up to N simultaneous subscribers. To do this, the BER formula given in [2] is modified as follows:

$$P_b = \frac{M}{2(M-1)} \sum_{t=t_{min}}^{t_{max}} P_E^t \,.\, P_T(t) \tag{4.2}$$

where M represents the signal multiplicity [5].

Moreover the probability distribution functions $P_T(t)$ and P_E^t are provided as below:

$$P_T(t) = \frac{\binom{p^2-p}{N-t}\binom{p-1}{t-1}}{\binom{p^2-1}{N-1}} \tag{4.3}$$

$$\begin{aligned} P_E^t \geq & \sum_{l_1=p+2}^{N-t} \binom{N-t}{l_1} \frac{1}{M^{l_1}} \left(1-\frac{1}{M}\right)^{N-t-l_1} \times \\ & \sum_{l_0=0}^{min\{l_1-p-2,\ N-t-l_1\}} \binom{N-t-l_1}{l_0} \frac{1}{(M-1)^{l_0}} (1-\frac{1}{M-1})^{N-t-l_0-l_1} \\ & + 0.5 \sum_{l_1=p+1}^{\frac{N-t+p+1}{2}} \binom{N-t}{l_1} \frac{1}{M^{l_1}} \left(1-\frac{1}{M}\right)^{N-t-l_1} \times \\ & \binom{N-t-l_1}{l_1-p-1} \frac{1}{(M-1)^{l_1-p-1}} \left(1-\frac{1}{M-1}\right)^{N-t-2l_1+p+1} \end{aligned} \tag{4.4}$$

where $t_{min} \stackrel{\text{def}}{=} max\{N+p-p^2, 1\}$

$t_{max} \stackrel{\text{def}}{=} min\{N, p\}$

$t \in \{t_{min}, t_{min}+1, \ldots, t_{max}\}$

4.2.2 PPM-OCDMA Systems with Both Manchester Codes and Interference Cancellation Scheme

Manchester codes were previously implemented in PPM-OCDMA systems in [4, 5]. Performing the similar calculations, the BER formula, for the systems employing UC-MPC, is obtained below:

$$P_b = \frac{M}{2(M-1)} \sum_{t=t_{min}}^{t_{max}} \sum_{r=r_{min}}^{r_{max}} P_E \,.\, P_{R|T}(r|t).\, P_T^1(t) \tag{4.5}$$

where the upper bounded error probability is presented as P_E.

Furthermore, the interference probabilities, $P_{R|T}(r|t)$ and $P_T^1(t)$ in [4, 5], are modified as follows:

$$P_E \le (M-1) \times \sum_{l_1=0}^{r} \binom{r}{l_1} \frac{1}{M^{l_1}} \left(1-\frac{1}{M}\right)^{r-l_1} \times \sum_{l_0=0}^{r-l_1} \binom{r-l_1}{l_0} \frac{1}{(M-1)^{l_0}} (1-\frac{1}{M-1})^{r-l_0-l_1} \times \exp(-Q.\frac{(p+1)^2}{4.(p+1+l_0+l_1)})$$

$$P_T^1(t) = \frac{\binom{p^2-2p+1}{N-t}\binom{p-2}{t-1}}{\binom{p^2-p-1}{N-1}}$$

$$P_{R|T}(r|t) = \frac{\binom{\frac{p^2-2p+1}{2}}{\mathrm{r}}\binom{\frac{p^2-2p+1}{2}}{N-t-r}}{\binom{p^2-2p+1}{N-\mathrm{t}}} \tag{4.6}$$

where $t_{min} \stackrel{\text{def}}{=} max\{N + 2p - p^2 - 1, 1\}$

$t_{max} \stackrel{\text{def}}{=} min\{N, p - 1\}$

$t \in \{t_{min}, t_{min} + 1, \dots, t_{max}\}$

$r_{min} \stackrel{\text{def}}{=} max\left\{N - t - \frac{p^2 - 2p + 1}{2}, 0\right\}$

$r_{max} \stackrel{\text{def}}{=} min\left\{N - t, \frac{p^2 - 2p + 1}{2}\right\}$

$r \in \{r_{min}, r_{min} + 1, \dots, r_{max}\}$

$Q \approx \mu \,.\, \frac{\ln M}{p + w}$

It should be noted that Q denotes the average received photon counts per pulse, and as $Q \to \infty$, the upper bounded error probability (P_E) approaches zero. Moreover, μ represents the average number of photons per pulse (photons/nat).

4.2.3 PPM-OCDMA Systems implementing Interference Cancellation

The integration process in this system is carried out over the entire chip time, not just half of it. Therefore, the error probability can be expressed as below [4, 5]. This can be mentioned as the only difference between the system with both interference cancellation and Manchester codes, and this system.

$$P_b = \frac{M}{2(M-1)} \sum_{t=t_{min}}^{t_{max}} P_E . P_T^1(t) \tag{4.7}$$

According to UC-MPC's correlation properties, the upper bounded error probability P_E can be modified and expressed as follows:

$$P_E \leq \sum_{l_1=0}^{N-t} \binom{N-t}{l_1} \frac{1}{M^{l_1}} \left(1-\frac{1}{M}\right)^{N-t-l_1} \times$$

$$\sum_{l_0=0}^{N-t-l_1} \binom{N-t-l_1}{l_0} \frac{1}{(M-1)^{l_0}} \left(1-\frac{1}{M-1}\right)^{N-t-l_0-l_1}$$

$$\exp\left(-Q.\frac{(p+1)^2}{4.(p+1+l_0+l_1)}\right) \tag{4.8}$$

4.3 Performance Analysis of UC-MPC

Performance of the proposed UC-MPC was analysed in three different synchronous OCDMA systems, based on the analysis discussed in Section 4.2. Then, for different values of prime numbers (p), these results were compared with those of the MPC code set. In addition, analysis provided in [2, 6] has been used to evaluate the MPC's performance.

The BER performance of the proposed code (UC-MPC) is demonstrated in Figure 4.1, in comparison with the well-known prime code set (MPC); as a function of p, and for the multiplicity factor M =16. As can be seen, UC-MPC outperforms in all the cases and offers a lower BER. Therefore, for a given prime number (p), the number of simultaneous active users (N) in the systems employing UC-MPC is greater than for those employing MPC.

For instance, for the given prime number *p=19*, MPC accommodates *N=48* simultaneous subscribers; whereas, in the same situation, UC-MPC can accommodate up to *N=74* users. Moreover, from the figure it can be seen that employing the higher value of prime number results in a lower BER.

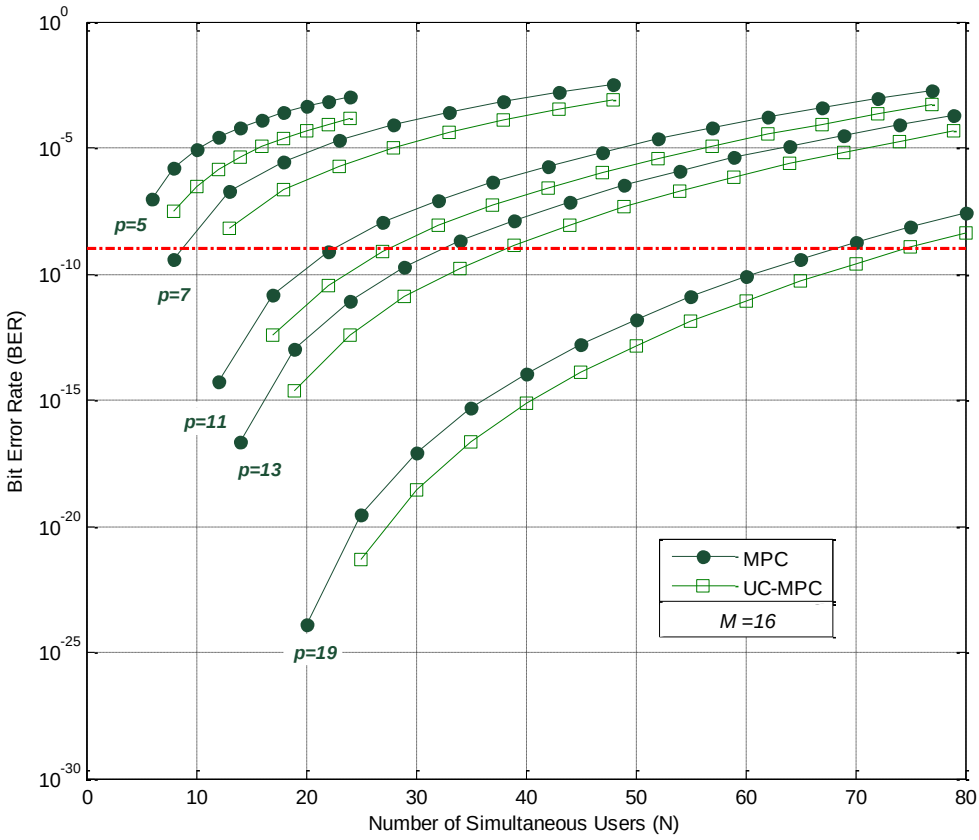

Figure 4.1 BER Performance of Lower Bounded PPM-OCDMA Systems for Various Prime Numbers (*p*)

The BER performance of the PPM-OCDMA systems for the previously mentioned three different cancellation techniques for the given characteristics *M=16, μ=100* and *p=19* are illustrated in Figure 4.2.

The performance of the OCDMA systems with cancellation scheme was found to be better. For instance, without a cancellation technique, the number of simultaneous active subscribers (N) under the communication with BER $\leq 10^{-9}$ are 65 for MPC, and 75 for UC-MPC, whereas the value of N for the systems implementing any of cancellation schemes is significantly higher.

Also, the systems with cancellation and no Manchester codes can accommodate up to 281 users in MPC and 300 users in UC-MPC, under a standard BER of 10^{-9}.

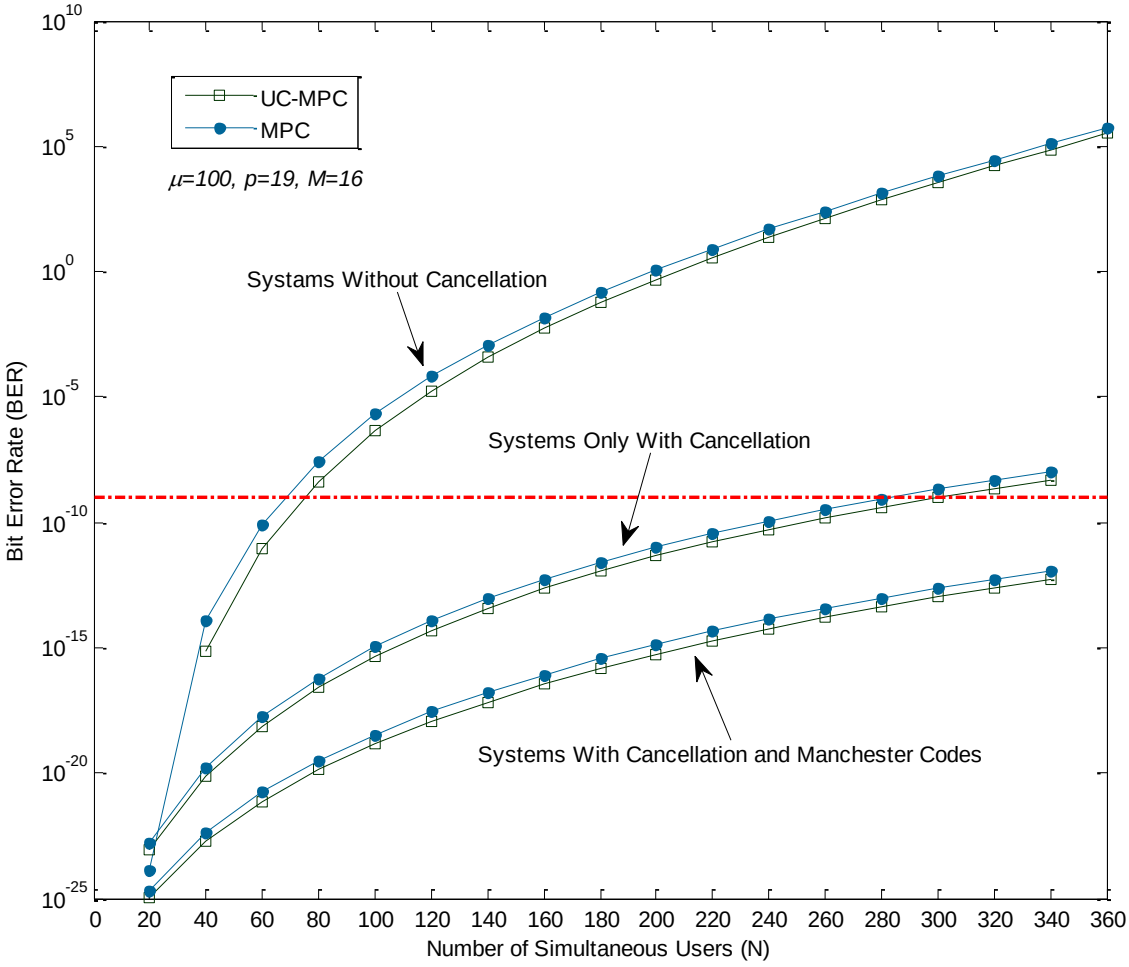

Figure 4.2 BER Performances of MPC and UC-MPC for PPM-OCDMA Systems with Different Cancellation Schemes

Moreover, systems employing both a cancellation scheme and Manchester codes can accommodate all of their 361 subscribers for a BER of 10^{-9}.

It was also found that, for systems using Manchester codes in the presence of a cancellation scheme, the performance is increased, in comparison with those not employing Manchester coding.

The enhanced performances of PPM-OCDMA systems using UC-MPC are shown in Figure 4.2, as compared with MPC. It should be also mentioned that increasing the signal multiplicity (M) results in further improvement of the performance, but it increases the system complexity as well.

4.4 Summary

In this chapter, the BER performances of PPM-OCDMA systems employing both the newly proposed prime code (UC-MPC) and the well-known MPC were analysed and investigated. It was found that for all the cases UC-MPC performs better than MPC.

An enhancement of the correlation properties results in a higher power efficiency. Also an increase in the code length improves the security. These are all advantages of the proposed UC-MPC. The Uniform cross-correlation prime code is the only prime code which offers the same probability of interference between each two selected code signatures, whereas other prime codes including MPC, new MPC (nMPC) [6], and double-padded MPC (DPMPC) [4], do not have such a characteristic.

All of the mentioned properties of UC-MPC would result in:

1. A decrease in the BER and enhancement of the performance
2. A higher difference between cross- and auto-correlation values which:
    a. Eases the decoding in the receivers.
    b. Enhances the performance of system employing asynchronous communications.

REFERENCES

[1] F. Liu and H. Ghafouri-Shiraz, "Analysis of PPM-CDMA and OPPM-CDMA communication systems with new optical code," in *Asia-Pacific Optical Communications*, pp. 602137-602137-9, 2005.

[2] H. M. H. Shalaby, "Cochannel interference reduction in optical PPM-CDMA systems," *Communications, IEEE Transactions on,* vol. 46, pp. 799-805, 1998.

[3] H. M. H. Shalaby, "Direct detection optical overlapping PPM-CDMA communication systems with double optical hardlimiters," *Lightwave Technology, Journal of,* vol. 17, pp. 1158-1165, 1999.

[4] M. M. Karbassian and H. Ghafouri-Shiraz, "Fresh Prime Codes Evaluation for Synchronous PPM and OPPM Signaling for Optical CDMA Networks," *Lightwave Technology, Journal of,* vol. 25, pp. 1422-1430, 2007.

[5] H. M. H. Shalaby, "Performance analysis of optical synchronous CDMA communication systems with PPM signaling," *Communications, IEEE Transactions on,* vol. 43, pp. 624-634, 1995.

[6] G. C. Yang and W. C. Kwong, *Prime codes with applications to CDMA optical and wireless networks*: Artech House Publishers, 2002.

Chapter 5

ANALYSIS OF IP TRANSMISSION AND ROUTING IN AN OPTICAL NETWORK UNIT

In this chapter the IP transmission and routing over FSK-OCDMA is studied, based on the proposed UC-MPC code set. It has been shown that this code enhances the system's security, BER, PER and the capacity of system, in comparison with the other prime code sets.

5.1 Introduction

During the last three decades, extensive investigations have been carried out on optical-CDMA codes which have been implemented in multimedia services [1-5]. However, development of a code family is of the interest for researchers working in this area to make it more efficient. In addition, the properties of the code, such as weight, length, as well as cardinality, are the parameters which extremely influence the number of subscribers accommodated in an optical communication system.

Moreover, the type of modulation, the receiver's topology, and also Multiple Access Interferences (MAI), all affect the system performance. On the other hand, Internet Protocol (IP) transmission has generated a great deal of interest during the past few decades, and will be discussed in different aspects, including modulations, protocols, receiver topologies and interference cancellation techniques. In addition, various coherent interference cancellers have been considered based, on different codes within different network architectures.

In addition, development of an appropriate novel orthogonal code can optimise the performance of an IP network which is implementing these code signatures. Subsequently, different achievements could be obtained, such as:

1. Enhancement of the system performance.
2. An increase in the number of simultaneous subscribers.
3. Provision of faster communication in both asynchronous and synchronous systems over IP.

This chapter covers the implementation analysis of the proposed UC-MPC code set in an IP transmission and routing within an optical network unit (ONU). This study has been carried out, based on Coherent Frequency Shift Keying Optical Code Division Multiple-Access (FSK-OCDMA) utilising an incoherent demodulation. As a result, the co-channel interference was reduced and subsequently the performance of the overall optical communication system was improved. In addition, it has been found that the correlation properties of the system, its BER, as well as its security, were all enhanced in comparison to the other prime codes.

5.2 Analysis of UC-MPC in IP Transmission and Routing over FSK-OCDMA

Figure 5.1 illustrates the architecture of the IP routing network over FSK-OCDMA [6]. The IP traffic to a *K* receiver are broadcasted by p^2 transmitters through a passive star coupler in this topology.

A FSK modulator as the OCDMA encoder, and UC-MPC as the signature code, are allocated for each transmitter. Moreover, each of the receivers has an FSK decoder, as well as a Multi Access Interference (MAI) canceller. Optical encoders and decoders implemented in *M-ary* FSK-OCDMA are discussed in [7].

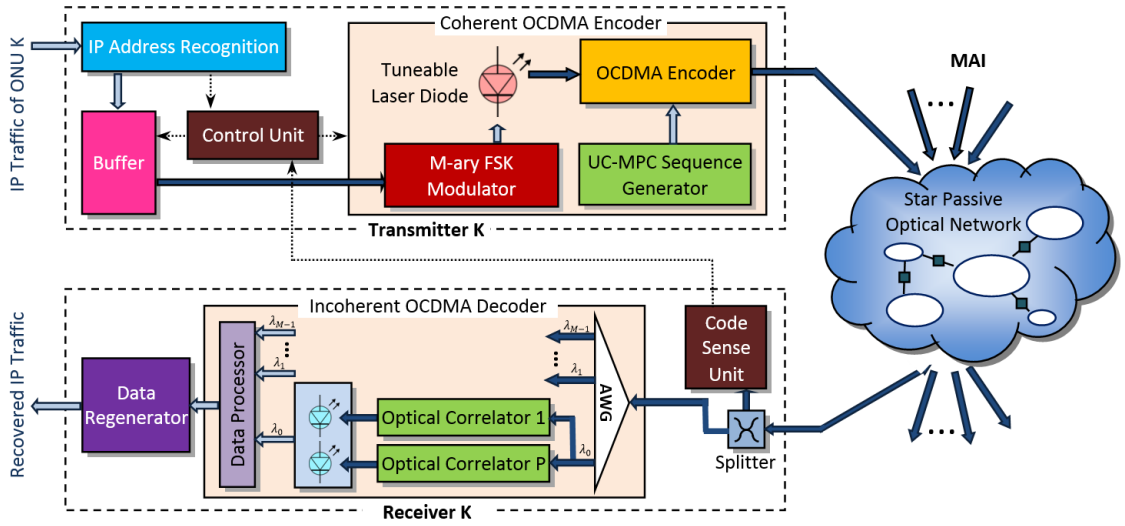

Figure 5.1 IP routing network architecture over OCDMA and employing UC-MPC

Based on the calculations provided in [6-8], the packet error rate (PER) formula is derived as follows:

$$PER = 1 - \left(1 - P_T(K)\right)^w \tag{5.1}$$

$$P_T(K) = \sum_{k=1}^{K} P_{IP}(k).P_b(k) \tag{5.2}$$

$$P_{IP}(K) = \binom{U}{K} P_{ac}^K (1 - P_{ac})^{U-K} \tag{5.3}$$

$$P_{ac} = \frac{1}{2}.\frac{K}{U}.B \tag{5.4}$$

$$\begin{aligned} P_b \leq \frac{M}{2} \sum_{r=r_{min}}^{r_{max}} \sum_{l_{0,0}=0}^{K-r} \sum_{l_{1,0}=0}^{K-r-l_{0,0}} & \binom{K-r-l_{0,0}}{l_{1,0}} \times \left(\frac{1}{\gamma.M}\right)^{l_{1,0}} \\ & \times \left(1 - \tfrac{1}{\gamma.M}\right)^{K-r-l_{0,0}-l_{1,0}} \times \exp\left[-\tfrac{\rho Q}{2}.\tfrac{p+1}{2}\right] \\ & \times \binom{K-r}{l_{0,0}} \times \left(\frac{1}{\gamma.M}\right)^{l_{0,0}} \times \left(1 - \frac{1}{\gamma.M}\right)^{K-r-l_{0,0}} \\ & \times \binom{p^2-2p+1}{K-r} \times \frac{\binom{p-2}{r-1}}{\binom{p^2-p-1}{K-1}} \end{aligned} \tag{5.5}$$

where

$$Q = \mu \cdot \frac{Ln\, M}{p+1} \quad , \quad \rho = \frac{p+1}{p+1+l_{0,0}+l_{1,0}} \, ,$$

$$r_{max} = min(K, p-1)\,, \qquad r_{min} = max(1, K-(p-1)^2) \quad and$$

$$B = \frac{Average\ Output\ Bitrate}{Maximum\ Transmission\ Bitrate}$$

where [6-8]:

P_T	Total probability of error
P_{IP}	Probability Density Function (PDF) of *K* simultaneous active subscribers transmitting IP packet
P_{ac}	Probability of *K* subscribers being active
P_b	Bit error rate of decoder employing UC-MPC as the signature code
B	Channel utilisation factor
Q	Average received photon count per pulse
ρ	Parameter which minimizes the interference
$\gamma \; or \; j$	Reception ratio
U	Total number of accommodated subscribers in the network
w	Average packet length
$l_{m,v}$	Number of subscribers which have a pulse in the *v*th slot with wavelength λ_m, except those in the first group
μ	Average number of photons per pulse
M	Number of wavelengths in the *M*-ary frequency signal distribution

5.3 Discussion of the Results

Performance analysis of the IP traffic over FSK-OCDMA employing UC-MPC, is demonstrated in Figure 5.2 for various numbers of prime numbers *(p)* and channel utilisation values *(B)*, against the number of active users.

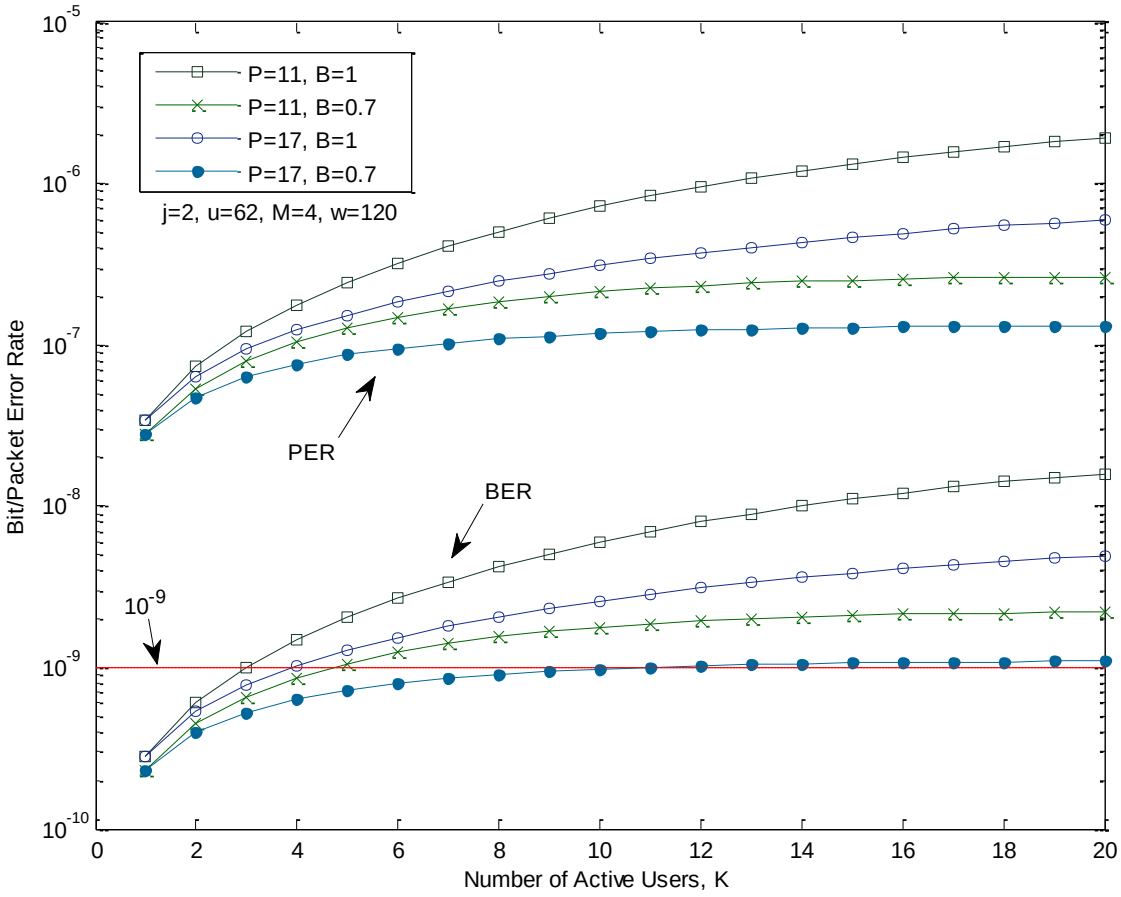

Figure 5.2 PER and BER of IP traffic over FSK-OCDMA employing UC-MPC, for various numbers of p and B against the number of active users (K)

The analysis has been carried out for the given values of *j=2*, *u=62*, *M=4* and *w=120*, using the Equations (5.1)-(5.5). The results show that increasing *p* would result in the performance enhancement; whereas increasing *B* increases the BER. For instance, a 30%

decrease in *B* from 1 to 0.7 when *p=17*, increases the capacity of the system by 200%, from *N=4* to *N=12*. Moreover, the Packet Error Rate (PER) has also has a direct relation to *B* and an indirect relation to *p*. For instance, again a 30% decrease in *B* from 1 to 0.7 when *p=17* and *K=12*, decreases the PER of system by about 67%. In addition, an increase of *p* from *p=14* to *p=17*, results in about 56% of a decrease in PER.

Figure 5.3 illustrates how the BER of MPC and UC-MPC vary against the maximum number of active users. It can be concluded from the results that UC-MPC offers a better BER, and hence accommodates more active users, for all the values of *B*.

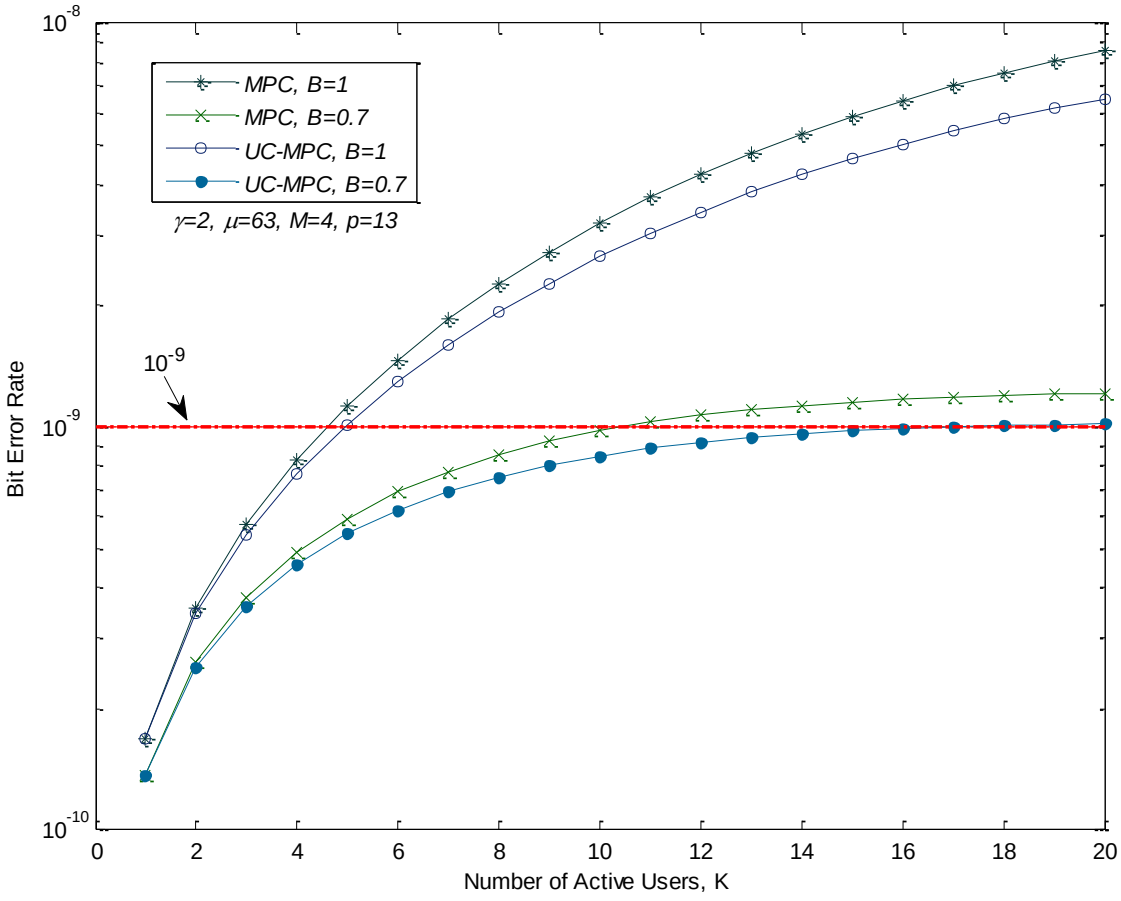

Figure 5.3 BER Performance comparison of IP traffic over FSK-OCDMA between MPC and UC-MPC

For instance, for *B=0.7*, the maximum number of users (*N*) that can be accommodated in the system for a reliable, standard BER $\leq 10^{-9}$, are 17 and 10, for UC-MPC and MPC, respectively. All in all, it can be concluded that, utilising UC-MPC's signature codes as a replacement for MPC could enhance the performance of the system.

It should be noted that the results has been cross-checked with the prior arts [6-8].

5.4 Summary

In this investigation, the Uniform Cross-Correlation Prime Code (UC-MPC) was utilised in the IP transmission and routing system over FSK-OCDMA. The performance of the system was examined for different prime numbers *(p)* and channel utilisation values *(B)*. It was concluded that the performance of the network was improved by increasing *p* as well as reducing *B* under the same conditions.

In addition, it was concluded that utilisation of UC-MPC resulted in an enhancement in the performance of the network. Consequently, the number of active user that could be supported was considerably increased, in comparison to the same case but employing the MPC.

REFERENCES

[1] H. M. H. Shalaby, "Cochannel interference reduction in optical PPM-CDMA systems," *Communications, IEEE Transactions on,* vol. 46, pp. 799-805, 1998.

[2] H. M. H. Shalaby, "Complexities, error probabilities, and capacities of optical OOK-CDMA communication systems," *Communications, IEEE Transactions on,* vol. 50, pp. 2009-2017, 2002.

[3] G. C. Yang and W. C. Kwong, *Prime codes with applications to CDMA optical and wireless networks*: Artech House Publishers, 2002.

[4] M. M. Karbassian and H. Ghafouri-Shiraz, "Performance analysis of heterodyne-detected coherent optical CDMA using a novel prime code family," *Journal of Lightwave Technology,* vol. 25, pp. 3028-3034, 2007.

[5] F. Liu, M. M. Karbassian, and H. Ghafouri-Shiraz, "Novel family of prime codes for synchronous optical CDMA," *Optical and Quantum Electronics,* vol. 39, pp. 79-90, 2007.

[6] M. M. Karbassian and H. Ghafouri-Shiraz, "IP Routing and Transmission Analysis in Optical CDMA Networks: Coherent Modulation With Incoherent Demodulation," *Lightwave Technology, Journal of,* vol. 27, pp. 3845-3852, 2009.

[7] M. M. Karbassian and H. Ghafouri-Shiraz, "Novel Channel Interference Reduction in Optical Synchronous FSK-CDMA Network Using a Data-Free Reference," *Lightwave Technology, Journal of,* vol. 26, pp. 977-985, 2008.

[8] M. M. Karbassian and H. Ghafouri-Shiraz, "IP Routing and Traffic Analysis in Coherent Optical CDMA Networks," *Lightwave Technology, Journal of*, vol. 27, pp. 1262-1268, 2009.

Chapter 6

PROPOSING THE TRANSPOSED UC-MPC

A novel codes set is proposed based on the Uniform Cross-Correlation Modified Prime Code (UCMPC), hereby referred to as the Transposed UC-MPC (T-UCMPC). This code set offers higher capacity, better spectral efficiency, lower BER and higher security, compared to other existing prime codes.

6.1 Introduction

Various optical orthogonal codes have been proposed and evaluated in different optical CDMA networks in the past few years [1-5], but proposing a novel code family which enhances the network capacity, and its spectral efficiency is still an on-going challenge. Many code families has been introduced recently which either are new prime code sets or are a modified versions of existing prime code families (e.g. padded MPC (PMPC) [1], the new MPC (nMPC) [2], double-padded MPC (DPMPC) [3], and Transposed Modified Prime Codes (T-MPC) [4].

In Chapter 3 a novel prime code family, named Uniform Cross Correlation Modified Prime Code (UCMPC), has been proposed which outperforms other available prime code families. It was discussed that UCMPC offers better spectral efficiency, lower bit error rate (BER), uniform and unity cross-correlation and higher security. In addition, this code set can be easily implemented in the existing networks with minimal cost and no change in the hardware.

In this section, the UCMPC is implemented in an optical network unit (ONU) for IP transmission and routing [6]. The results indicated that UCMPC enhances both the bit error rate (BER) and packet error rate (PER) of the system.

6.2 Construction of T-UCMPC Conclusion

The novel T-UCMPC is constructed, based on the Uniform Cross-Correlation Modified Prime Code, which is explained in detail in the previous chapters. Table 6.1 shows code and binary sequences of UCMPC over a Galois Field of 3 (i.e. *p=3*) which is obtained by using the algorithms and formulas provided in Chapter 3 . In this table, *p* is a prime number, *i* is the group number, *x* is the code index within a group, *j* is the sub-sequence index, *n* is the code index and *k* is the bit index within the binary code sequence. The transposed version of UCMPC can be expressed as:

$$C_{T-UCMPC}(n,k) = C_{UCMPC}(k,n) \tag{6.1}$$

TABLE 6.1
UC-MPC CODE SET OVER GF(3)

Index			$S_{UC\text{-}MPC}$				$C_{UC\text{-}MPC}$											
							j=0			*j=1*			*j=2*			*j=3*		
i	*x*	*n*	*j=0*	*j=1*	*j=2*	*j=3*	*k*											
							0	1	2	3	4	5	6	7	8	9	10	11
0	0	0	1	4	4	2	0	0	1	1	0	0	1	0	0	0	1	0
	1	1	2	5	0	4	0	1	0	1	0	1	0	0	0	1	0	0
	2	2	4	6	1	0	1	0	0	1	1	0	0	0	1	0	0	0
1	0	3	1	1	3	0	0	0	1	0	0	1	0	1	1	0	0	0
	1	4	2	2	2	2	0	1	0	0	1	0	0	1	0	0	1	0
	2	5	4	0	6	4	1	0	0	0	0	0	1	1	0	1	0	0
2	0	6	1	2	0	5	0	0	1	0	1	0	0	0	0	1	0	1
	1	7	2	0	5	1	0	1	0	0	0	0	1	0	1	0	0	1
	4	8	4	1	0	3	1	0	0	0	0	1	0	0	0	0	1	1

Table 6.2 illustrates the transposed version of Table 6.1 which has been produced using Equation (6.1). UCMPC has p groups of code sequences where each group contains p codes, and it can accommodate up to $N_{UCMPC}=p^2$ subscribers. The code length of each subscriber is $L_{UCMPC}= p^2+p$. On the other hand, T-UMPC contains $p+1$ groups of code sequences, each have p codes and can handle up to $N_{T\text{-}UCMPC} =p^2+p$ subscribers. This means the capacity of network is increased by p. It should be mentioned that codes in T-UCMPC have the length of $L_{T\text{-}UCMPC} =p^2$.

TABLE 6.2
TUC-MPC CODE SET OVER GF(3)

Index			$S_{TUC\text{-}MPC}$			$C_{TUC\text{-}MPC}$								
						j=0			*j=1*			*j=2*		
i	*x*	*n*	*j=0*	*j=1*	*j=2*	*k*								
						0	1	2	3	4	5	6	7	8
0	0	0	1	1	1	0	0	1	0	0	1	0	0	1
	1	1	2	2	2	0	1	0	0	1	0	0	1	0
	2	2	4	4	4	1	0	0	1	0	0	1	0	0
1	0	3	7	0	0	1	1	1	0	0	0	0	0	0
	1	4	1	2	4	0	0	1	0	1	0	1	0	0
	2	5	2	4	1	0	1	0	1	0	0	0	0	1
2	0	6	4	1	2	1	0	0	0	0	1	0	1	0
	1	7	0	7	0	0	0	0	1	1	1	0	0	0
	2	8	1	4	2	0	0	1	1	0	0	0	1	0
3	0	9	2	1	4	0	1	0	0	0	1	1	0	0
	1	10	4	2	1	1	0	0	0	1	0	0	0	1
	4	11	0	0	7	0	0	0	0	0	0	1	1	1

6.3 Analysis and Discussion of Results

Each T-UCMPC binary code sequence can be presented as:

$$C_{T-UCMPC}(n,p) = (c_{n,0}, c_{n,1}, \dots, c_{n,k}, \dots, c_{n,p^2+p-1}) \quad (6.2)$$

In addition, the discrete correlation function $R_{C_{n_1}C_{n_2}}$ at the m^{th} chip position for two binary sequences $C_{n_1} = C_{T-UCMPC}(n_1,p)$ and $C_{n_2} = C_{T-UCMPC}(n_2,p)$ is defined as [5]:

$$R_{C_{n_1}C_{n_2}}(m) = \sum_{k=0}^{L-1} c_{n_1,k} \cdot c_{n_2,k+m} \quad (6.3)$$

Where C_{n_1} & C_{n_2} ϵ {0, 1}, L is the code length and $|m| \leq L-1$. Figure 6.1(a) to Figure 6.1(d) show the correlation functions of all possible pairs of the code sequences for p=5 synchronised UCMPC and T-UCMPC. All these correlation values are calculated at the chip synchronization position (i.e. m=0 in (3)), which is referred to as the synchronised correlation between each pair code sequences. As figures indicate, for all UCMPC combinations, the auto-correlation values (diagonal values) and cross-correlation values are $p+1$=6 and 1, respectively. The correlation function $R_{C_{n_1}C_{n_2}}(m)$ for a given pair of T-UCMPC sequences at the synchronous time is given as:

$$R_{C_{n_1}C_{n_2}}(0) = \begin{cases} p, & n_1 = n_2 \\ 0 \text{ or } 1, & n_1 \neq n_2 \end{cases} \quad (6.4)$$

Figure 6.1(d) clearly shows that the cross-correlation, for each two distinct code sequences within the group, is zero.

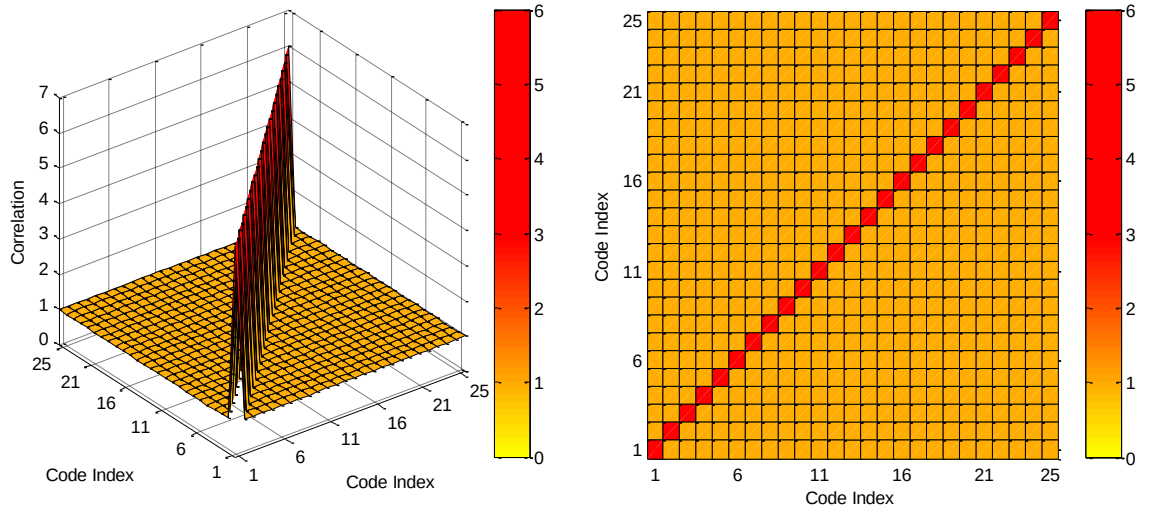

(a) (b)

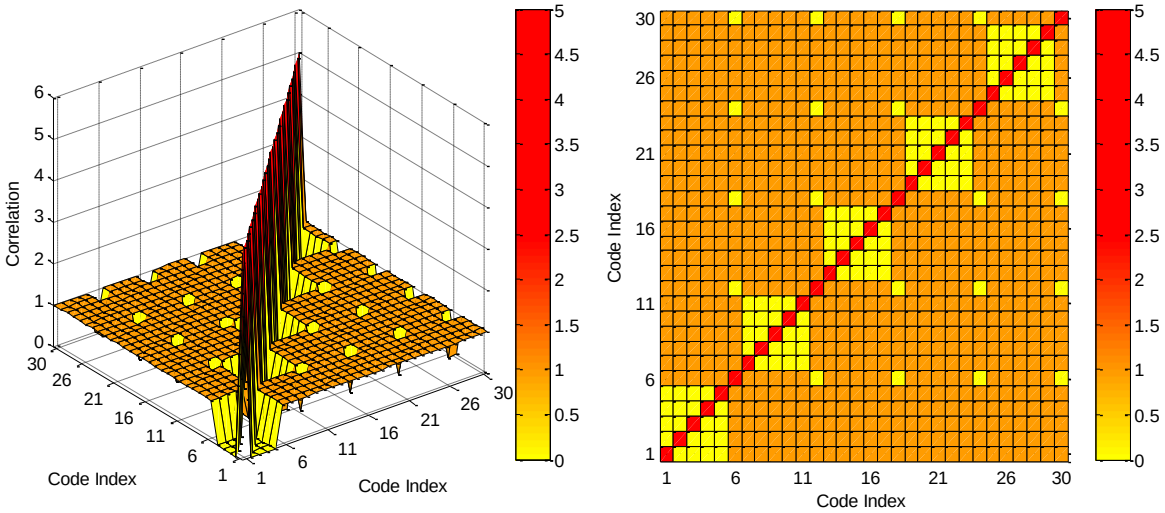

(c) (d)

Figure 6.1 Correlation functions of UCMPC and T-UCMPC families over GF(5) in a synchronised system (a) UCMPC (3D View), (b) UCMPC (Top View), (c) T-UCMPC (3D View), (d) T-UCMPC (Top View)

Moreover, based on the hit possibility between '1s' within different signature codes, the BER of an intensity-modulated On-Off Keying (OOK) system can be expressed as [4, 7]:

$$BER = \frac{1}{2}\sum_{i=0}^{w/2}(-1)^i \binom{\frac{w}{2}}{i}\left(1-\frac{2.f.i}{w}\right)^{K-1}$$
$$f = \frac{w^2}{4L} \tag{6.5}$$

where w and K are the code weight and number of active subscribers, respectively. Figure 6.2 illustrates the bit error rates of both UCMPC and T-UCMPC in a system with OOK modulation, as a function of number of simultaneous users (K) and for different prime codes (i.e T-MPC [4], MPR [7], UCMPC [5] and T-UCMPC).

In this figure, T-UCMPC families with greater length are padded by zeroes. As the figure shows, the T-UCMPC outperforms the others and the maximum number of active subscribers (*N*) increases in a system that employs T-UCMPC as its signature code. For example, for a low-weight modified prime code MPR [7] with code weight of w=24, the maximum number of simultaneous users which the system can accommodate is *N*=60, whereas *N=165* for a zero-padded T-UCPMC that has the same code weight and length (i.e. a 175% increase). In addition, this figure illustrates the higher the value of *L*, the lower the value of BER.

6.4 Summary

In this chapter a novel family of optical orthogonal codes, hereby referred to as T-UCMPC, is proposed for optical CDMA systems. T-UCMPC correlation properties have been analysed and compared its results with those of the newly proposed UCMPC [5].

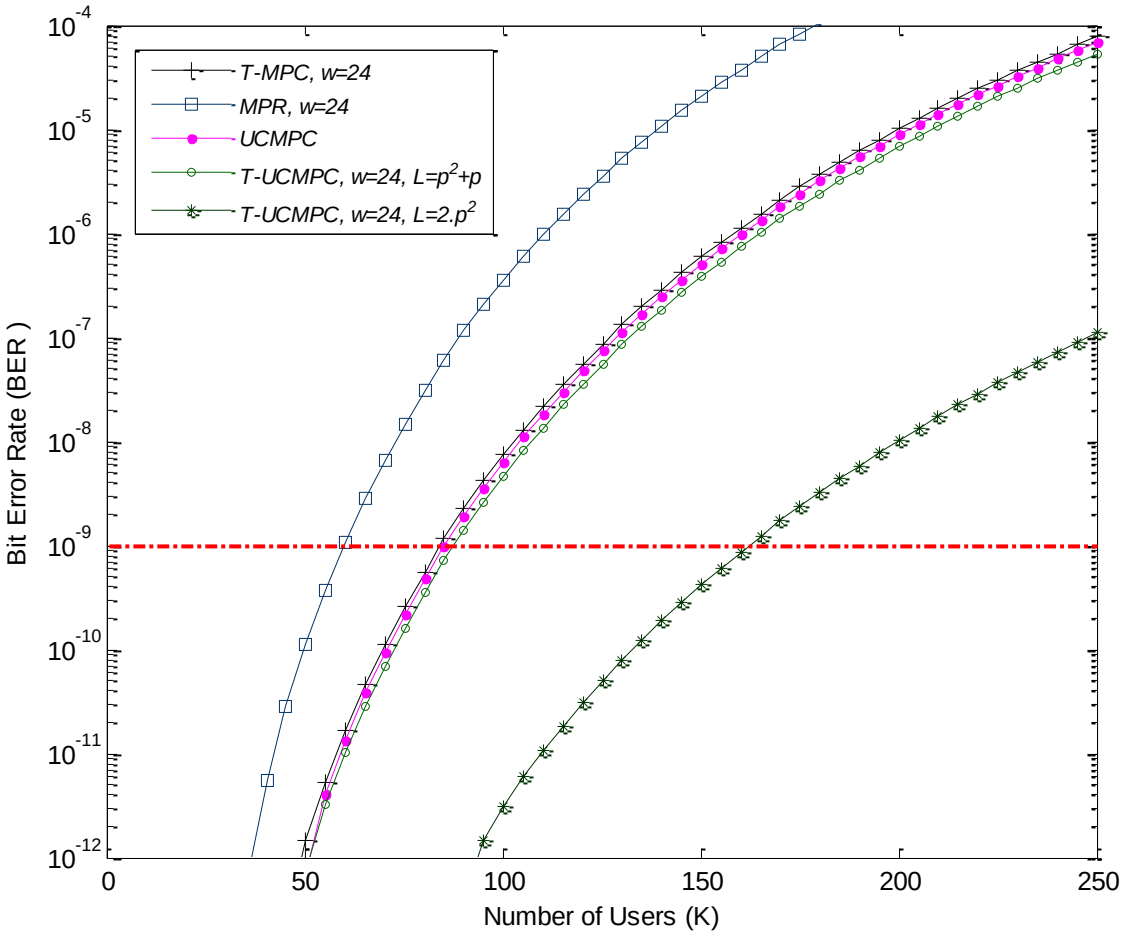

Figure 6.2 BER Performance of Lower Bounded PPM-OCDMA Systems for Various Prime Numbers (p)

It has been found that the cardinality of the T-UCMPC has increased to p^2+p, as compared with p^2 in MPC, PMPC nMPC, DPMPC and UCMPC. This means more users can be accommodated within the system and hence the system's capacity increases considerably. In addition, the new code set offers a secure transmission and results in lowering the system BER and enhancing the number of active simultaneous users in the OCDMA systems.

REFERENCES

[1] M. Y. Liu and H. W. Tsao, "Cochannel interference cancellation via employing a reference correlator for synchronous optical CDMA systems," *Microwave and Optical Technology Letters,* vol. 25, pp. 390-392, 2000.

[2] F. Liu, M. M. Karbassian, and H. Ghafouri-Shiraz, "Novel family of prime codes for synchronous optical CDMA," *Optical and Quantum Electronics,* vol. 39, pp. 79-90, 2007.

[3] M. M. Karbassian and H. Ghafouri-Shiraz, "Performance analysis of heterodyne-detected coherent optical CDMA using a novel prime code family," *Journal of Lightwave Technology*, vol. 25, pp. 3028-3034, 2007.

[4] M. M. Karbassian and F. Kueppers, "OCDMA code utilization increase: capacity and spectral efficiency enrichment," in *Global Telecommunications Conference (GLOBECOM 2010), 2010 IEEE*, pp. 1-5, 2010.

[5] M. H. Zoualfaghari and H. Ghafouri-Shiraz, "Uniform cross-Correlation modified prime code for applications in synchronous optical CDMA communication systems," *Lightwave Technology, Journal of*, vol. 30, pp. 2955-2963, 2012.

[6] M. Zoualfaghari and H. Ghafouri‐Shiraz, "Analysis of a novel prime code in IP transmission and routing over FSK‐OCDMA in an optical network unit," *Microwave and Optical Technology Letters,* vol. 54, pp. 2852-2856, 2012.

[7] J.-G. Zhang, A. Sharma, and W. C. Kwong, "Cross-correlation and system performance of modified prime codes for all-optical CDMA applications," *Journal of Optics A: Pure and Applied Optics*, vol. 2, p. L25, 2000.

Chapter 7

PROPOSING A NOVEL MUI CANCELLATION SCHEME

In this chapter a novel multi-user interference (MUI) cancellation scheme is proposed for OCDMA systems employing prime code families. Also the feasibility and implementation of this novel scheme is discussed in detail. In addition, the performance analysis of a few prime code families are evaluated experimentally using this newly proposed MUI cancellation scheme. The results reveal that the proposed scheme is easy to implement, and totally removes the MUI effect.

7.1 Introduction

The optical code division multiple-access (OCDMA) method makes several transmitters able to transmit data simultaneously, using the same channel [1]. In an OCDMA receiver, the desired subscriber signal is correlated by the corresponding code sequence, decoded and detected. However, interferences due to other subscribers' signals result in multi-user interferences (MUI) which severely limit the capacity of OCDMA networks [2, 3].

As the number of simultaneous subscribers increases, the performance of an OCDMA system decreases dramatically, due to the increase in MUI. Generally speaking, this problem can be overcome by using appropriate orthogonal code sets [1, 4-6] and interference cancellation scheme [2, 3, 7, 8].

In this chapter a novel MUI cancellation scheme is proposed, which is derived from the author's proposed theorem that can be applied to all prime code families. This scheme is simple and can also be easily implemented in the existing systems with minimal cost. In this chapter the background theory and proposed scheme are explained. Then, methodology and implementation techniques are discussed and finally the conclusion is given.

7.2 Theory and the Proposed Scheme

A novel prime code family was introduced in Chapter 3 , referred to as the ”Uniform Cross-Correlation Modified Prime Code (UC-MPC)”, which has excellent correlation properties, and delivers a very low receiver BER [5, 6]. However, a close inspection of UC-MPC [6], the modified prime code (MPC) [1], and the double-padded modified prime code (DPMPC) [4] have inspired the development of the following scheme, as all these codes have some common properties and characteristics.In general, a prime code family with weight *w* and length *L* can accommodate *U* unique prime code sequences, where any code pair has a maximum cross-correlation of unity. Starting with UC-MPC, the proposed scheme will be developed, which will then be generalized to include all other prime codes. Table 7.1 shows all possible values of $C_{UC\text{-}MPC}(n,p)$ for $p = 3$ [6], where *n* is the code index ($0 \leq n < p^2$), *j* is the sub-sequence index within the code ($0 \leq j \leq p$), $i=\left\lfloor \frac{n}{p} \right\rfloor$ is the group number, and $x=n \pmod p$ is the code index within a group.

7.2.1 Theorem

> “A **unique** sequence, C_T, is obtained by adding any *N* number of UC-MPC sequences which contains useful information about the source transmitters.”

All injected bits (IBs) are highlighted in Table 7.1, where the k^{th} column shows the location of the injected bits. For given values of both *j* ($0< j \leq p$) and *p*, then $k=j(p+1)$. That is, in Table 7.1 since $p=3$ for $j=1, 2$ and 3 the IBs are located in the $k=4^{th}$, $k=8^{th}$ and

$k=12^{th}$ columns. For all codes in the i^{th} group, the injected '1' bits are located in the $j=i+1$ sub-sequence. As an example, consider $C_{UC-MPC}(0,3)$=*(001 100 100 010)*, the group number is $i = \left\lfloor \frac{0}{3} \right\rfloor = 0$ and hence $j=1$. This implies that all injected '1' bits are located in the 4th column. Moreover, the injected bits (i.e. IBs) in the same column (i.e. $k=4$) of the other groups (i.e. $i=1$ and $i=2$) are all zeros.

TABLE 7.1
UC-MPC CODE SET FOR $p = 3$

Index				$C_{UC\text{-}MPC}$											
				j=0			*j=1*			*j=2*			*j=3*		
i	*x*	*n*	C_n	*k=1*	*k=2*	*k=3*	***k=4***	*k=5*	*k=6*	*k=7*	***k=8***	*k=9*	*k=10*	*k=11*	***k=12***
0	0	0	C_0	0	0	1	1	0	0	1	0	0	0	1	0
	1	1	C_1	0	1	0	1	0	1	0	0	0	1	0	0
	2	2	C_2	1	0	0	1	1	0	0	0	1	0	0	0
1	0	3	C_3	0	0	1	0	0	1	0	1	1	0	0	0
	1	4	C_4	0	1	0	0	1	0	0	1	0	0	1	0
	2	5	C_5	1	0	0	0	0	0	1	1	0	1	0	0
2	0	6	C_6	0	0	1	0	1	0	0	0	0	1	0	1
	1	7	C_7	0	1	0	0	0	0	1	0	1	0	0	1
	2	8	C_8	1	0	0	0	0	1	0	0	0	0	1	1

In general, for any given group number *i*, only the injected '*1*' bits are located in the k^{th} column, and this is the reason that makes this group *i* unique, when compared with other groups.

In other words, any code sequence or summation of code sequences in a given group (say i_1) cannot be replaced by any code sequence or summation of code sequences in any other group (say i_2 and $i_2 \neq i_1$), to produce the same C_T (Fact 1).

In addition, because the cross-correlation of each pair code in UC-MPC is one, hence, for $k \neq j(p+1)$, there are p '1's in each group code sequence that are not in the same position of any other '1's in the other code sequences within the same group. Therefore, any code sequence, or any summation of code sequences within a specific group which constructs C_T, cannot be replaced by any code sequence or summation of code sequences from the same group (Fact 2).

Hence, based on the above Facts 1 and 2, it can be concluded that C_T is a unique sequence, and that there are no other N code sequences that can be added to produce C_T. This new sequence (C_T) contains useful information, which will be discussed in the coming sections.

7.2.2 Construction of the unique sequence

For example, consider four digital code sequences, C_0, C_1, C_2 and C_3 (hereby referred to as simultaneous user codes) from Table 7.1. A unique sequence C_T is obtained by adding the corresponding bit of each four sequences as shown in Table 7.2. In addition Figure 7.1 shows their associated optical pulse sequences.

As Table 7.1 shows, the weight of each sequence is the same ($w = p + 1 = 4$), which implies the optical energy 'E' of each code sequence is identical. On the other hand, based on the energy conservation law, the total energy should remain constant which implies:

$$E_{C_T} = \sum_{n=1}^{N} E_{C_n} = N.E_C.$$

Therefore, the number of simultaneous users, N, can be obtained as:

$$N = \frac{E_{C_T}}{E_c} = \frac{E_{C_T}}{w.E_p} \tag{7.1}$$

where E_c is the average energy per simultaneous user, E_{C_T}, E_{C_n} and E_p are, respectively, optical energies of C_T, the n[th] code sequence C_n and each pulse within the sequence.

TABLE 7.2
FOUR UC-MPC CODES AND THEIR UNIQUE CODE C_T

C_0	0	0	1	1	0	0	1	0	0	0	1	0
C_1	0	1	0	1	0	1	0	0	0	1	0	0
C_2	1	0	0	1	1	0	0	0	1	0	0	0
C_3	0	0	1	0	0	1	0	1	1	0	0	0
C_T	1	1	2	3	1	2	1	1	2	1	1	0

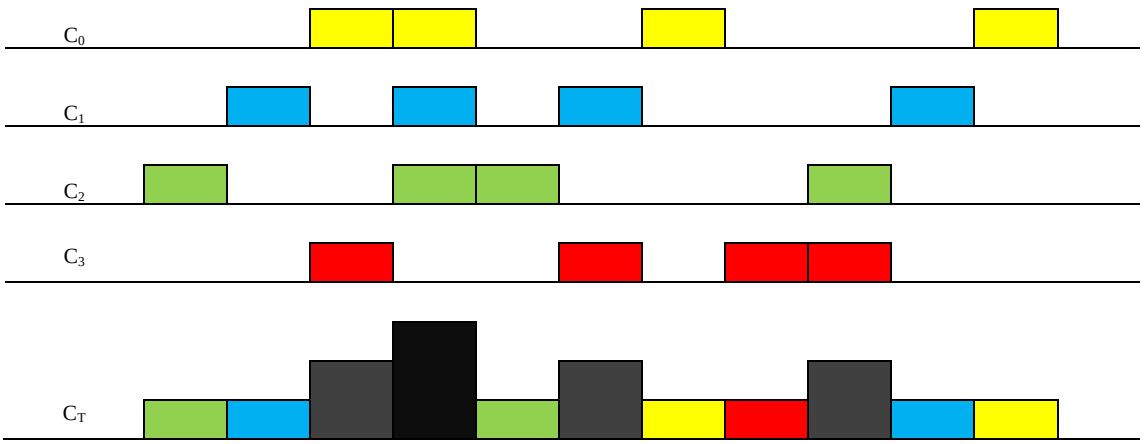

Figure 7.1 C_0, C_1, C_2, C_3 and C_T optical pulse sequences

For example, referring to the code C_T given in Table 7.2 and Figure 7.1:

$$E_c = E_{C_{UC\_MPC}} = w.E_p = 4.E_p$$

$$E_{C_T} = (1+1+2+3+1+2+1+1+2+1+1+0).E_p$$

$$= 16.E_p$$

Hence:

$$N = \frac{E_{C_T}}{E_c} = \frac{16.E_p}{4.E_p} = 4$$

7.2.3 Extraction of the constructor code sequences

In general, for any prime number 'p' and any code family having $N \leq p^2$ simultaneous active users, there are $\sum_{N=1}^{p^2} \binom{p^2}{N}$ unique sequences. This is because there are p^2 groups, each containing $\binom{p^2}{N}$ unique sequences. The look-up Table 7.3 shows all possible unique code sequences, C_T, and their associated constructor code sequences for the UC-MPC over GF($p = 3$). This table consists of three main columns: (i) index (i.e. group number and N); (ii) all unique code sequences in each group for a given N; and (iii) all constructor code sequences which are used to construct the corresponding unique sequences. This table has $p^2 = 9$ groups, where each group contains $\binom{9}{N}$ unique sequences. Hence, in the fourth group $(N = 4)$ there are 126 unique sequences, where each one of them is obtained by adding four constructor sequences, as indicated by tick marks in the look-up Table 7.3.

In general, for a given C_T, Table 7.3 can be used to extract all possible C_i. In doing so, the following algorithm may be used:

(i) Find the number of simultaneous users, *N*, using Equation (7.1)
(ii) Enter the table with this value of N and locate C_T
(iii) Finally, constructor code sequences (C_i) can be found in the same row of this table, next to the located C_T

As an example, let us find all possible constructor code sequences for the received signal $C_T = 112,312,112,110$. Following the above algorithm, from Equation (7.1) there are $N = 4$ and hence the locations of C_T and their corresponding constructor code sequences C_0, C_1, C_2 and C_3 can be easily found in Table 7.3, as highlighted. As explained in later sections, in each optical receiver the received signal C_T is correlated with the corresponding code sequence and after photo-detection the resulting electrical signal passes through a threshold detecting system which generates the data bits. The discrete correlation function for the received signal C_T and the corresponding code sequence C_n of the n^{th} receiver is:

$$R_{C_T C_n}(m) = \sum_{k=0}^{L-1} c_{T,k}.c_{n+m} \tag{7.2}$$

where L is the sequence length, n is the code index ($0 \leq n < p^2$) and $|m| \leq L - 1$. It should be noted that in a synchronised OCDMA system $m = 0$. Also $L = p^2 + p$ for UC-MPC [6]. γ and ψ_n are defined as the correction coefficient array and the corrected correlation parameter, respectively, as $\gamma = \{\gamma_0, \gamma_1, \dots, \gamma_n, \dots, \gamma_{p^2-1}\}$, where:

$$\gamma_n = \begin{cases} 1, & \text{When } C_n \text{ is a constructor code sequence} \\ 0, & \text{Otherwise} \end{cases}$$

and $$\psi_n = R(C_T, C_n) \times \gamma_n$$

Table 7.4 shows values of $R(C_T, C_n)$, γ_n and ψ_n for the code $C_T = 112,312,112,110$. In this case as Figure 7.1 shows:

$$\gamma_n = \begin{cases} 1, & 0 \le n \le 3 \\ 0, & \text{Otherwise} \end{cases}$$

Equation (7.2) can be used to calculate the in-phase ($m = 0$) correlation value of the received signal for each receiver. For example, referring to Figure 7.1, then:

$$R(C_T, C_0) = 0 + 0 + 2 + 3 + 0 + 0 + 1 + 0 + 0 + 0 + 1 + 0 = 7$$

TABLE 7.3
THE LOOK-UP TABLE WITH ALL POSSIBLE UNIQUE CODE SEQUENCES, C_T, AND THEIR ASSOCIATED CONSTRUCTOR CODE SEQUENCES FOR THE UC-MPC OVER GF($p = 3$)

Index		Unique Code Sequence C_T												Constructor Code Sequences C_i								
Group	*N*													C_0	C_1	C_2	C_3	C_4	C_5	C_6	C_7	C_8
1	1	0	0	1	1	0	0	1	0	0	0	1	0	✓								
	1	0	1	0	1	0	1	0	0	0	1	0	0		✓							
	1	1	0	0	1	1	0	0	0	1	0	0	0									
	…	…			…			…			…			…			…			…		
2	2	0	1	1	2	0	1	1	0	0	1	1	0	✓	✓							
	2	1	0	1	2	1	0	1	0	1	0	1	0	✓		✓						
	2	0	0	2	1	0	1	1	1	1	0	1	0	✓			✓					
	…	…			…			…			…			…			…			…		
3	3	1	1	1	3	1	1	1	0	1	1	1	0	✓	✓	✓						
	3	0	1	2	2	0	2	1	1	1	1	1	0	✓	✓		✓					
	3	0	2	1	2	1	1	1	1	0	1	2	0	✓	✓			✓				
	…	…			…			…			…			…			…			…		
4	**4**	**1**	**1**	**2**	**3**	**1**	**2**	**1**	**1**	**2**	**1**	**1**	**0**	✓	✓	✓	✓					
	4	1	2	1	3	2	1	1	1	1	1	2	0	✓	✓	✓		✓				
	4	2	1	1	3	1	1	2	1	1	2	1	0	✓	✓	✓			✓			
	…	…			…			…			…			…			…			…		
	⋮	⋮			⋮			⋮			⋮			⋮			⋮			⋮		
p^2=9	9	3	3	3	3	3	3	3	3	3	3	3	3	✓	✓	✓	✓	✓	✓	✓	✓	✓

The first column of Table 7.4 lists values of $R(C_T, C_n)$ for each constructor sequence (C_i, $i = 0\ to\ 3$) and each non-constructor sequence (C_i, $i = 4\ to\ 8$) which are 7 and 4, respectively. Also listed in the table are the values of γ_n and ψ_n. Usually, in an OCDMA receiver, the threshold value is set to be equal to the code weight, w, which means the receiver detects bit "1" when $R(C_T, C_i) \geq w$ and bit "0" otherwise. In this example, the receiver not only detects the constructor sequences, but also detects the unwanted non-constructor sequences ($C_4\ to\ C_8$). However, in the proposed novel MUI Canceller block (i.e. Section 7.3), each $R(C_T, C_n)$ value is multiplied by an associated correction coefficient to produce a new corrected correlation signal ψ_n which is free from the MUI (see Table 7.4).

TABLE 7.4
CORRELATION CORRECTION FOR $C_T = 112{,}312{,}112{,}110$.

$R(C_T, C_n)$			γ_n		ψ_n	
$R(C_T, C_0)$	7	✓: Correct	γ_0	1	ψ_0	7
$R(C_T, C_1)$	7	✓: Correct	γ_1	1	ψ_1	7
$R(C_T, C_2)$	7	✓: Correct	γ_2	1	ψ_2	7
$R(C_T, C_3)$	7	✓: Correct	γ_3	1	ψ_3	7
$R(C_T, C_4)$	4	×: Wrong	γ_4	0	ψ_4	0
$R(C_T, C_5)$	4	×: Wrong	γ_5	0	ψ_5	0
$R(C_T, C_6)$	4	×: Wrong	γ_6	0	ψ_6	0
$R(C_T, C_7)$	4	×: Wrong	γ_7	0	ψ_7	0
$R(C_T, C_8)$	4	×: Wrong	γ_8	0	ψ_8	0

7.2.4 Other Prime Code Families and their Problems

Since all the prime code families have some common properties, the proposed method can also be used for other prime code families including modified prime code (MPC) [1], new MPC (nMPC) [9] and double-padded MPC (DPMPC) [4]. As an example, let us consider the MPC with $p = 3$. Table 7.5 shows all possible values of $C_{MPC}(n, p)$ [1, 6] where 'j' is the sub-sequence index within the code ($0 \leq j < p$).

In the UC-MPC [6] the cross-correlation between any code pair, regardless of the group that each code belongs to, is "1" whereas in MPC, the cross-correlation between any code pair is either 0 or 1 depending on whether the codes belong to the same group or not, respectively. Consequently any C_T sequence that is generated from constructor codes which all belong to the same group is not unique.

TABLE 7.5
MPC CODE SET FOR $p = 3$

Index			C_{MPC}			
i	x	n	C_n	j=0	j=1	j=2
0	0	0	C_0	100	100	100
	1	1	C_1	010	010	010
	2	2	C_2	001	001	001
1	0	3	C_3	100	010	001
	1	4	C_4	010	001	100
	2	5	C_5	001	100	010
2	0	6	C_6	100	001	010
	1	7	C_7	010	100	001
	2	8	C_8	001	010	100

C_0	1	0	0	1	0	0	1	0	0
C_1	0	1	0	0	1	0	0	1	0
C_2	0	0	1	0	0	1	0	0	1
C_T	1	1	1	1	1	1	1	1	1

Group i=0

C_3	1	0	0	0	1	0	0	0	1
C_4	0	1	0	0	0	1	1	0	0
C_5	0	0	1	1	0	0	0	1	0
C_T	1	1	1	1	1	1	1	1	1

(b) Group i=1

C_6	1	0	0	0	0	1	0	1	0
C_7	0	1	0	1	0	0	0	0	1
C_8	0	0	1	0	1	0	1	0	0
C_T	1	1	1	1	1	1	1	1	1

(c) Group i=2

Figure 7.2 Examples of MPC family where C_T is not unique

For example, as shown in Figure 7.2 (see also Table 7.5), the code $C_T = 111,111,111$ can be obtained by adding different constructor codes such as (i) C_0, C_1 and C_2 (Figure 7.2(a)) or (ii) C_3, C_4 and C_5 (Figure 7.2(b)) or (iii) C_6, C_7 and C_8 (Figure 7.2(c)).

To overcome this problem, and hence makes C_T a unique sequence for all prime code families, the following method is proposed, hereby referred to as the "Generalisation Strategy" (GS):

C_0	1	0	0	1	0	0	1	0	0
C_1	0	1	0	0	1	0	0	1	0
C_2	0	0	1	0	0	1	0	0	1
C_T	1	1	1	1	1	1	1	1	1
S_T	1	0	0	0	0	0	0	0	0
C'_T	2	1	1	1	1	1	1	1	1

(a) Group i=0

C_3	1	0	0	0	1	0	0	0	1
C_4	0	1	0	0	0	1	1	0	0
C_5	0	0	1	1	0	0	0	1	0
C_T	1	1	1	1	1	1	1	1	1
S_T	0	1	0	0	0	0	0	0	0
C'_T	1	2	1	1	1	1	1	1	1

(b) Group i=1

C_6	1	0	0	0	0	1	0	1	0
C_7	0	1	0	1	0	0	0	0	1
C_8	0	0	1	0	1	0	1	0	0
C_T	1	1	1	1	1	1	1	1	1
S_T	0	0	1	0	0	0	0	0	0
C'_T	1	1	2	1	1	1	1	1	1

(c) Group i=2

Figure 7.3 Manipulating CT to make it unique

C_0	1	0	0	1	0	0	1	0	0
C_1	0	1	0	0	1	0	0	1	0
C_2	0	0	1	0	0	1	0	0	1
C_3	1	0	0	0	1	0	0	0	1
C_4	0	1	0	0	0	1	1	0	0
C_5	0	0	1	1	0	0	0	1	0
C_6	1	0	0	0	0	1	0	1	0
C_T	3	2	2	2	2	3	2	3	2
S_T	1	1	0	0	0	0	0	0	0
C''_T	4	3	2	2	2	3	2	3	2
C'_T	3	3	2	2	2	3	2	3	2

Figure 7.4 Manipulating CT to make it unique

(i) Suppose that C_T is obtained by adding all code sequences of a given group (let say the ith group). A new sequence S_T is introduced, which has the same length as C_T where its ith bit is "1" and its other bits are "0". Then the new unique sequence $C_T' = C_T + S_T$ (see Figure 7.3(a)-Figure 7.3(c))

(ii) If C_T is obtained by adding the code sequences of different groups (i.e. ith, mth and nth groups) then, in the new sequence S_T', the ith, mth and nth bits are "1", and its other bits are "0".

(iii) In both of the above cases, if any digit of C_T' is greater than p then that digit should be changed to the value of p. This is shown in Figure 7.4, where digit 4 is reduced to $p = 3$.

It should be noted that the GS can be applied to any prime code families including UC-MPC; although, as discussed before, C_T sequences for UC-MPC are unique and hence there is no need to apply GS to it.

7.3 Methodology and Implementation

In this section implementation and feasibility of the proposed novel cancellation scheme when employed in an OCDMA network are discussed. Figure 7.5 shows a detailed block diagram of the proposed OCDMA network with its MUI cancellation scheme. It consists of '*k*' optical transmitters, a star coupler, and '*k*' optical receivers. Each transmitter has (i) a de-multiplexer that separates the data and its address, (ii) an optical sampler which converts the Non-Return to Zero (NRZ) electrical data into the high speed optical pulses, (iii) an optical encoder and (iv) a prime code sequence generator. The optical encoder has an optical power splitter, parallel optical fibre delay lines, optical switches and an optical power combiner that converts the optical pulses into the optical code sequences [1]. The prime code sequence generator selects a prime code sequence based on the input electrical address signal, and passes it to the optical switches on the optical fibre delay lines of the encoder.

On the other hand, each receiver consists of (i) an optical decoder, (ii) a threshold detector which detects the auto-correlation peaks and (iii) a pulse generator for recovering the electrical data bits. Both the transmitter MUI controller unit and the star coupler are proposed to cancel the MUI effect.

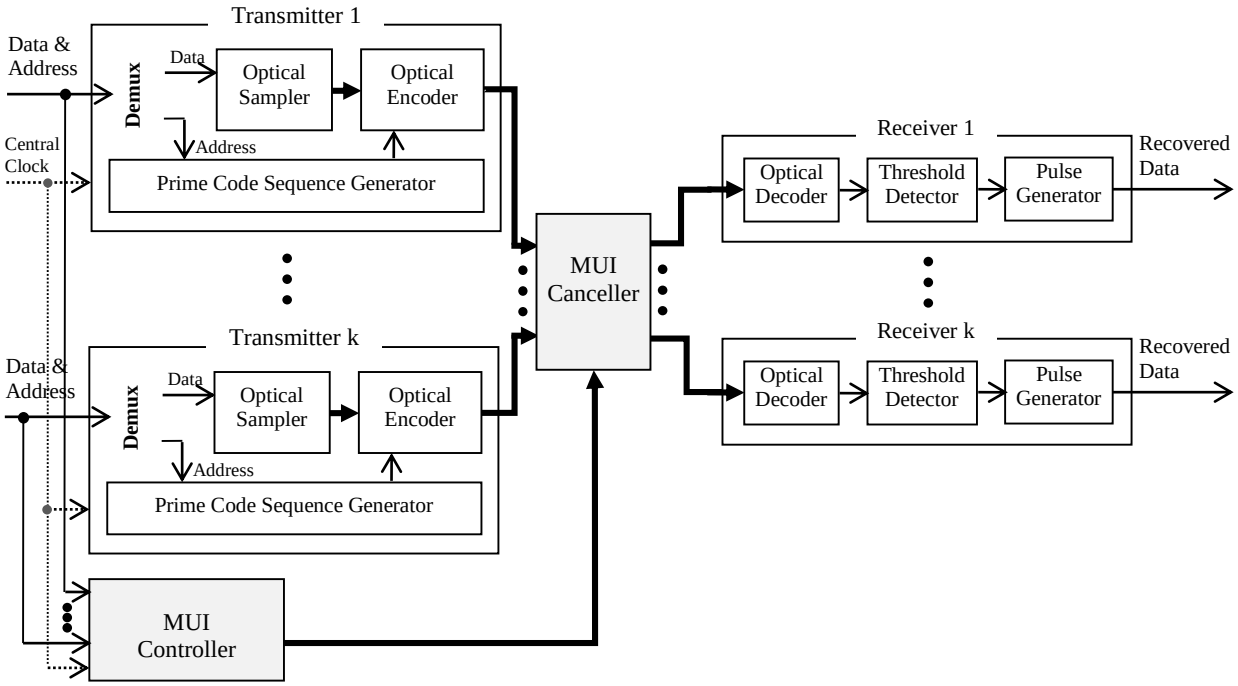

Figure 7.5 Proposed system with MUI cancellation block diagram

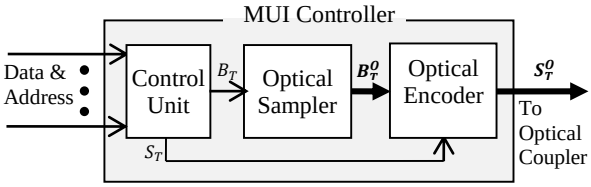

Figure 7.6 Proposed MUI controller detailed block diagram

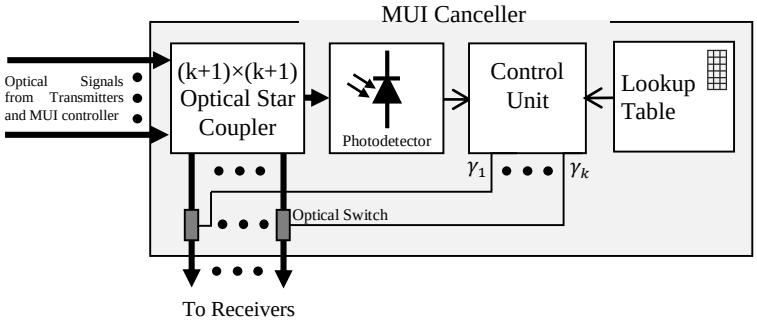

Figure 7.7 Proposed MUI canceller detailed block diagram

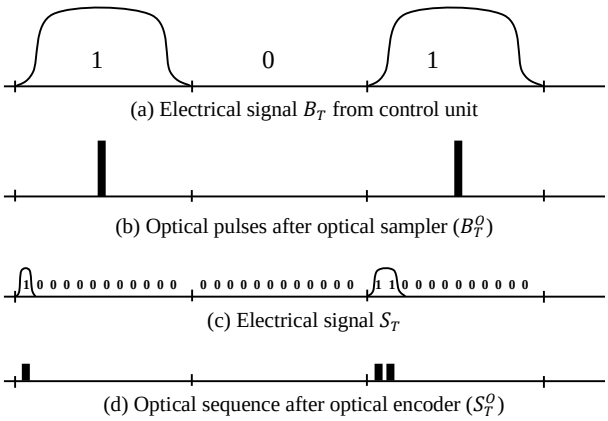

Figure 7.8 Optical signal waveforms corresponding to the proposed MUI controller

Figure 7.6 shows the MUI controller unit in more detail. It consists of a control unit, an optical sampler and an optical encoder. The control unit separates the data and addresses of all transmitters and checks whether all constructor codes belonging to the same group are used as recipient addresses. If used, then, based on the group number and the proposed GS, the sequence S_T will be generated and added to C_T to produce the unique sequence C_T' (see Figure 7.4).

In short, as shown in Figure 7.6, the control unit generates an electrical sequence (S_T) and a '0' or '1' single bit (B_T) which is converted into an optical pulse B_T^O by the optical sampler.

Then, both B_T^O and S_T waveforms are fed into the optical encoder to produce an optical sequence S_T^O. Figure 7.7(a)-Figure 7.7(d) show an example of all B_T, B_T^O, and S_T^O waveforms for three instances, where $S_T = 100{,}000{,}000{,}000$ (Figure 7.3(a)), $S_T = 000{,}000{,}000{,}000$ (Figure 7.2) and $S_T = 110{,}000{,}000{,}000$ (Figure 7.4). It should be

noted that, in case all codes in a given group are not used as constructor codes, both S_T and S_T^O become zero electrical and optical sequences of length 'L'.

Figure 7.7 shows the proposed MUI canceller. It consists of a (k+1)×(k+1) optical star coupler, a photodetector, a control unit, and a Read-Only Memory (ROM) which stores the pre-calculated look-up table described Section 7.2 (i.e. Table 7.3). The inputs to MUI canceller consists of "k" optical sequences from transmitters and the output of MUI controller unit (Figure 7.6). These sequences are combined in the optical star coupler to produce (k+1) OCDMA waveforms (C_T). One of these waveforms is detected by the Photo-Detector (PD) and the remaining k waveforms enter the receivers (Figure 7.8). The electrical signal C_T at the output of PD enters the control unit which computes the number of simultaneous users (N). The control unit also extracts the C_T as well as all associated constructor sequences from the look-up table. Also, the correction coefficients (γ_n) signals are generated which control the optical switches located between the star coupler and the receivers as shown in Figure 7.8.

For the receivers that are carrying the constructor code sequences C_i, optical switches are ON (i.e. $\gamma_n = 1$). However, for the other receivers, their associated optical switches are OFF ($\gamma_n = 0$), implying that the correlation between each wrong received signal and its associated receiver's signature sequence is zero. In fact, these optical switches that are controlled by γ_n signals perform the correlation correction, and hence totally eliminate the MUI effect in the proposed OCDMA system. Using the look-up table as a data structure, runtime computation can be replaced with a simple array indexing operation and hence, processing time decreases significantly.

It should be noted that the above MUI cancellation scheme is general and can be implemented easily in existing systems with any prime code family. Also there is no need to manipulate the hardware of transmitters and/or receiver, as it is only necessary to add two blocks (MUI Controller and MUI Canceller) to existing systems. Moreover it is simple to implement and fast, due to its indexed search algorithm and the use of a cached look-up table.

7.4 Summary

A novel method that can totally remove the MUI in OCDMA networks presented and discussed in detail. The proposed scheme is then implemented in a proposed apparatus with a high-level block diagram design. Based on this design, this MUI cancellation scheme is shown to be low-cost, less-complex and easy-to-implement, in compare with those in [2, 3, 7, 8]. Furthermore, another cancellation scheme has been analysed in Chapter 4 . None of the prior arts omits the MUI effect totally. In the next chapter, it will be demonstrated that the proposed MUI cancellation scheme removes all of the interferences, in a noise-free channel.

Also, experimentally the BER performances of two OCDMA networks have been compared in the next chapter, one with and the other without using this proposed MUI cancellation method. The results reveal that the proposed cancelation technique totally removes the MUI in all three code families (i.e. MPC, DPMPC and UC-MPC), and if the MUI canceller is not used, the UC-MPC performs better (i.e. gives lower BER), as compared with the other mentioned prime codes.

REFERENCES

[1] G. C. Yang and W. C. Kwong, *Prime codes with applications to CDMA optical and wireless networks*: Artech House Publishers, 2002.

[2] H. Khoshbin-Ghomash and R. Ormondroyd, "An adaptive neural network receiver for CDMA multi-user interference cancellation in multipath environments," in *Military Communications Conference, 1998. MILCOM 98. Proceedings., IEEE*, pp. 767-771, 1998.

[3] W.-B. Yang and K. Sayrafian-Pour, "A low complexity interference cancellation technique for multi-user DS-CDMA communications," in *Communications (ICC), 2010 IEEE International Conference on*, pp. 1-5, 2010.

[4] M. M. Karbassian and H. Ghafouri-Shiraz, "Performance analysis of heterodyne-detected coherent optical CDMA using a novel prime code family," *Journal of Lightwave Technology*, vol. 25, pp. 3028-3034, 2007.

[5] M. Zoualfaghari and H. Ghafouri‐Shiraz, "Analysis of a novel prime code in IP transmission and routing over FSK‐OCDMA in an optical network unit," *Microwave and Optical Technology Letters*, vol. 54, pp. 2852-2856, 2012.

[6] M. H. Zoualfaghari and H. Ghafouri-Shiraz, "Uniform cross-Correlation modified prime code for applications in synchronous optical CDMA communication systems," *Lightwave Technology, Journal of*, vol. 30, pp. 2955-2963, 2012.

[7] R. Fantacci, "Proposal of an interference cancellation receiver with low complexity for DS/CDMA mobile communication systems," *Vehicular Technology, IEEE Transactions on,* vol. 48, pp. 1039-1046, 1999.

[8] R. Lupas and S. Verdu, "Near-far resistance of multiuser detectors in asynchronous channels," *Communications, IEEE Transactions on*, vol. 38, pp. 496-508, 1990.

[9] F. Liu, M. M. Karbassian, and H. Ghafouri-Shiraz, "Novel family of prime codes for synchronous optical CDMA," *Optical and Quantum Electronics,* vol. 39, pp. 79-90, 2007.

Chapter 8

EXPERIMENTAL INVESTIGATION ON OCDMA MULTI ACCESS TRANSMISSION

For the final step of this research, as an essential stage, an experimental setup has been modelled in optical software named OptiSystem, to accredit all the theoretical and analytical results obtained in the previous chapters. Furthermore, the modelled node-to-node optical code division multiple access (OCDMA) link was set up in the laboratory and various experiments were performed. This chapter discusses this experimental setup and its results in detail.

8.1 Introduction

As discussed previously in the literature review, research has been carried out to model an OCDMA network experimentally [1-7]. Some of these experiments investigated the synchronous OCDMA (S-OCDMA) networks (e.g. [6]), while some others focused on asynchronous OCDMA (A-OCDMA) systems, such as [8] and [2].

To validate the theoretical and analytical results of this research, an experimental investigation has been carried out, where an OCDMA fibre optic network was modelled in the laboratory. As a result, the real BER of a system employing specific code signatures has been obtained.

Moreover, the system performances of a few prime code families using a laboratory based optical link were analysed and compared, both with- and without the proposed MUI cancellation scheme.

Finally, the same system has been modelled in the OptiSystem software form Optiwave package, to verify the results and achieve a faster transmission in the simulation.

8.2 Experimental Setup

Figure 8.1 and Figure 8.2 show the experimental setup and its block diagram, respectively, which consist of a transmitter block (Figure 8.2(a)), an optical transceiver (Figure 8.2(b)) and a receiver block (Figure 8.2(c)). The laser used in the transmitter operated at 785nm with an output power of about 4.5mW. In this experiment a 1m and a 1168m long MMF was used with a measured attenuation coefficient of 3.85dB/km at 785nm. Also, the receiver is a silicon pinFET, with a sensitivity of 1μw.

This setup could be used for all the prime code families, and is capable of accommodating $k = p^2$ simultaneous users (in this case up to 25 users are employed, as $p = 3\ or\ 5$).

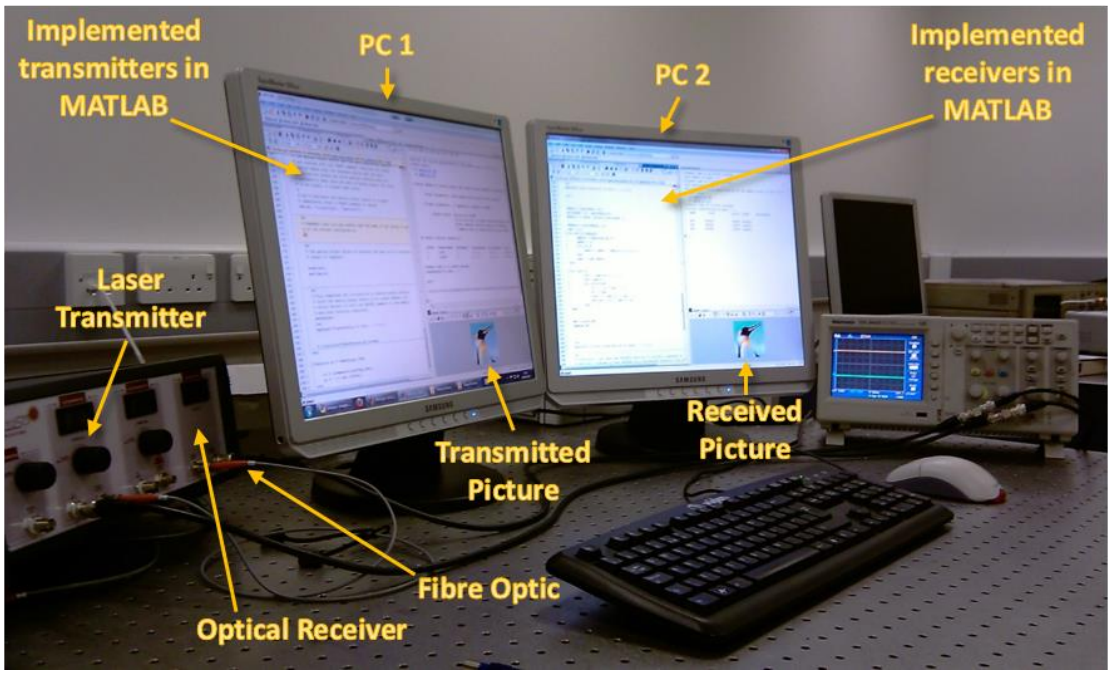

Figure 8.1 OCDMA experiment test bed

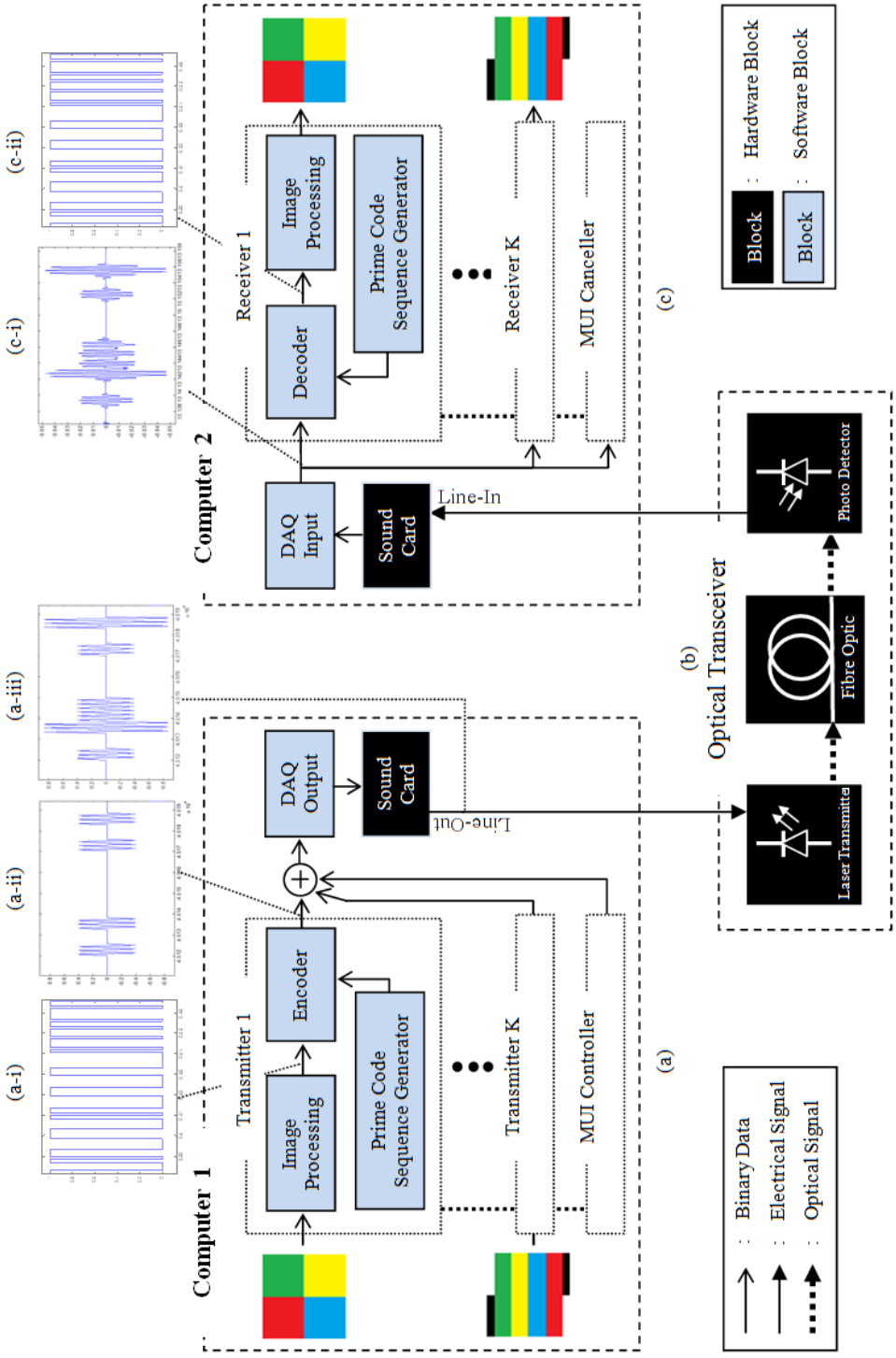

Figure 8.2 Block diagram of modelled OCDMA fibre optic network.
(a) First computer: transmitters and MUI controller, (b) Optical transceivers: laser transmitter, fibre optic and photo receiver, (c) Second computer: receivers and MUI canceller.
(a-i) Binary data, (a-ii) Encoded signal, (a-iii) Combined signal, (c-i) Received signal and (c-ii) Recovered data

Each transmitter in the first node consisted of an image processing block which loaded a picture from a local hard disk and converted it to a three-dimensional unsigned 8-bit integer (unit8) array. This array consisted of three, two-dimensional matrixes, each of which represented a constructor colour (Red, Green and Blue). Each of these two-dimensional matrixes also consisted of *R* rows and *C* columns; where *R* and *C* correspond to the width and height of the picture (number of pixels), respectively. Each element of these matrices contained a number valued between 0 and 255, according to the intensity of the corresponding colour in the respective pixel of the image. These numbers were then converted into the binary data as a long, one-dimensional array (waveform a-i in Figure 8.2(a)).

Both the image binary data and the signature code sequence generated by the prime code sequence generator were input to the encoder and produced the waveform a-ii in Figure 8.2(a).

The encoded data from each transmitter, together with that from the MUI controller unit (S_T), were combined to produce the binary sequence C_T^B, which was then fed into the data acquisition block (DAQ); this was used to control the sound card of the computer-1 (waveform a-iii in Figure 8.2(a)). The sound card was used to convert the digital waveform to its associated analogue signal. The produced analogue waveform C_T at the sound card line-out was fed into the laser transmitter unit of the optical transceiver block, as shown in Figure 8.2(b).

The generated optical waveform C_T^O, was transmitted via an optical fibre and detected by the photodetector (PD). The detected signal was then fed into the line-in of the receiver's

sound card (computer-2), and was converted into the binary data in MATLAB by the DAQ block (waveform c-i in Figure 8.2(c)). As Figure 8.2(c) shows, in each receiver there was a prime code sequence generator, similar to that in the transmitters, which generated the corresponding signature sequence. The received binary data was then correlated with the corresponding code sequence in the decoder block, and the transmitted data was recovered (waveform c-ii in Figure 8.2(c)).

It should be mentioned that the MUI canceller unit was implemented in Computer 2. The waveform c-ii (i.e. the recovered data) was then converted back to an image matrix which was stored in the local hard disk of computer-2. The bit-error rate (BER) of the system could be obtained by comparing the data of both the original and received pictures bit-by-bit.

In this experiment, 9 and 25 different coloured images were allocated to 9 and 25 users respectively, as shown in Figure 8.2, and On-Off keying modulation was employed in the encoders. All 9 transmitters sent their data simultaneously via an optical link to the receiver, where they were recovered and processed. At the output, the number of different bits between the transmitted and received data (errors) was obtained and normalized with respect to the total number of input data bits, which resulted in the system BER. To enhance the accuracy of the BER measurement, the experiment was repeated 10 times to compute the average BER.

8.3 Software Model and Algorithm

In this section the detailed algorithm and the software model used in Computer 1 and 2, implemented in the experiment setup in Figure 8.2, are explained. These models were implemented in MATLAB.

8.3.1 Transmitters-Side Software Model

Figure 8.3 illustrates the algorithm used in the transmitter side (Computer 1). This algorithm modelled the plurality of transmitters, transmitting different colourful images as the data source and consists of:

1. Data initialisation
2. Transmission of each mesh
    a. Processing of each user
        i. Processing of each colour
    b. Data modulation and transmission

As it can be seen in this flowchart, the data initialisation initialises the variables and configurations. The model could be configured, based on the following parameters:

- *p:* The constructor prime number.
- *Code Set:* The code set which should be used to encode the data.
- *Picture Size:* The size of sample pictures to be transmitted from each transmitter.

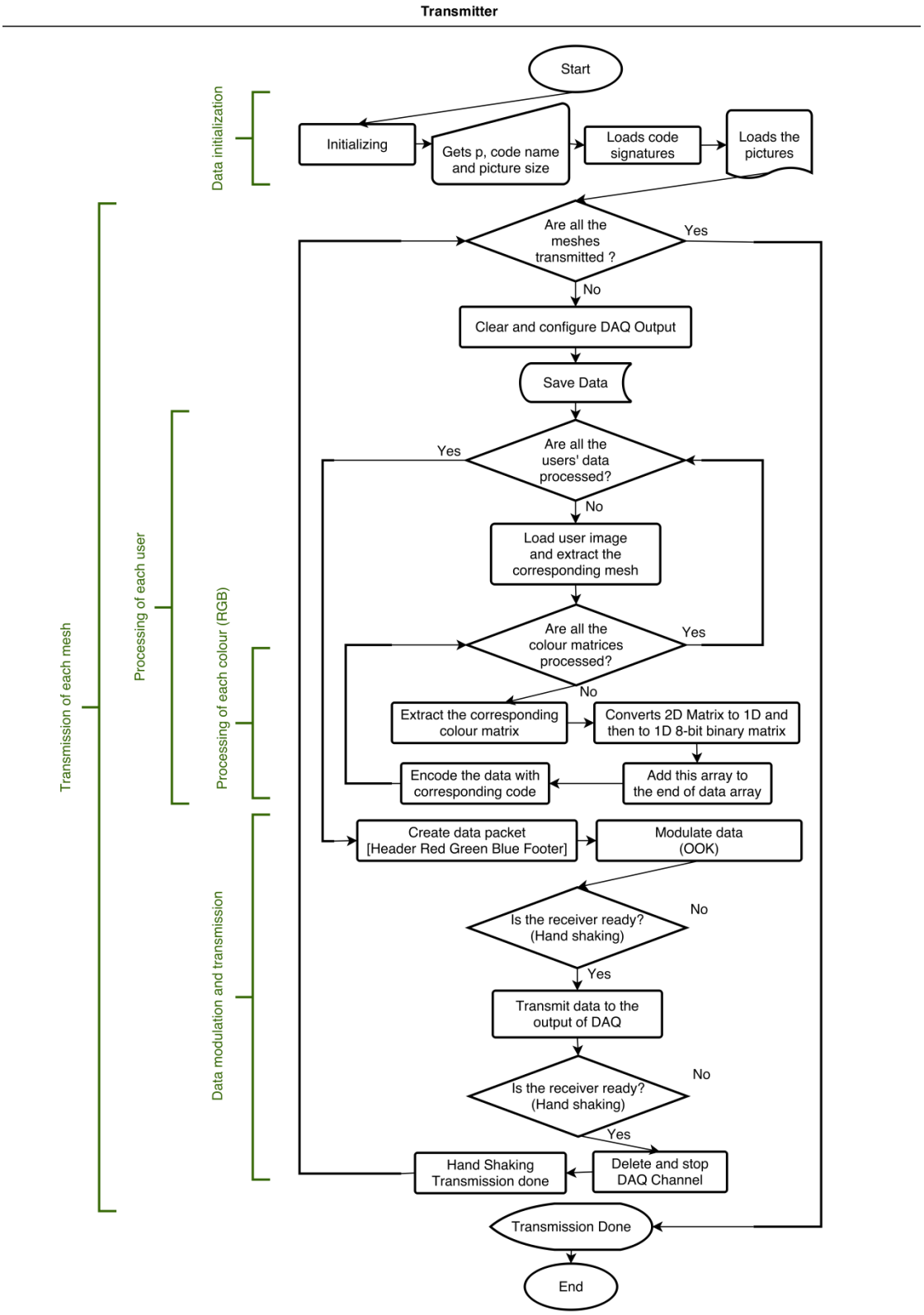

Figure 8.3 Transmitter-Side Software Model - Flowchart

Moreover, both data and DAQ sampling frequencies, bit rate and channel configurations on the DAQ were also initialised at this stage. Then the code signatures were constructed and imported, based on the initialised prime number '*p*' and the selected code set (Default: *p=3* and *Code=UC-MPC* [9]). Finally, at this stage, the sample images were loaded in the workspace.

To make this model faster, more practical and closer to reality, each image was divided into n^2 meshes (i.e. 'n' rows and 'n' columns). This variable could be configured. After the calibration, 'n' was configured in a way such that the size of each mesh was 10×10 pixel.

Each mesh from each transmitter was transmitted, along with the corresponding meshes from the other transmitters, at the same time. After this transmission, the next set of meshes was transmitted correspondingly. This process was repeated until all of the whole pictures (i.e. all the meshes in all the images) were transmitted. This is labelled as "Transmission of each mesh" in the flowchart.

To carry out this process, the data acquisition (DAQ) output of MATLAB had to be cleared and initialised. Then, the configurations including, the prime number and code name, were written into a file. Then, the processing of each user began. All the images corresponding to the users were loaded, and each corresponding mesh was extracted from them.

The next step was to process the RGB colours of each mesh; in doing so, each colour matrix was extracted from each mesh. Then, the programme converted this 2D matrix to

a 1D decimal, and then to a 1D, 8-bit binary matrix, as explained in Section 8.2. This bit train then was added to the end of the data array. Finally, this data was encoded with the corresponding signature code, and this process was then repeated for all the three colour matrices (i.e. red, green and blue).

If the configurations were set to have the MUI cancellation unit, then the MUI controller unit, which is proposed in Chapter 7 , generated its signature bits to be added to the superposition data from the plurality of the transmitters.

After processing each user's data individually, and creating the superposition bit train, the data modulation and transmission process happened. As the first step, a packet was generated: [Header Red Green Blue Footer]. The header and footer not only helped to handle the setup and release times of the DAQ, but also were essential to indicate the start and end of the transmission in an asynchronous communication. Moreover, the encoded RGB data was encapsulated in the packet.

After receiving the handshaking acknowledgement from the receiver side (i.e. Computer 2), then the transmission to the output channel of the DAQ was started. Another handshaking happened after the reception of data from the receiver side. After receiving this handshaking, the DAQ channel was stopped and a handshake acknowledgement was sent to the receivers.

All of these steps were repeated until all the meshes were transmitted.

8.3.2 Receivers-Side Software Model

The software model flowchart of this experiment is shown in Figure 8.4. This algorithm models the plurality of receivers, receiving and retrieving different colourful images as the received data, and consisted of:

1. Data initialisation
2. MUI canceller unit
3. Reception of each mesh
    a. Data reception
    b. Data processing
    c. Processing of each subscriber/user
        i. Processing of each pixel
            1. MUI remover
            2. Detector
        ii. Image processing

As with the transmitter-side model, this algorithm also started with the data initialisation, which consisted of:

1. Configuring the MUI cancellation settings
2. Data initialisation and loading the preserved data
3. Generating and loading the code signatures.

To include an MUI canceller in the model, this unit was initialised by loading all of the C_T combinations discussed in Table 7.3. After initialising the MUI canceller, the process of the reception of each mesh began. The first step of this process was to clear, initialise, and configure the DAQ input of Computer 2.

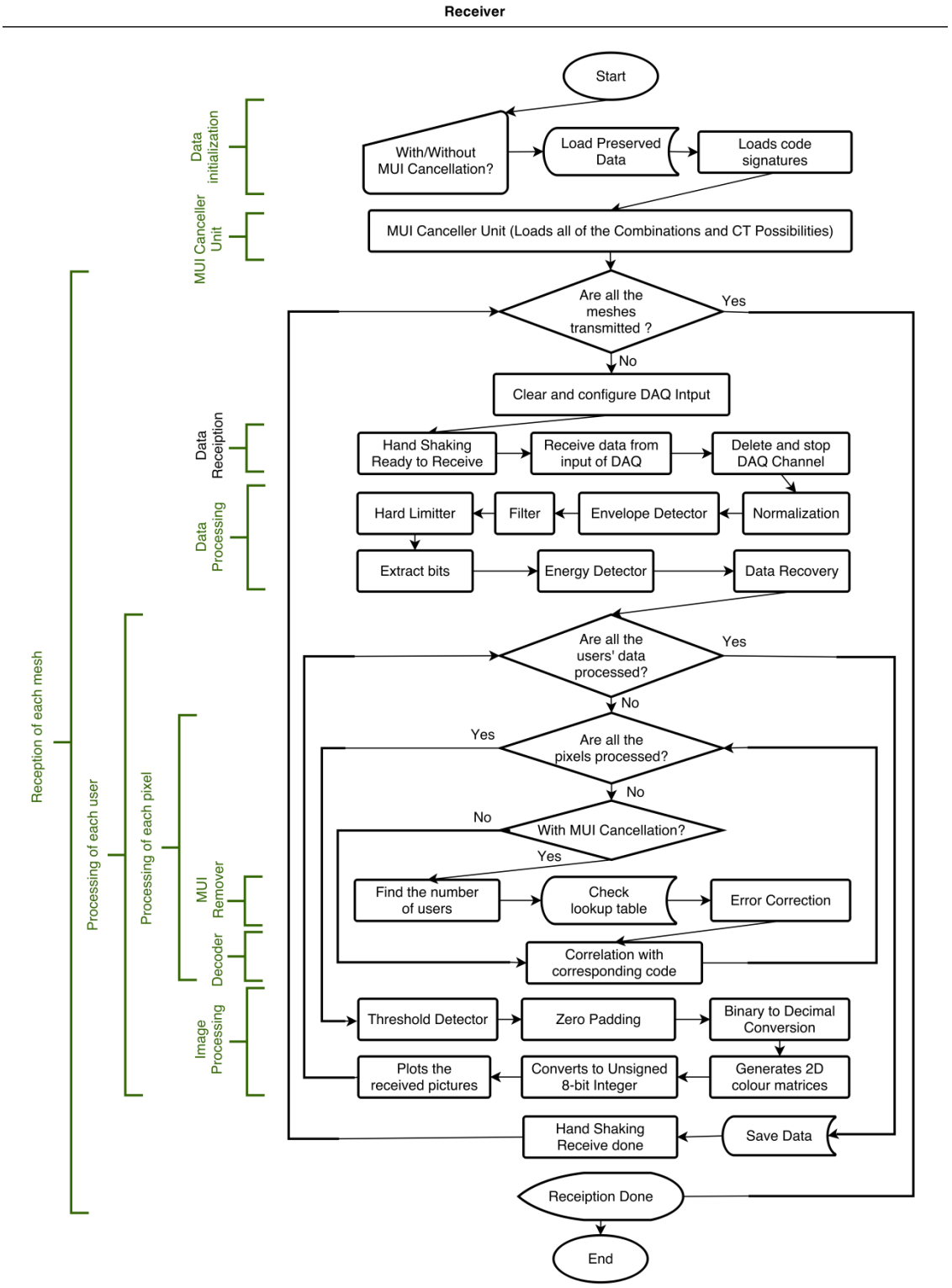

Figure 8.4 Receiver-Side Software Model - Flowchart

Then, the handshaking process took place with the transmitter side, to announce that Computer 2 was ready to receive the data. After a successful handshake, the data was read from the input of the DAQ. Finally, the corresponding DAQ was stopped and deleted. This set of processes is named as data reception in the flowchart.

The next step is the data processing, in which the received data from the DAQ channel was normalised so that the received data signal was independent of the medium conditions, such as the length of the fibre and hence the amount of distortion. Then, an envelope detector function generated the envelope over the received signal. Thereafter this envelope was filtered by a low pass filter to remove the noise. The filtered signal was then hard limited with a dynamic threshold to detect the different levels of the received signal. Afterwards the bit duration was detected and the bits were separated. The energy of each bit was then, calculated and the data bits were finally recovered, based on their received energies.

In this step the processing of each user began; which itself included the processing of each pixel of the transmitted pictures corresponding to each user. If the MUI cancellation scheme was set to be included in this model, then the MUI removal process began at this stage. This process consisted of: (i) finding the number of transmitters/users by detecting the energy of the signal; (ii) checking the MUI look up table to find the most similar signal and (iii) bit error correction by generating correction coefficients.

Then, in the decoder unit, the processed received signal was correlated by the corresponding signature code. The pixel processing loop was repeated until all the pixels of the corresponding user in the corresponding mesh were retrieved.

The next step was the image processing. In this step, the calculated correlation values were compared against a threshold, which was usually equal to the code weight, to detect bits ones and zeros. Then, if it was necessary, the retrieved bit train was zero-padded to fit the size of the picture matrices. Afterwards, the binary values were converted to the decimal values, and 2D colour matrices were generated. Then these matrices were converted to the unsigned 8-bit integer type, so that they could easily construct the images in MATLAB. At the end, these mesh images, which were the part of the transmitted images, were plotted for the corresponding user.

The processing of each user was then repeated for all the users. When the processing of all users' data was finished, the retrieved data was then saved for (a) post processing, (b) finding the differences between the retrieved images and the original images, and (c) calculating the BER. Finally, the last handshake took place, which announced the end of the reception process to the transmitter side.

These processes were then repeated until the transmission of all the meshes was finished successfully.

8.4 Practical Results and Discussion

In this section, the effects of different parameters which were examined in this experiment are discussed. These included employing different code families, using different fibre lengths, and the implementation of the proposed MUI cancellation scheme. Moreover, in this experiment, different numbers of simultaneous users (up to the full capacity of the system) were accommodated in the systems with different numbers of constructor prime numbers (p).

8.4.1 Performance Analysis of Different Code Families

This setup provided a good opportunity to analyse and compare different code families, not only analytically, but also practically.

Figure 8.5 shows nine 300px by 300px coloured pictures which were transmitted in the explained system with 1km fibre over $GF(p=3)$. Figure 8.6 to Figure 8.9 illustrate the recovered pictures in the system without the proposed MUI cancellation scheme under full capacity ($N=9$), employing different code families, including MPC, DPMPC, TPMPC and UC-MPC. Table 8.1 compares the performance of UC-MPC with various known prime code families.

As it can be seen in this table, the experimental results followed the analytical results, and the proposed UC-MPC outperforms among the other prime code families.

TABLE 8.1
PERFORMANCE ANALYSIS OF UC-MPC IN COMPARISON WITH OTHER CODE FAMILIES
GF(3)

Code Name	MPC	DPMPC	TPMPC	UC-MPC
Total BER	0.19357	0.17262	0.15577	0.14183

8.4.2 Investigation of MUI Canceller Effect

Figure 8.10 clearly illustrates the dramatic effect of using the proposed MUI canceller scheme [10] in the network. This experiment was performed by implementing UC-MPC over *GF(3)* and fibre length of 1km, under the full capacity utilisation of the system.

As can be seen in this figure, the retrieved images are identical to the transmitted images with zero BER. It should be mentioned that the MUI cancellation scheme removes the multi user interference totally (100%) and reduces the noise dramatically; but it does not mean that it can remove the noise completely. Zero BER presented in this figure is a result of a short length (1km) communication. This length was chosen intentionally to have a semi-ideal and noise-free medium, and to investigate the effect of multi user interference and an MUI canceller scheme only.

8.4.3 Investigation of Different Number of Constructor Prime Numbers (p)

Figure 8.11 shows the transmitted 200px by 200px coloured pictures in the system implementing UC-MPC over *GF(p=5)*, under full capacity (*N=25*). Figure 8.12 and Figure 8.13 illustrate the pictures in the system with 1km fibre, both without and with the proposed MUI cancellation scheme, respectively.

As can be seen in the systems without the MUI cancellation scheme, implementing the higher constructor prime numbers, or in other words, higher code cardinality and hence higher accommodated active users, would result in more interference and higher BER.

However, Figure 8.13 shows that the MUI cancellation scheme removes the interferences totally, independent of the constructor prime numbers "*p"*.

8.4.4 Investigation of Different Number of Simultaneous Users

In this section the effect of accommodating different numbers of simultaneous users in the system was investigated and compared for two different code sets, MPC and UC-MPC. The transmitted 300px by 300px coloured pictures in the system under partial capacity (*N=4*) over *GF(p=3)* are shown in Figure 8.14.

Figure 8.15 and Figure 8.16 illustrate the recovered pictures in the system with 1km fibre, without the proposed MUI cancellation scheme under partial capacity (*N=4*) and

employing MPC and UC-MPC signatures, respectively. These results show that MPC over *GF(p)* can accommodate up to "*p"* users without being affected by multi user interference. While the first three pictures are not affected, the fourth picture in Figure 8.15 is distorted. However, UC-MPC can accommodate up to "*p+1"* users with no MUI effect (no picture is affected in Figure 8.16). This is more evidence that proves UC-MPC outperforms in comparison with the well known MPC code.

Furthermore, Figure 8.18 shows the recovered pictures in the system with 1km fibre, without the proposed MUI cancellation scheme under partial capacity (*N=6*) employing UC-MPC signatures over GF(p=3). All of the six pictures are now distorted, and the overall BER is more than accommodating the (*N=4*) users (Figure 8.16), and at less than full capacity of (*N=9*) users (Figure 8.9).

Moreover, the recovered pictures in the identical systems with the MUI cancellation scheme employing both MPC and UC-MPC codes are shown in Figure 8.17 and Figure 8.19. Again it has been shown that the MUI canceller system removes the interferences totally, for both MPC and UC-MPC code signatures, independent of the number of simultaneous users.

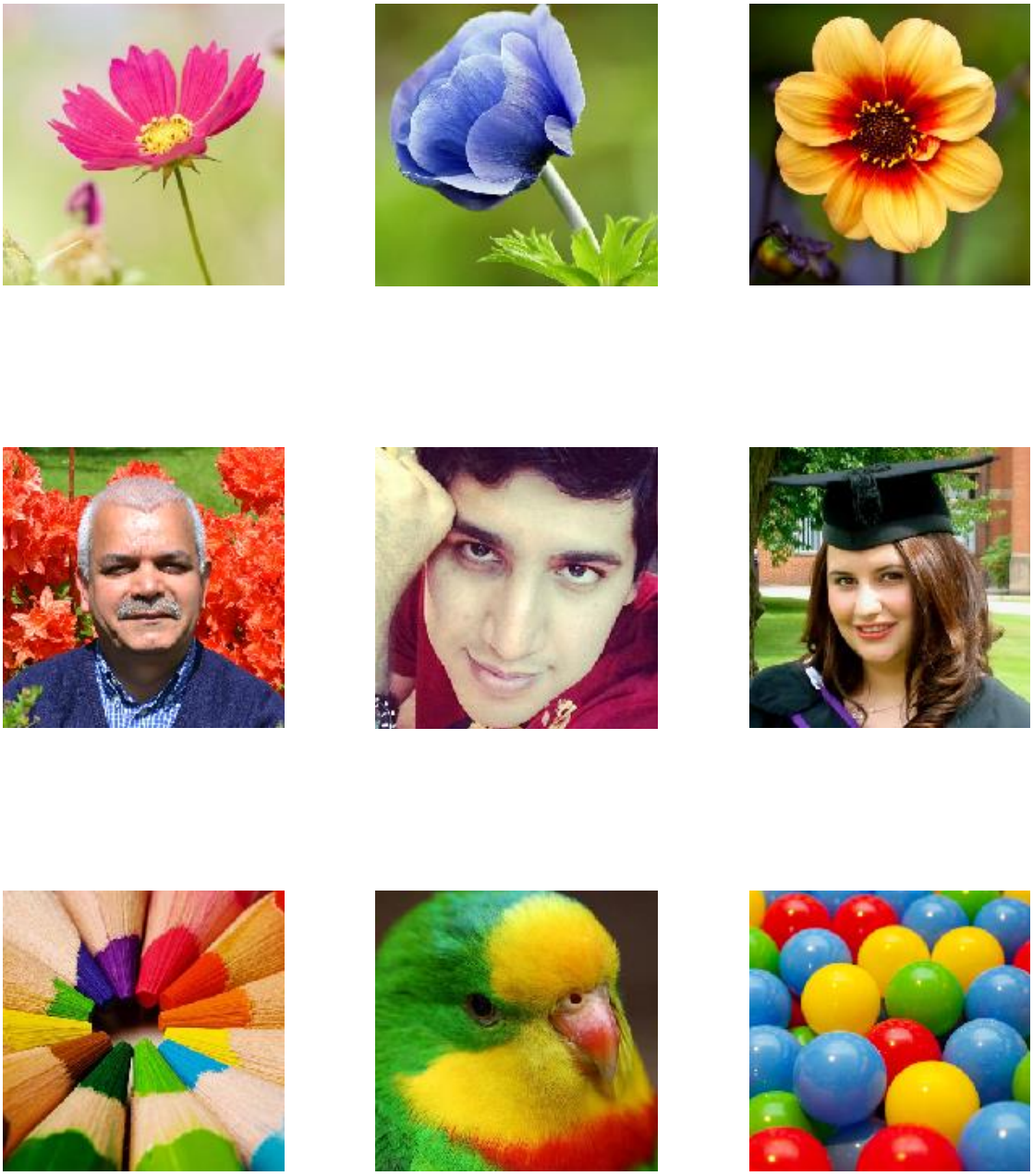

Figure 8.5 Transmitted pictures in the system over *GF(p=3)*
300px by 300px – Coloured

1. BER = 0.16483 2. BER = 0.18246 3. BER = 0.18279

4. BER = 0.18175 5. BER = 0.18025 6. BER = 0.21801

7. BER = 0.20087 8. BER = 0.21043 9. BER = 0.2207

Figure 8.6 Recovered pictures in the system with 1km fibre without the proposed MUI cancellation scheme under full capacity ($N=9$) employing MPC signatures over $GF(p=3)$

1. BER = 0.14741

2. BER = 0.15815

3. BER = 0.16589

4. BER = 0.16499

5. BER = 0.16021

6. BER = 0.19321

7. BER = 0.17967

8. BER = 0.19263

9. BER = 0.19144

Figure 8.7 Recovered pictures in the system with 1km fibre without the proposed MUI cancellation scheme under full capacity (*N=9*) employing DPMPC signatures over *GF(p=3)*

1. BER = 0.13328 2. BER = 0.14379 3. BER = 0.15333

4. BER = 0.14135 5. BER = 0.13994 6. BER = 0.17358

7. BER = 0.1637 8. BER = 0.17526 9. BER = 0.17772

Figure 8.8 Recovered pictures in the system with 1km fibre without the proposed MUI cancellation scheme under full capacity ($N=9$) employing TPMPC signatures over $GF(p=3)$

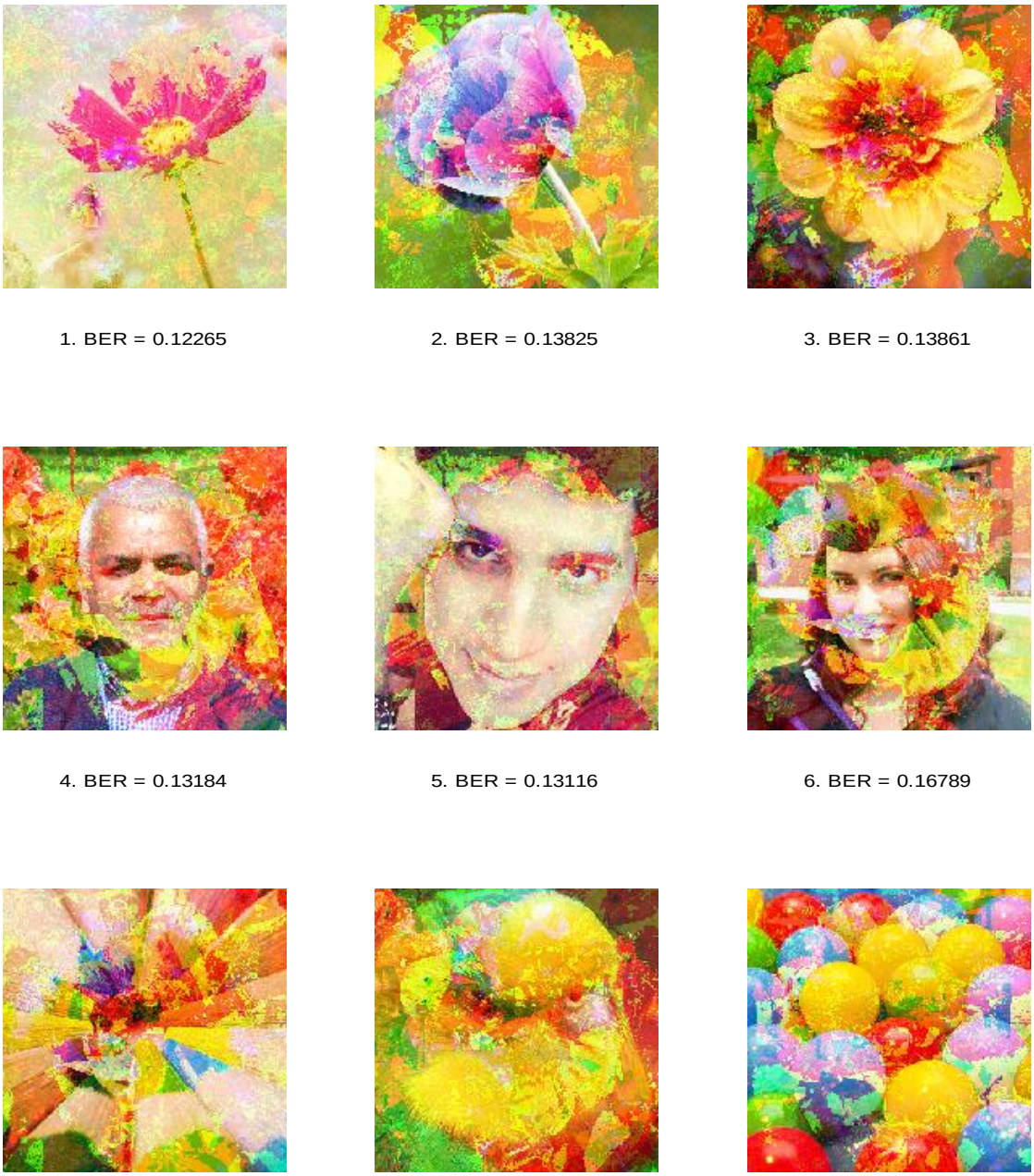

Figure 8.9 Recovered pictures in the system with 1km fibre without the proposed MUI cancellation scheme under full capacity (*N=9*) employing UC-MPC signatures over *GF(p=3)*

1. BER = 0

2. BER = 0

3. BER = 0

4. BER = 0

5. BER = 0

6. BER = 0

7. BER = 0

8. BER = 0

9. BER = 0

Figure 8.10 Recovered pictures in the system with 1km fibre with the proposed MUI cancellation scheme under full capacity (*N=9*) employing MPC, DPMPC, TPMPC and UC-MPC signatures over *GF(p=3)*

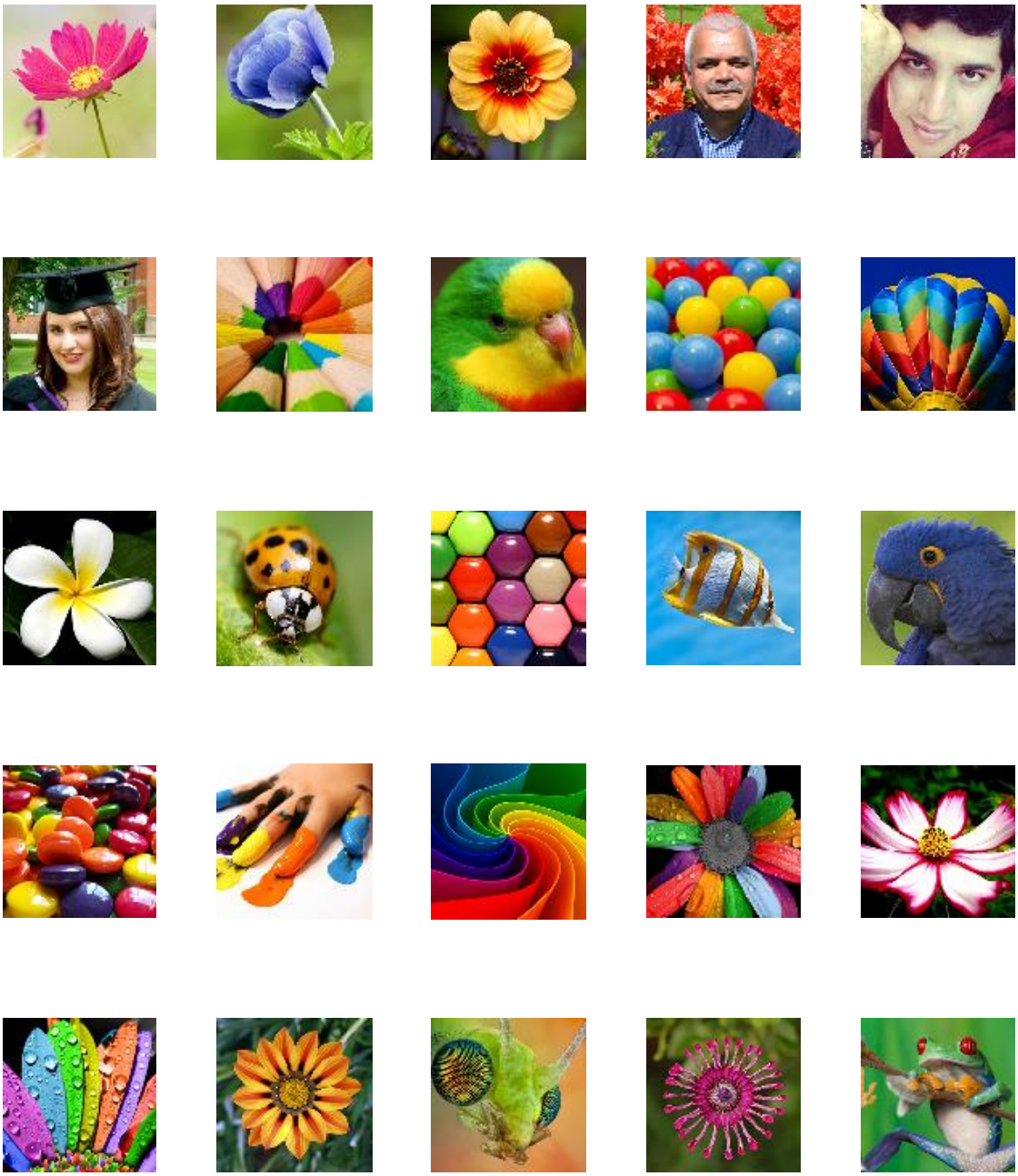

Figure 8.11 Transmitted pictures in the system implementing UC-MPC over *GF(p=5)*
200px by 200px – Coloured

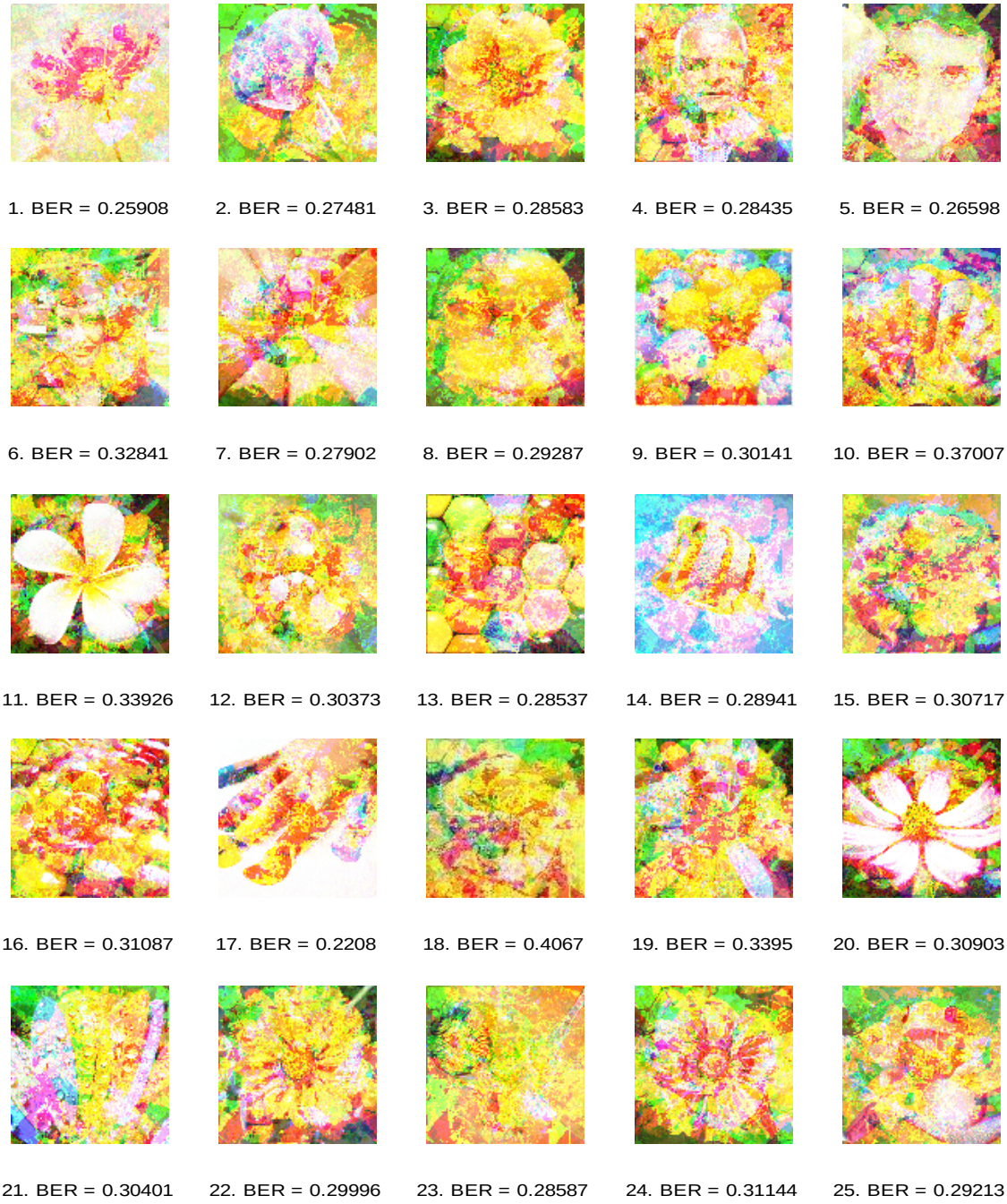

Figure 8.12 Recovered pictures in the system with 1km fibre without the proposed MUI cancellation scheme under full capacity (*N=25*) employing UC-MPC signatures over *GF(p=5)*

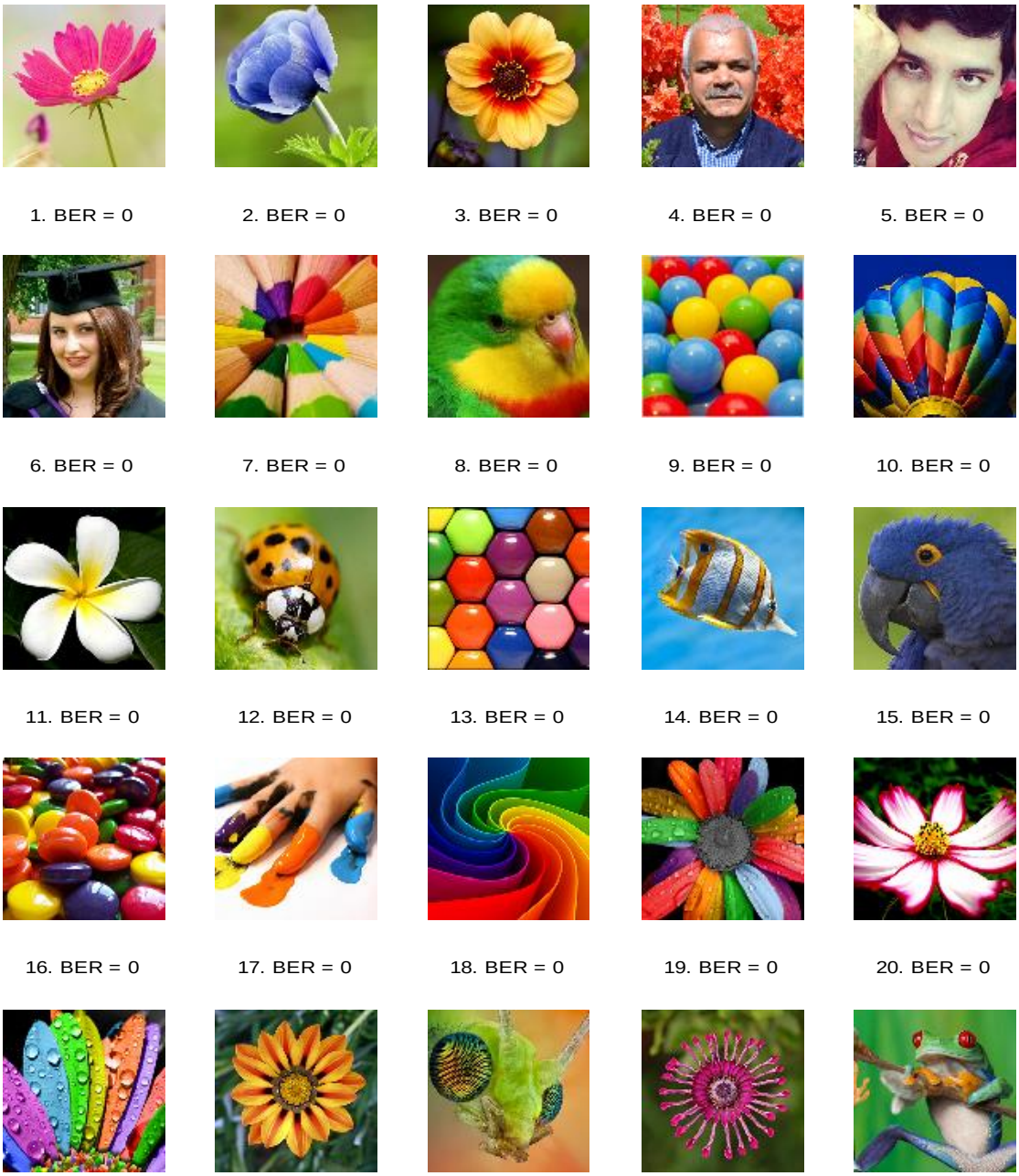

Figure 8.13 Recovered pictures in the system with 1km fibre with the proposed MUI cancellation scheme under full capacity (*N=25*) employing UC-MPC signatures over *GF(p=5)*

Figure 8.14 Transmitted pictures in the system under partial capacity (*N=4*) over *GF(p=3)*
300px by 300px – Coloured

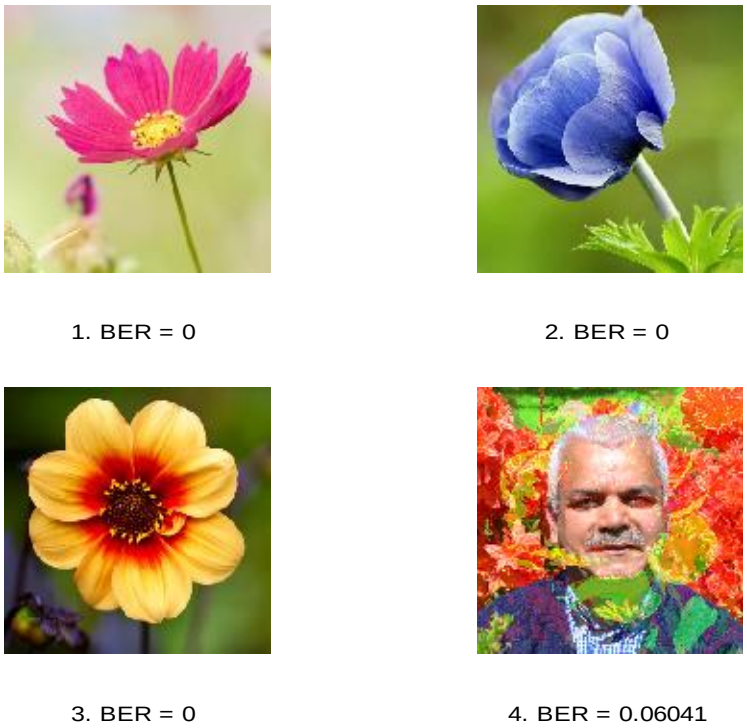

Figure 8.15 Recovered pictures in the system with 1km fibre without the proposed MUI cancellation scheme under partial capacity (*N=4*) employing MPC signatures over *GF(p=3)*

1. BER = 0

2. BER = 0

3. BER = 0

4. BER = 0

Figure 8.16 Recovered pictures in the system with 1km fibre without the proposed MUI cancellation scheme under partial capacity (*N=4*) employing UC-MPC signatures over *GF(p=3)*

1. BER = 0

2. BER = 0

3. BER = 0

4. BER = 0

Figure 8.17 Recovered pictures in the system with 1km fibre with the proposed MUI cancellation scheme under partial capacity (*N=4*) employing MPC and UC-MPC signatures over *GF(p=3)*

1. BER = 0.036906 2. BER = 0.042277 3. BER = 0.041733

4. BER = 0.044275 5. BER = 0.042365 6. BER = 0.057168

Figure 8.18 Recovered pictures in the system with 1km fibre without the proposed MUI cancellation scheme under partial capacity (*N=6*) employing UC-MPC signatures over *GF(p=3)*

1. BER = 0 2. BER = 0 3. BER = 0

4. BER = 0 5. BER = 0 6. BER = 0

Figure 8.19 Recovered pictures in the system with 1km fibre with the proposed MUI cancellation scheme under partial capacity (*N=6*) employing MPC and UC-MPC signatures over *GF(p=3)*

8.4.5 Comparison of BER in Systems with and without the Proposed MUI Cancellation Scheme

Figure 8.20 compares the bit error rate (BER) of two systems one with and the other one without the proposed cancellation scheme. In each system MPC, DPMPC and UC-MPC families were employed over *GF(p=3)*. This figure shows that in the system without the proposed MUI cancellation scheme, the UC-MPC code family outperform of both MPC and DPMPC; the effect of MUI increased with the number of simultaneous users. The results clearly show that, by employing the proposed cancellation scheme, the effect of MUI in all the above mentioned code families can be completely removed.

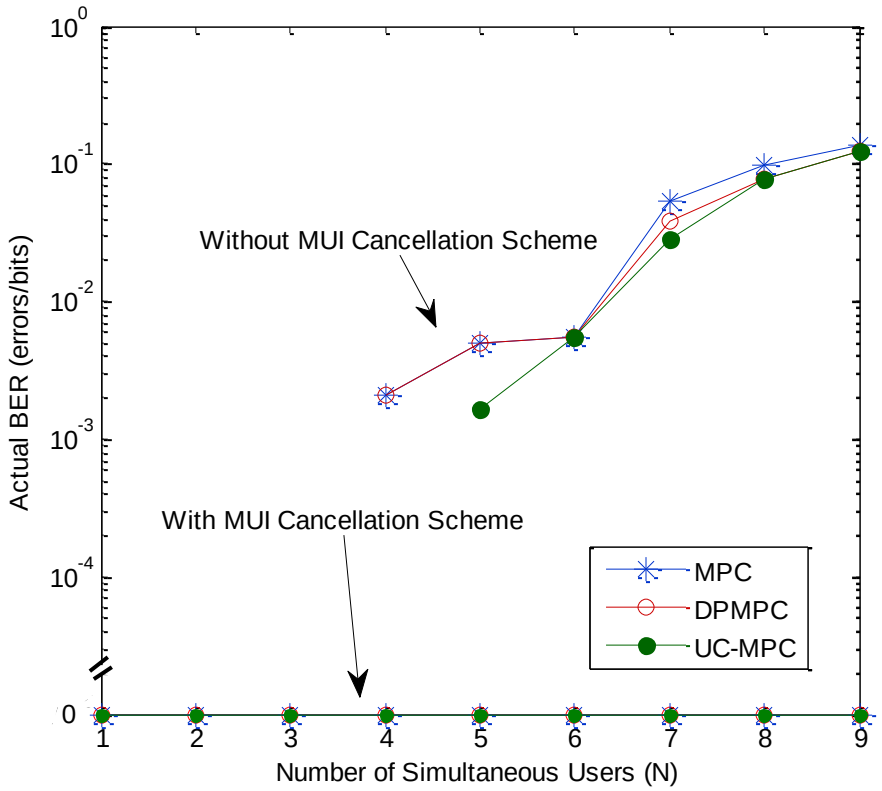

Figure 8.20 Comparison of BER in systems with and without the proposed MUI cancellation scheme

8.5 Simulation of an OCDMA Network in OptiSystem

As a part of this research, the experiment setup was simulated in an optical software design suite, named OptiSystem from the Optiwave package, under the 30-day trial licence. This software can simulate optical components and links of modern networks in the transmission layer. This was done to validate the results of previous sections, using faster communication up to 10 Gb/s.

Figure 8.21 below shows this setup. This model consisted of two MATLAB components which handled the communications between the OptiSystem and MATLAB. These components pointed to the almost identical codes which were introduced in Section 8.3.

The transmitter side and the receiver side in this figure are the modelled versions of Computer 1 and Computer 2 in Figure 8.3, respectively. Moreover, the optical transceiver in Figure 8.2 were modelled in OptiSystem (i.e. optical link in Figure 8.21).

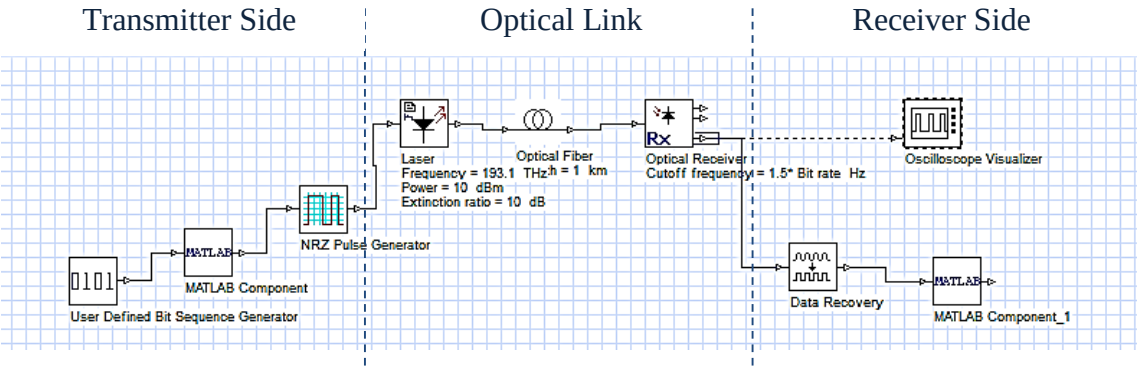

Figure 8.21 OptiSystem network model

8.5.1 Transmitter Side

The bit sequence generator unit in the transmitter side handled the bit rate of this communication. Also, a non-return to zero (NRZ) pulse generator was used to convert the binary signal at the output of the MATLAB component of the transmitter side into the electrical signal for the input of the laser model.

8.5.2 Receiver Side

On the receiver side, a data recovery unit was used to retrieve the transmitted signal and convert the electrical signal at the output of the optical receiver into the binary signal, so it could be used as an input for the MATLAB component on the receiver side. Also, an oscilloscope visualizer was implemented on the receiver side to monitor the electrical output of the optical receiver.

8.5.3 Optical Link

The laser block, optical fibre and the optical receiver block in the optical link were configured with the exact same specifications of the real components used in the experiment in Section 8.2.

8.6 Simulation Results and Discussion

Figure 8.22 illustrates the performance comparison of UC-MPC and DPMPC, using OptiSystem in the system with 2km fibre without the proposed MUI cancellation scheme under partial capacity (N=2).

As it can be seen in the picture, the recovered images in the mentioned system employing UC-MPC as the signature code were not affected by the interferences and the noises. On the other hand, those with DPMPC as the code sequences were corrupted. It should be mentioned that, before UC-MPC, DPMPC had introduced a better BER and properties in comparison with the other prime codes.

At it was discussed previously, although UC-MPC was constructed with a lower code weight (i.e. $w=p+1$) in comparison with DPMPC (i.e. $w=p+2$), UC-MPC offers much better correlation properties and its codes are more orthogonal.

Figure 8.23 shows the output of the oscilloscope visualizer (i.e. the electrical output of the optical receiver), for implementing of both UC-MPC and DPMPC in the above mentioned experiment. As it can be seen, the received signal encoded with UC-MPC was received with much higher power, whereas in the case of DPMPC, the received signal was distorted and hence error bits were introduced.

Figure 8.24, just as in Figure 8.15 and Figure 8.17, shows the effect of multi-user interference in the system under partial capacity ($N=4$) over $GF(p=3)$; but this experiment was performed in the introduced OptiSystem model with 10px by 10px coloured pictures and it compared employing UC-MPC with DPMPC.

Similarly to MPC in Figure 8.15, the fourth user in DPMPC (bottom-right image in Figure 8.24(c)) suffered from the interferences, whereas all the four users in UC-MPC had an interference-free communication.

Furthermore, the effect of the MUI canceller scheme in the system employing UC-MPC over *GF(p=3)* under full capacity (*N=9*) was investigated separately in the OptiSystem model. The model outcomes in Figure 8.25(a)-Figure 8.25(c) validate the practical results in Figure 8.5, Figure 8.9 and Figure 8.10, respectively.

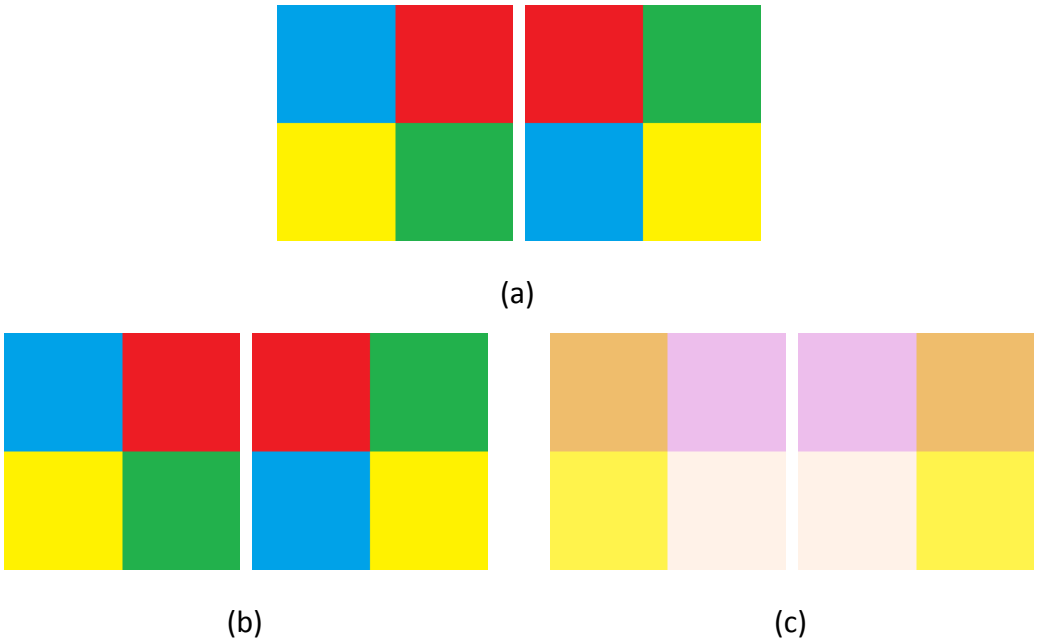

Figure 8.22 Performance comparison of UC-MPC and DPMPC, using OptiSystem in the system with 2km fibre without the proposed MUI cancellation scheme under partial capacity (*N=2*)
(a) Transmitted 10px by 10px coloured pictures; recovered pictures employing (b) UC-MPC and (c) DPMPC signatures over *GF(p=3)*

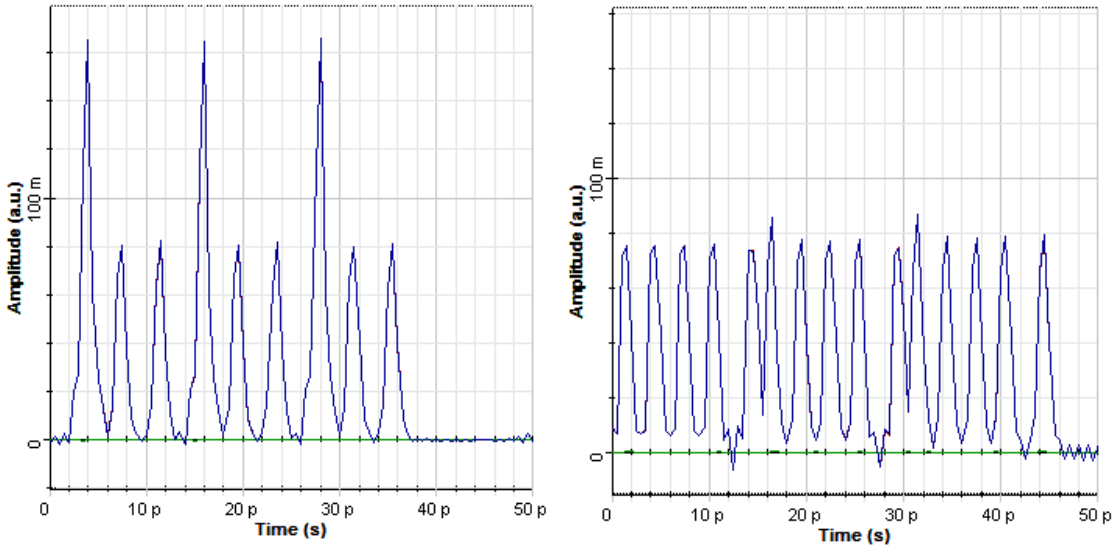

(a) UC-MPC (b) DPMPC

Figure 8.23 Optical receiver's output in oscilloscope visualizer

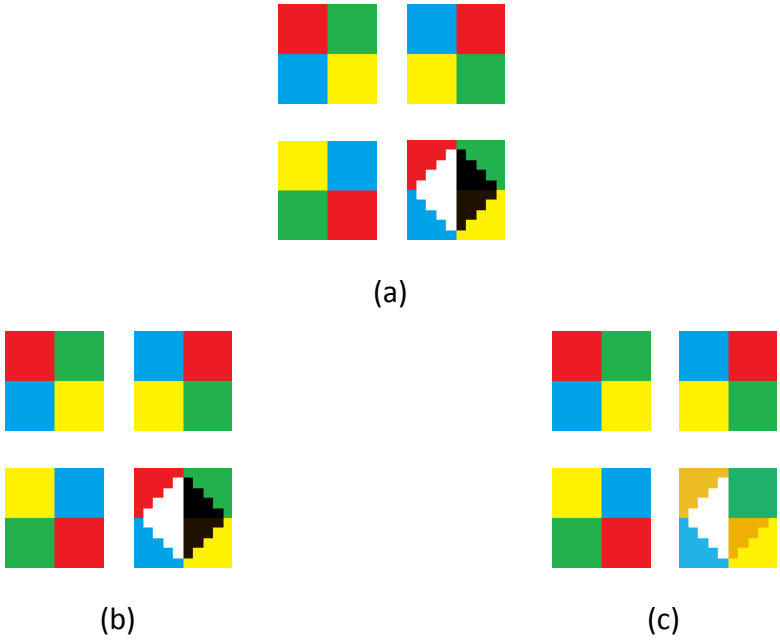

(a)

(b) (c)

Figure 8.24 Effect of multi user interference, using OptiSystem in the system under partial capacity (*N=4*) (a) Transmitted 10px by 10px coloured pictures; recovered pictures employing (b) UC-MPC and (c) DPMPC signatures over *GF(p=3)*

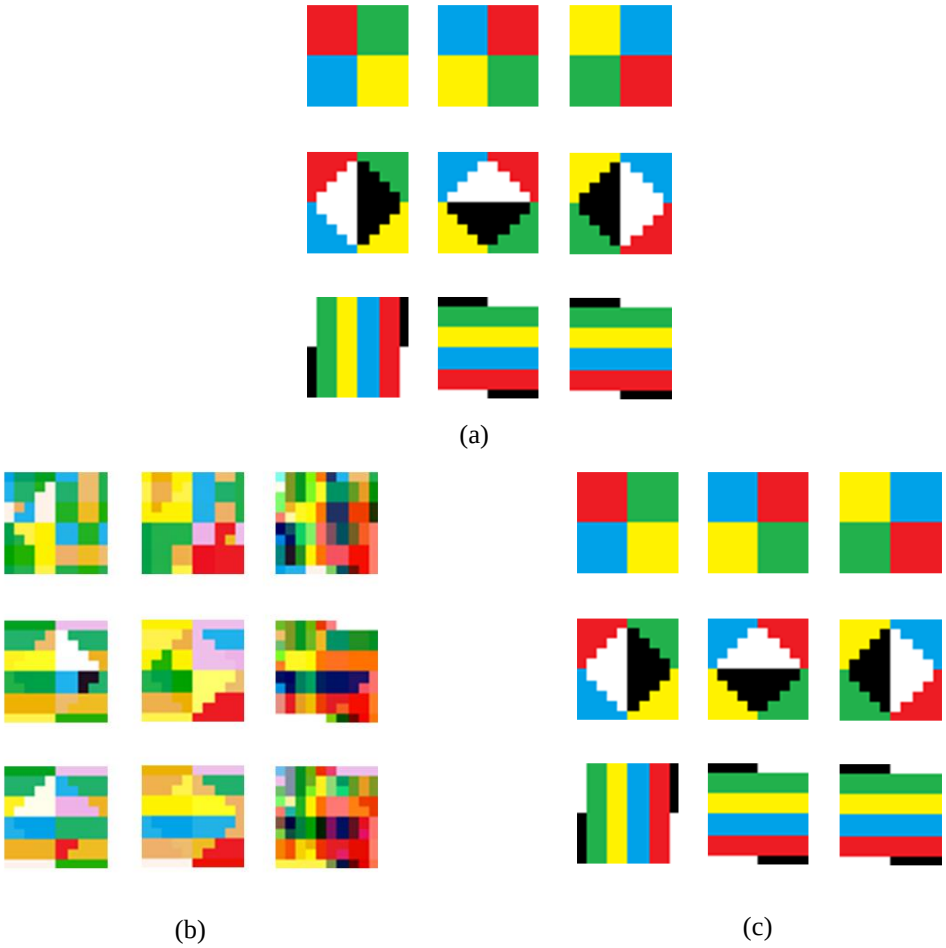

(a)

(b) (c)

Figure 8.25 Effect of MUI canceller scheme, using OptiSystem in the system employing UC-MPC over *GF(p=3)* under full capacity (*N=9*)
(a) Transmitted 10px by 10px coloured pictures; recovered images in the system (b) without and (c) with the proposed MUI cancellation scheme

8.7 Summary

A practical implementation of an optical link setup was introduced and explained in this chapter. Also the software model, algorithm and codes used in this experiment were discussed in detail, followed by the practical results of these experiments. Moreover, it was shown how this experiment setup had been modelled in OptiSystem. Finally, the simulation results of modelled experiments were discussed and compared with the practical results.

In conclusion, it was shown that the practical, simulation and analytical results identically followed each other. Additionally, it was shown that both the implementation of the proposed code set and the MUI canceller scheme are practically feasible. Furthermore, this experimental setup presented this opportunity to compare different systems and code sets together, not only on paper, but also practically.

REFERENCES

[1] J. P. Heritage and A. M. Weiner, "Advances in Spectral Optical Code-Division Multiple-Access Communications," *Selected Topics in Quantum Electronics, IEEE Journal of*, vol. 13, pp. 1351-1369, 2007.

[2] R. Matsumoto, T. Kodama, S. Shimizu, R. Nomura, K. Omichi, N. Wada, *et al.*, "40G-OCDMA-PON System With an Asymmetric Structure Using a Single Multi-Port and Sampled SSFBG Encoder/Decoders," *Lightwave Technology, Journal of*, vol. 32, pp. 1132-1143, 2014.

[3] Y. Tanaka, T. Kodama, S. Yoshima, N. Kataoka, J. Nakagawa, S. Shimizu, *et al.*, "Ultimate reach 10Gbps dispersion-compensation-free WDM-TDM-OCDMA-PON: Experimental demonstration and theoretical validation," in *Optical Fiber Communication Conference and Exposition (OFC/NFOEC), 2012 and the National Fiber Optic Engineers Conference*, pp. 1-3, 2012.

[4] Y. Yi, K. G. Petrillo, T. Hong-Fu, J. B. Khurgin, A. B. Cooper, and M. Foster, "Simulation and experimental demonstration of coherent OCDMA using spectral line pairing and heterodyne detection," in *Information Sciences and Systems (CISS), 2013 47th Annual Conference on*, pp. 1-6, 2013.

[5] H. Brahmi, G. Giannoulis, M. Menif, V. Katopodis, D. Kalavrouziotis, C. Stamatiadis, *et al.*, "Experimental Demonstration of an Elastic Packet Routing

Node Based on OCDMA Label Coding," *Photonics Technology Letters, IEEE,* vol. 24, pp. 721-723, 2012.

[6] S. Idris, T. Osadola, and I. Glesk, "Towards self-clocked gated OCDMA receiver," *Journal of the European Optical Society-Rapid Publications vol 8 13013, 6 pages,* vol. 8, p. 3013, 2013.

[7] F. Uherek and J. Chovan, "2-D Wavelength-Time Optical CDMA System - Experiment and Simulation," in *Transparent Optical Networks, 2007. ICTON '07. 9th International Conference on*, pp. 118-121, 2007.

[8] X. Linhui, F. Qingqing, and Y. Hongxi, "A new optical code translation scheme for multi-hop network and simulation of multi-user asynchronous OCDMA system," in *Optical Communications and Networks (ICOCN 2010), 9th International Conference on*, pp. 201-203, 2010.

[9] M. H. Zoualfaghari and H. Ghafouri-Shiraz, "Uniform cross-Correlation modified prime code for applications in synchronous optical CDMA communication systems," *Lightwave Technology, Journal of*, vol. 30, pp. 2955-2963, 2012.

[10] M. H. Zoualfaghari and H. Ghafouri-Shiraz, "A Novel Multi User Interference Cancellation Scheme for Synchronous OCDMA Networks," *Lightwave Technology, Journal of,* vol. 31, pp. 1813-1820, 2013.

Chapter 9

Conclusion and Future Works

The final chapter of this work summarises and concludes the outcome of this research, and also includes novel contributions. Moreover, recommendations for further studies in this field of research are included in this chapter.

9.1 Conclusion and Contributions

This thesis presented a new transceiver architecture implementing new spreading codes and a pioneer multi-user interference cancellation scheme, to reduce the co-channel interference in OCDMA networks. This research was in line with the essential need to improve the existing industrial network infrastructures, in order to have high capacity, faster and more reliable communication.

To achieve these aims, this research focused on three main objectives: (1) to introduce new optical orthogonal codes and analyse their performances in different networks; (2) to propose a novel OCDMA network infrastructure and (3) to validate the analytical results in a practical experiment carried out in an end-to-end optical link in the laboratory, as follows:

1. Uniform Cross-Correlation Modified Prime Code (UC-MPC)
    a. Co-channel Interference Reduction Using UC-MPC
    b. Analysis of IP Transmission and Routing in an Optical Network Unit
    c. Proposing Transposed UC-MPC.
2. Proposing a Novel MUI Cancellation Scheme.
3. Simulation and Modelling of an OCDMA Network in the Laboratory.

9.1.1 Uniform Cross-Correlation Modified Prime Code (UC-MPC)

The first step to reduce the co-channel interference reduction and increase the efficiency of the network was to propose a novel code family which introduces enhanced optical orthogonal codes.

In line with this objective, a few prime code families were proposed. Among these novel code sets, the most efficient set was chosen and introduced as Uniform Cross-Correlation Modified Prime Code (UC-MPC). It was found that this code enhances the overall optical communication system's performance. In short, the proposed code has (i) excellent correlation properties, (ii) reduces the co-channel interference, (iii) improves the system security and (iv) reduces the BER in the receiver [1].

The weight, cardinality and length of this new code were introduced as $p+1$, p^2 and p^2+p, respectively. Moreover, the value of auto-correlation and cross-correlation were $p+1$ and 1, respectively [1].

Furthermore, the following outcomes can be highlighted for this section:

1. Regenerated the Prime Code (PC), Modified Prime Code (MPC), Fresh Prime Code (FPC), Padded Modified Prime Code (PMPC) and Double Padded Modified Prime Code (DPMPC) families in MATLAB.
2. Analysed correlation properties of all above code families in MATLAB, using 3D graphs.

3. Performed performance analyses and evaluation of synchronous Pulse Position Modulation (PPM) for OCDMA networks, including calculation of error probability and BER for mentioned code families.

4. Proposed three kinds of Zero Padded Modified Prime Code (ZPMPC) families, and evaluated correlation properties and BER analysis for this family.

    a. Zero Padded Modified Prime Code (ZP-MPC)

    b. Distributed Zero Padded Modified Prime Code (DZP-MPC)

    c. Shifted Zero Padded Modified Prime Code (SZP-MPC).

5. Proposed three kinds of Unit Padded Modified Prime Code (UPMPC) families, and evaluated correlation properties and BER analysis for this family.

    a. Unit Padded Modified Prime Code (UP-MPC)

    b. Distributed Unit Padded Modified Prime Code (DUP-MPC).

6. Proposed Uniform Cross-Correlation Modified Prime Code (UC-MPC) for applications in OCDMA communication systems.

7. Evaluated correlation properties and BER analysis for UC-MPC family.

9.1.2 Co-channel Interference Reduction Using UC-MPC

Thereafter, it was essential to expand the performance analysis of the novel UC-MPC code, from correlation analysis to efficiency analysis of this code set in different communication systems.

To comply with this aim, the performance of the proposed spreading code was analysed and compared in PPM-OCDMA systems (i) without interference cancellation (ii) with interference cancellation and Manchester codes and (iii) with cancellation only.

It was found that the proposed UC-MPC enhances the bit error rate (BER) as compared with the other existing prime code families.

The BER performances of PPM-OCDMA systems using this new family code and MPC are also analysed and compared. The results show that, in all cases, UC-MPC outperforms the others [1].

The following is the breakdown of the achievements for this section:

1. Applied and analysed UC-MPC in PPM-OCDMA network
    a. Simple receiver
    b. Receiver with MAI cancellation
    c. Receiver with MAI cancellation and Manchester encoding.
2. Applied and analysed UC-MPC in overlapping PPM-OCDMA network
    a. Simple receiver

b. Receiver with MUI cancellation

c. Receiver with MUI cancellation and Manchester encoding

d. Throughput analysis.

3. Applied and analysed UC-MPC in a coherent network (Homodyne BPSK-OCDMA)

a. Analysis of phase modulation with Mach-Zehnder interferometer (MZI)

b. Applied the effect of different noises (AWGN, shot noise, thermal noise) and MAI in calculation of bit error rate (BER).

4. Applied and analysed UC-MPC in FSK-OCDMA network

a. Analysis of M-ary FSK-OCDMA with MUI cancellation.

9.1.3 Analysis of IP Transmission and Routing in an Optical Network Unit

Good performance of the proposed UC-MPC led to an investigation of the possible approach of CDMA from an access protocol in the data-link layer to the IP routing in the network layer. Therefore, the performance of IP traffic loaded over this system was analysed to examine its feasibility and efficiency [2].

The results showed that the bit error rate (BER) and packet error rate (PER) improved, when UC-MPC was employed and analysed in the IP transmission and routing in the network over FSK-OCDMA modulation. An increase in the number of simultaneous active subscribers was the other benefit of this system. Moreover, it was discussed that this system is more power efficient and offers better security in comparison with systems employing other prime codes [2]. This analysis was carried out for various channel utilization values *(B)* and against different prime numbers *(p)*. It was found that decreasing "*B*" improves the performance of the network, whereas it was derived that prime number "*p*" has a direct effect on the performance. Some of the achievements are as follows:

1. Applied UC-MPC in IP over FSK-OCDMA network.

2. Analysed the BER and PER performance of IP traffic over FSK-OCDMA employing UC-MPC, for various numbers of *p* and *B* against the number of active users.

3. Analysed the BER performance comparison of IP traffic over FSK-OCDMA between MPC and UC-MPC.

9.1.4 Proposing Transposed UC-MPC

Like some other prime codes, UC-MPC was a generic code set, which could be modified easily to offer more spreading signatures with different properties. Therefore, it was modified, and a novel code was created, named as Transposed UC-MPC (T-UCMPC). The new code set increased the capacity, offered better BER and spectral efficiency and improved the security, as compared with conventional prime codes [3].

Then, the correlation properties of T-UCMPC were calculated, analysed and compared with those of UC-MPC [1]. It was found that the T-UCMPC introduces higher cardinality (i.e. p^2+p), compared to many other prime families (i.e. p^2) [3]. Therefore it was able to accommodate more simultaneous subscribers, under a secure communication. The outcome includes:

1. Proposed Transposed Uniform Cross-Correlation Modified Prime Code (T-UCMPC) for applications in OCDMA communication systems.
2. Introduced Low-Weight T-UCMPC (LW-T-UCMPC).
3. Analysed performance of Low-Weight T-UCMPC in On-Off Keying (OOK) systems.

9.1.5 Proposing a Novel MUI Cancellation Scheme

To enhance and maintain the conventional OCDMA networks, it was essential but not sufficient to introduce the new code sets. It was also necessary to optimise, enhance or redesign the network infrastructures. As an example, existing systems were suffering from multi user interferences dramatically. This was limiting the capacity and performance of the conventional systems [4].

To tackle this limitation, a new multi user interference (MUI) cancellation scheme was introduced, which was developed based on the proposed hypothesis on the uniqueness of the superposition signal created from the plurality of transmitters employing prime codes. Furthermore, the implementation, feasibility and cost effectiveness of the proposed novel cancellation scheme, when employed in an optical CDMA network were investigated.

It was found that the proposed system completely eliminates the effects of MUI. The low-cost and complexity, as well as being easy-to-implement, are the main advantages of this scheme [4]. It can directly and significantly affect network providers commercially and causes big savings in resources and expenses by:

1. Upgrading the existing OCDMA networks with the least amount of effort, cost and time, because:
    a) There are few changes in the system hardware, by adding few blocks to the system.
    b) There is no need to change the transceiver designs and hardware.

c) The software is compatible with existing software.

2. Benefitting from the full capacity of the current network.

3. Extending the highest possible number of accommodated active users in the current system.

4. Improving the accuracy, quality and performance of the network.

To summarise, the following are the achievements of this chapter. The author has:

1. Proposed and proved a hypothesis on the uniqueness of the superposition signal created from the plurality of transmitters employing prime codes.

2. Introduced a novel scheme for MUI cancellation for systems employing UC-MPC, based on the proposed hypothesis.

3. Developing and expanding the MUI cancellation scheme to support other prime families.

4. Designed and implemented the MUI cancellation scheme in the conventional OCDMA networks.

9.1.6 Experimental Investigation on OCDMA Multi Access Transmission

An optical link was setup in the laboratory, where an OCDMA fibre optic network was modelled. The experimental setup consisted of several transmitter nodes, an optical transceiver and several receiver nodes. This setup was able to implement all the prime code families and was capable of accommodating $k=p^2$ simultaneous users. In this case at least 9 users were employed ($p=3$). This link was able to transmit any data and multi-media files simultaneously when the system accommodated k active subscribers [4].

Then, different prime code sets, including UC-MPC, were employed and their performances were investigated in the presence of different modulations schemes. This analysis contained real-time bit error rate (BER) and attenuation analysis. In contrast with previous research, the realistic performance analysis of an OCDMA system was measured, while all the relevant noises, such as optical transmitter phase noise and optical receiver thermal and shot noises, were taken into account, whereas, in other research, an analytical approach or a simulation was performed.

For the next step the proposed MUI canceller unit in this setup was used, which consisted of an MUI controller unit and an MUI canceller unit [4]. Then, the performance of the system, and also the performance of different code families in this system, were analysed and measured.

Meanwhile, this network was modelled and simulated in OptiSystem and MATLAB software. Then, the experimental results were discussed and compared with the analytical

and simulation results. By these actions, a beneficial reference for the enhancement of the proposed theoretical models and identification of existing practical limitations was obtained. As the achievements of this chapter, the author has:

1. Developed a real file transmission over fibre optic employing different networks and modulations in the laboratory.
    a. Accommodated two simultaneous subscribers in different networks (e.g. On-Off Keying) employing different code signatures (e.g. UC-MPC, MPC, n-MPC and DPMPC).
    b. Accommodated a multi access scheme up to the whole capacity of the network (i.e. p^2 subscribers) in different networks (e.g. On-Off Keying) employing different code signatures (e.g. UC-MPC, MPC, n-MPC and DPMPC).
    c. Investigated the effect of multi user interference (MUI) and also an MUI cancellation scheme comparing different codes and networks.
    d. Transmitted different types of files (i.e. grey scale and colour images, audio and text files).
2. Applied OptiSystem software to plan, test and simulate optical links in the transmission layer of modern optical networks:
    a. Simulated optical networks with OptiSystem under the same conditions as a real experiment.

b. Connected MATLAB and OptiSystem to run in parallel.

c. Modelled and configured the existing setup in the lab.

d. Compared the results of simulations and the actual optical devices and elements.

e. Transmitted a file in the simulated networks.

f. Investigated the file transfer over up to a 10 Gb/s data transmission rate and speeded up the process more than 300 times faster, using programming techniques, error handling and optimised use of simulation blocks.

g. Implemented the proposed “Splitter” or “Mesh” technique to simulate the transmission of large pictures in the presence of software and hardware limitations.

h. Implemented the simulation of the multi access scheme up to the whole capacity of the network (i.e. p^2 subscribers).

i. Repeated and compared the results under different circumstances (e.g. different fibre lengths, various number of simultaneous subscribers and different code signatures).

j. Investigated the effect of multi user interference (MUI) and also an MUI cancellation scheme comparing different codes and networks.

9.2 Future Works

All the mentioned achievements are the first steps to greater enhancements in the current CDMA/OCDMA systems, working towards the next generation of networks. On the whole, the main objective of the future studies could be to examine the ultimate architecture to make it efficient, maintainable, extensible and importantly compatible with current technologies.

It could be a time to investigate the current industrial networks' infrastructures, standards and protocols and to negotiate with leading communication companies like British Telecom (BT). This would help to demonstrate a realistic approach to get an intellectual property (IP) for the proposed codes and schemes. Then the focus could be on the implementation of research in the real world and investigation of its impact in today's communication industry. For this reason, this setup will also be targeted to be IP compatible supporting self-synchronous multi-rate services.

The following detailed possible research opportunities, based on the backbones of the proposed methods and schemes, are mentioned here; which it is believed, will result in revolutionary academic and industrial achievements, and could be a path towards faster and more reliable communication:

- To setup a high-speed, fully optical and electronic network with optical transceivers and electronic elements, which employs the proposed MUI cancellation scheme, UC-MPC and other prime code families in:

a) OptiSystem and MATLAB software, to investigate the performance of the proposed code set and system in the simulated environment.

b) A laboratory with corresponding hardware and software, to develop a real file transmission over fibre optic employing different networks and modulations and develop a realistic approach to employ this system in today's communication networks.

- To accommodate a multi access scheme up to the whole capacity of the network in various networks (e.g. On-Off Keying and Pulse-Position Modulation) employing different code signatures (e.g. UC-MPC, MPC, n-MPC and DPMPC).
- To evaluate the performance of the proposed MUI cancellation scheme in different networks using different codes, both analytically and experimentally.
- To compare the analytical and experimental results with simulations.
- To investigate a novel Forward Error Correction (FEC) over OCDMA, applying UC-MPC.
- To propose the asynchronous MUI cancellation scheme for asynchronous OCDMA networks.
- To develop the compatibility of IP-mapped coding and/or OCDMA-PON architecture through simulation and signalling.
- To demonstrate, optimise and manage IP-over-OCDMA technology and/or OCDMA-PON prototype in the networking perspective through hardware/software platforms.
- To investigate the current industrial networks' infrastructures, standards and protocols.

- To patent and obtain intellectual properties (IP) for the proposed UC-MPC and MUI cancellation scheme.
- To negotiate with leading communication companies to implement the proposed code and scheme in the current network infrastructures.

REFERENCES

[1] M. H. Zoualfaghari and H. Ghafouri-Shiraz, "Uniform cross-Correlation modified prime code for applications in synchronous optical CDMA communication systems," *Lightwave Technology, Journal of,* vol. 30, pp. 2955-2963, 2012.

[2] M. Zoualfaghari and H. Ghafouri‐Shiraz, "Analysis of a novel prime code in IP transmission and routing over FSK‐OCDMA in an optical network unit," *Microwave and Optical Technology Letters,* vol. 54, pp. 2852-2856, 2012.

[3] M. H. Zoualfaghari and H. Ghafouri-Shiraz, "A Novel Transposed Uniform Cross-Correlation Modified Prime Code for Enhancement of Capacity and Spectral Efficiency of Networks," *Microwave and Optical Technology Letters,* vol. 55, pp. 2952-2955, 2013.

[4] M. H. Zoualfaghari and H. Ghafouri-Shiraz, "A Novel Multi User Interference Cancellation Scheme for Synchronous OCDMA Networks," *Lightwave Technology, Journal of,* vol. 31, pp. 1813-1820, 2013.

UNIVERSITY OF
BIRMINGHAM